Engineering nanoparticle-based vaccines: Implications for the quality of humoral and cellular immunity

THÈSE N^{O} 6848 (2016)

PRÉSENTÉE LE 14 JANVIER 2016

À LA FACULTÉ DES SCIENCES DE LA VIE
LABORATOIRE DE RECHERCHE INTÉGRATIVE DU SYSTÈME LYMPHATIQUE ET DU CANCER
PROGRAMME DOCTORAL EN BIOTECHNOLOGIE ET GÉNIE BIOLOGIQUE

ÉCOLE POLYTECHNIQUE FÉDÉRALE DE LAUSANNE

POUR L'OBTENTION DU GRADE DE DOCTEUR ÈS SCIENCES

PAR

Marcela RINCÓN-RESTREPO

acceptée sur proposition du jury:

Prof. A. Radenovic, présidente du jury
Prof. M. Swartz, Dr S. Hirosue, directrices de thèse
Prof. A. Mondino, rapporteuse
Prof. P. Romero, rapporteur
Prof. B. Correia, rapporteur

ÉCOLE POLYTECHNIQUE
FÉDÉRALE DE LAUSANNE

Suisse
2016

ACKNOWLEDGEMENTS

This thesis involves the help and the input of many valuable people that made my PhD possible.

First, I would like to thank my supervisor, Melody Swartz, for her support during the last years and for transmitting me her incredible energy and passion for science. I also have to acknowledge her for the independence and trust she deposited on me, and for always generating novel ideas that strongly stimulated me. Finally, I do need to thank her for her capacity to select great people in the lab, which made work much more fun!

I also thank deeply Dr. Sachiko Hirosue, my co-advisor, for all her help, trust and encouragement during my PhD. Your support helped me to go through many good and bad moments during my thesis. Thanks for teaching me how to work in the lab and how to set up properly experiments: I learnt enormously from your rigorous scientific approach, you helped me paved the way.

To our lab assistants, Patricia Corthésy, Yassin Ben Saida, and to our secretary, Ingrid Margot; infinite thanks for managing perfectly the lab, for the preparation of all the BMDCs, for the mouse genotyping, and for their invaluable administrative help.

I am also immensely grateful to all my friends and colleagues in the LLCB lab:

The girls: Valentina Triacca, Esra Guc and Laura Jeanbart: I thank you immensely for your friendship and for being always a support and a source of smiles and happiness for me. Thanks for all the moments we shared, our trips, and our brushing sessions: they were an oasis of relaxation during the intense times of the PhD.

The guys: Manuel and Marco, you were always bringing excitement to the lab with your funny stories. Thank you for your friendship and for sharing with me awesome moments inside and outside the EPFL.

To Lambert and Sylvie: I enjoyed being your neighbor and sharing with you songs, tape, staplers, and pens; that somehow we manage always to find, despite having a messy corner!.

To the LLCB, thanks for being the best group I have ever worked!. The collaborative spirit of the team and the support from all the members helped me enormously in the progress of my thesis.

To my thesis Jury, Professor Anna Mondino, Professor Aleksandra Radenovic, Professor Pedro Romero, and Professor Bruno Correia: many thanks for accepting being part of my committee and taking the time to read and contribute to my thesis project.

I am very grateful to Shaun, Cara, Effy, Laura, Sylvie and Sachiko: thanks for taking the time to read, comment and correct my thesis draft.

To Giuseppe, for his support and encouragement, for keeping me up during all the bad moments and celebrating with me during the good times. It would have been a tough journey without you by my side.

Finally, to my family, for whom this thesis is dedicated, infinite thanks for all your unconditional support and love. Thanks for believing in me, you got me here.

ABSTRACT

Vaccines have diminished the burden and spread of infectious diseases by inducing protection against pathogens hence reducing disability and mortality. The success of standard methods of vaccination, such as immunizations with live attenuated vectors, relies on the recognition of microbial components by the innate immune system, which in turn influences the response of the adaptive immune system in order to eradicate the pathogen. However, safety concerns associated with live attenuated vectors prevented their wide application. As a consequence, subunit vaccines, composed of microbial components and proteins, have emerged to elicit protective immunity, thus offering a more simplified, safer and standardized mode of immunization.

Single components, such as proteins and immunostimulatory agents (adjuvants) are not as immunogenic as whole pathogens, and thus there is a need for novel strategies to enhance their immunogenicity. Nanoparticle carriers (<1000 nm) are a promising mean of protein and adjuvant delivery, since they enhance immune responses by protecting the antigen from early degradation, promoting antigen retention in lymphoid organs and allowing dendritic cell (DC) targeting in lymphoid organs. Considering the efficacy of nanoparticle-based systems for vaccination, our laboratory has recently developed two delivery platforms based on poly(ethylene glycol) (PEG) and poly(propylene sulfide) (PPS): nanoparticles (NPs) and polymersomes (PSs) differ in size, method of antigen loading and method of antigen release.

In this thesis, we evaluated the impact of antigen delivery by nanocarriers on the magnitude, and more importantly, on the quality of cellular and humoral responses. We first assessed how NPs modified the CD8+ T cell response to a viral MHCI epitope and demonstrated that presentation by NPs can significantly enhance the magnitude of the cellular response. Next, we asked how the quality of the cellular response differed from a standard method of immunization, a DC-based vaccine. We showed that the quality of the memory CD8+ T cells was considerably altered, with NPs promoting a robust pool of memory CD8+ T cells with an effector-like phenotype characterized by high expression of KLRG-1 and low expression of CD43, CD27 and CD62L. By contrast, DC vaccination promoted a central memory-like phenotype.

Recent work by our group showed that T cell responses induced by NPs and PSs differ significantly depending on the delivery vehicle, with NPs enhancing cytotoxic T cell responses and PS augmenting CD4+ T cells. Herein, we demonstrated that the preferential T cell activation is a consequence of distinct intracellular trafficking and differential organ biodistribution of the antigen, which is promoted by the properties of the nanocarrier. Furthermore, we found that PSs are better at enhancing CD4+ T cell activation and inducing T follicular helper (Tfh) cells, which translated in an increase in germinal center B cells, which is beneficial for the development of vaccines based on humoral responses. Based on these results, we decided to evaluate the feasibility of a PS-based vaccine for the delivery of the Lassa virus antigen, Glycoprotein 1 (LASV-GP1). Although in terms of quantity we observed no differences between the PS-loaded protein and the soluble form, our data displayed an enhancement in the quality of the antibodies elicited, which had an increased binding to

LASV-GP1 when displayed in its native conformation and displayed a broader epitope targeting.

Finally, we demonstrated that, besides classical antigen-presenting cells, non-hematopoietic stromal cells also scavenge foreign antigens. We showed that lymph node lymphatic endothelial cell (LECs) internalize and process exogenous proteins in inflammatory and non-inflammatory conditions *in vivo*. Although with our approach we could not detect the implications of LECs presentation in the functional outcome of immune responses, we hypothesize that the elucidation of the roles of LECs on the tuning of immunity will bring novel modes of immunomodulation of vaccines.

In summary, this thesis describes a comprehensive study of the adaptive immune responses generated after intradermal delivery of particulate-based vaccines. Furthermore, this thesis accomplishes the aims to establish new insights and immediately applicable guidelines for vaccine design.

Keywords:

Nanoparticles, polymersomes, antibodies, Lassa, lymph node, vaccine, quality, CD8 T cell, CD4 T cell, B cell, dendritic cell

RÉSUMÉ

Les vaccins ont diminué la prépondérance et les épidémies de maladies infectieuses en induisant une protection contre les pathogènes, réduisant ainsi la morbidité et mortalité. Le succès des méthodes standard de vaccination, telles que les immunisations avec des vecteurs vivant atténués, dépend de la reconnaissance des composants pathogéniques par le système immunitaire, qui à son tour influence la réponse immunitaire adaptative afin d'éradiquer le pathogène. Néanmoins, les soucis de sécurité associés avec les vecteurs vivant atténués n'ont pas permis une application large de ces vaccins. Par conséquent, les vaccins sous-unités, composés de composants microbiaux et protéiques, sont apparus pour induire une immunité protectrice, offrant ainsi un mode d'immunisation plus simplifié, sûr et standardisé.

Les composants uniques d'un vaccin, tels que les protéines et les adjuvants, ne sont pas aussi immunogéniques que les pathogènes entiers, donc il y a un réel besoin de nouvelles stratégies pour augmenter leur immunogénicité. Les nanovecteurs (< 1000 nm) sont un moyen prometteur pour le transport de protéines et d'adjuvants : ils peuvent augmenter les réponses immunitaires en empêchant la dégradation rapide des protéines, promouvant la rétention des antigènes dans les organes lymphoides, et permettant le ciblage des cellules dendritiques (DC) dans les ganglions lymphatiques. Au vu de l'efficacité des vaccinations basées sur les nanovecteurs, notre laboratoire a développé deux plateformes basées sur le poly(éthylène glycol) (PEG) et le poly(propylène sulfide) (PPS) : les nanoparticules (NPs) et les polymersomes (PSs) diffèrent par leur taille, la méthode de cargaison et de le livraison de l'antigène.

Dans cette thèse, nous avons évalué l'impact de la livraison antigénique par les nanovecteurs sur la magnitude et la qualité des réponses immunitaires cellulaires et humorales. Nous avons d'abord étudié comment les NPs modulent la réponse CD8+ T cellulaire face à un épitope MHCI viral et avons démontré que le chargement des NPs peut augmenter drastiquement la magnitude de la réponse cellulaire. Ensuite, nous avons demandé quelle est la différence dans la réponse cellulaire face à un vaccin basé sur les DCs, qui est un type d'immunisation standard. Nous avons montré que la qualité de la réponse CD8+ T mémoire était changée de manière drastique, les NPs promouvant des cellules T CD8+ avec un phénotype effecteur caractérisé par une fort expression de KLRG-1 et un faible marquage de CD43, CD27 et CD62L. En contraste, la vaccination DC a promu un phénotype type mémoire centrale chez les cellules T CD8+.

Les travaux récents de notre laboratoire ont montré que les réponses T induites par les NPs et PSs diffèrent de manière significative selon le vecteur, avec les NPs qui augmentent les réponses cytotoxiques et les PSs qui augmentent les réponses T CD4+. Ici, nous avons démontré que l'activation préférentielle des cellules T est une conséquence d'un trafic intracellulaire distinct et d'une biodistribution de l'antigène à travers les organes différente, qui est promue par les propriétés du nanovecteur. De plus, nous avons observé que les PSs sont de meilleurs activateurs des cellules T CD4+ et inducteurs plus efficaces des cellules T folliculaires (Tfh), ce qui s'est traduit par une augmentation des centres germinaux de

cellules B, qui sont bénéfiques pour le développement de vaccins basés sur les réponses humorales. Sur la base de ces résultats, nous avons décidé d'évaluer la faisabilité d'un vaccin PS pour la livraison de l'antigène du virus Lassa, glycoprotéine 1 (LASV-GP1). Bien qu'en terme de quantité nous avons observé aucune différence entre la protéine libre et la protéine sur les PSs, nos résultats suggèrent une augmentation de la qualité des anticorps induits par les PSs : les anticorps se liaient davantage à LASV-GP1 dans sa conformation native et ciblaient un panel plus large d'épitopes.

A la fin, nous avons aussi démontré que, en plus des cellules présentatrices d'antigène classiques, les cellules stromales hématopoiétiques pouvaient aussi pourchasser les antigènes étrangers. Nous avons montré que les cellules endothéliales lymphatiques (LECs) dans les ganglions pouvaient internaliser et digérer des protéines exogènes dans des conditions inflammatoires et homéostatiques in vivo. Même si nous n'avons pas détecté l'implication des LECs dans le résultat fonctionnel des réponses immunitaires, nous posons l'hypothèse que l'élucidation des rôles joués par les LECs dans la modulation de l'immunité forgera de nouvelles méthodes d'immunomodulation par les vaccins.

En résumé, cette thèse décrit une étude compréhensive des réponses immunitaires adaptatives générées après la livraison intradermale de vaccins basés sur des nanovecteurs. De plus, cette thèse accomplit le but d'établir de nouvelles informations et lignes directrices pour le design de nouveaux vaccins.

Mots-clefs

Nanoparticule, polymersome, anticorps, Lassa, ganglion lymphatique, vaccin, qualité, cellule T CD4+, cellule T CD8+, cellule B, cellule dendritique

TABLE OF CONTENTS

LIST OF FIGURES

CHAPTER 1

CHAPTER 2

CHAPTER 3

CHAPTER 4

CHAPTER 5

COMMON ABBREVIATIONS

NP: Nanoparticle

PS: Polymersome

OVA: Ovalbumin

LCMV: Lymphochoriomeningitis virus

LASV: Lassa Virus

LASVGP1: Lassa virus Glycoprotein 1

LN: Lymph node

DC: Dendritic cell

APC: Antigen presenting cells

Tfh: T follicular helper

LEC: Lymphatic endothelial cell

FRC: Fibroblastic reticular cells

α**R3**: anti-VEGFR3

Chapter 1 INTRODUCTION

Motivation, background and outline of the thesis

1.1 MOTIVATION

The need for subunit vaccines

It is indisputable that vaccines have diminished the burden of infectious diseases by reducing disability and mortality [1]. Vaccination has proven to be a safe and cost-effective mean of prevention of illness that has brought enormous economic benefits, especially in the developing world [2,3].

The goal of vaccines is to program the immune system to rapidly respond and protect in case of pathogen exposure. To date, the most successful vaccines are live attenuated viruses, which were developed empirically in the nineteenth-century and consist of weakened pathogens that simulate natural infection without promoting disease. The success of this type of vaccine is inherent to the pathogens used, since they encode for a broad set of immunostimulatory molecules that efficiently trigger the immune response. However, the great efficacy of these approaches comes with a safety cost, as some of these vectors regain virulence and convert into a pathogenic form [3–6]. Furthermore, for chronic diseases such as infection with human immunodeficiency virus (HIV), mimicking the natural infection is not enough to promote protection, and thus new strategies of vaccination are needed [7].

There has been enormous progress in the understanding of how vaccines and the immune system work, which has made possible the development of rationally designed vaccines. For instance, we know that innate immunity has evolved to recognize and respond to pathogens, and moreover, that it has the ability to tune the adaptive immune system in order to react in a way that eradicate the infection [8,9]. This is achieved by pattern recognition of molecules associated with microbes (pathogen-associated molecular patterns, PAMPs) through different receptors (pattern recognition receptors, PRRs), whose activation will determine the magnitude and quality of the immune response. Thus, innate immune cells, such as antigen presenting cells (APCs) not only modified the adaptive immune system through antigen presentation, but also delivering key signals for the differentiation of lymphocytes into distinct subsets (Fig1-1). In fact, live attenuated vaccines such as the yellow fever vaccine (YF-17D) and smallpox vaccine activate various PRRs that synergistically activate T cells and B cells to promote long-lasting immunity [10,11]

Understanding which components of existing vaccines enable a potent activation of the immune system made it now possible to isolate antigenic parts from a pathogen, thereby avoiding the inclusion of virulent factors that promote disease. Subunit vaccines made use of these antigenic components and thus offer a much safer, controlled and targeted mode of immunization [12,13]. Yet, the immunity induced by single pathogen components is currently not comparable to that offered by live attenuated vaccines. Subunit vaccines are usually comprised of small molecules that lack enough immunogenicity and that are rapidly cleared from the circulation, and thus their changes to encounters immune cells are limited. Consequently, parameters such as the route of administration, method of delivery, and selection of immunostimulatory compounds (adjuvants) must all be specifically tuned to enhance not only the magnitude, but also the quality of the immune response to novel subunit vaccine candidates.

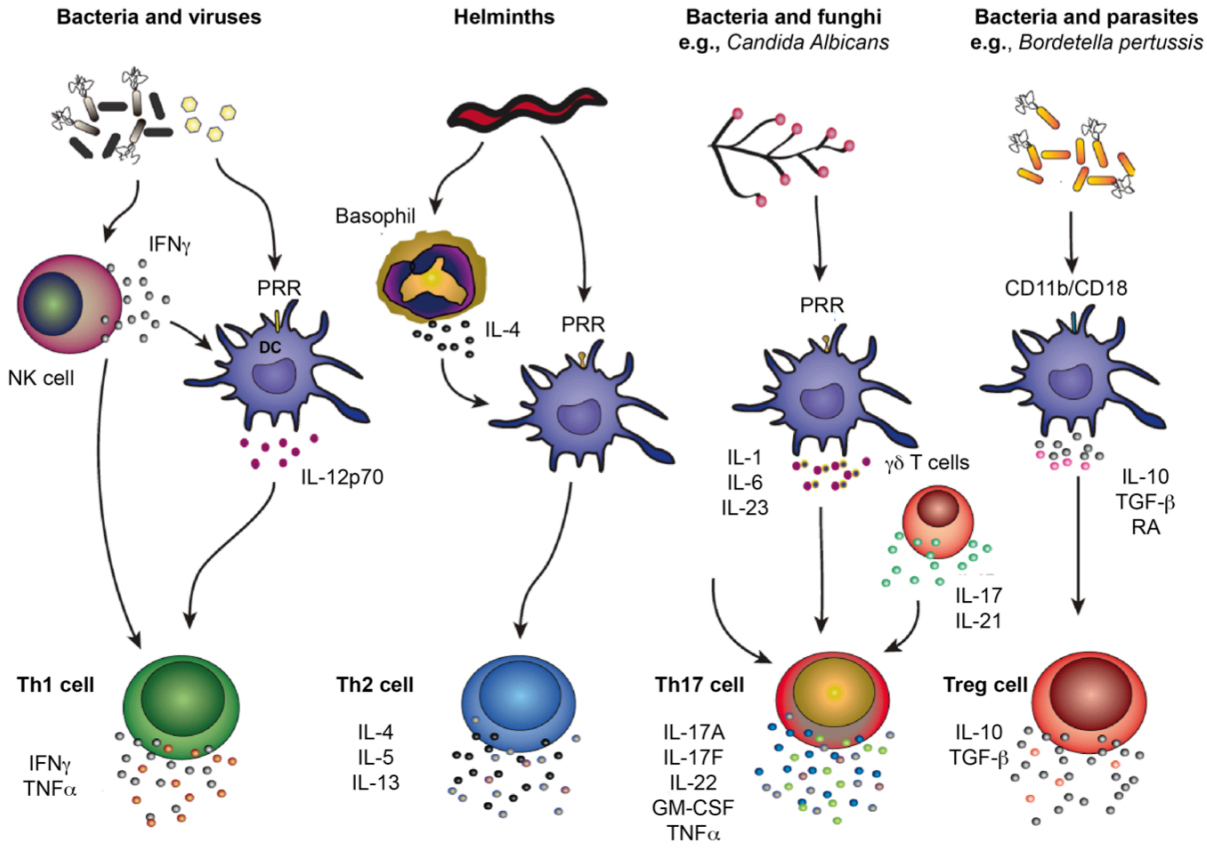

Figure 1–1 Types of helper responses promoted by pattern recognition receptors (PRRs) in innate immune cells. Antigen presenting cells, such as Dendritic cells (DCs) integrate signals from diverse pathogens through PRRs, secreting key signals that influence the type of T helper (Th) cell induced. Image adapted from [14].

Targeting Emerging diseases: Lassa fever

The Lassa virus (LASV) belongs to the *Arenaviridae* family, a rodent-borne group of viruses that are causative agents of severe hemorrhagic fevers in regions of Africa and in South America. Structurally, arenaviruses have a bisegmented negative single-stranded RNA genome, which encode for four proteins: the Glycoprotein precursor (GPC), the nucleoprotein (NP), the RNA polymerase (L) and the Matrix protein (Z). The genome is enclosed in a lipid membrane bearing trimers of the glycosylated proteins, GP1 and GP2, which interact closely with each other forming spikes that adorn the surface of the virus. GP1 and GP2 are derived from the GPC precursor: GP1 is responsible for interacting with the receptor for cell infection, whereas the GP2 is the fusion-active transmembrane protein (Fig1-2) [15–17].

Lassa hemorrhagic fever is caused by the LASV, which is endemic in countries of West Africa, mainly Sierra Leona, Guinea and Liberia. Currently, the only treatment available is an antiviral drug, Ribavirin, although it is only effective when delivered early in the course of the disease [18]. Approximately 5,000-10,000 people die yearly from Lassa fever [19]. A study from 2014 indicated that the mortality rate of patients diagnosed with the disease could reach values as high as 60%. This mortality rate was observed even after Ribavirin treatment, which suggests that current therapeutic methods for LASV are inefficient, and underscores the need for an effective vaccine or treatment [20].

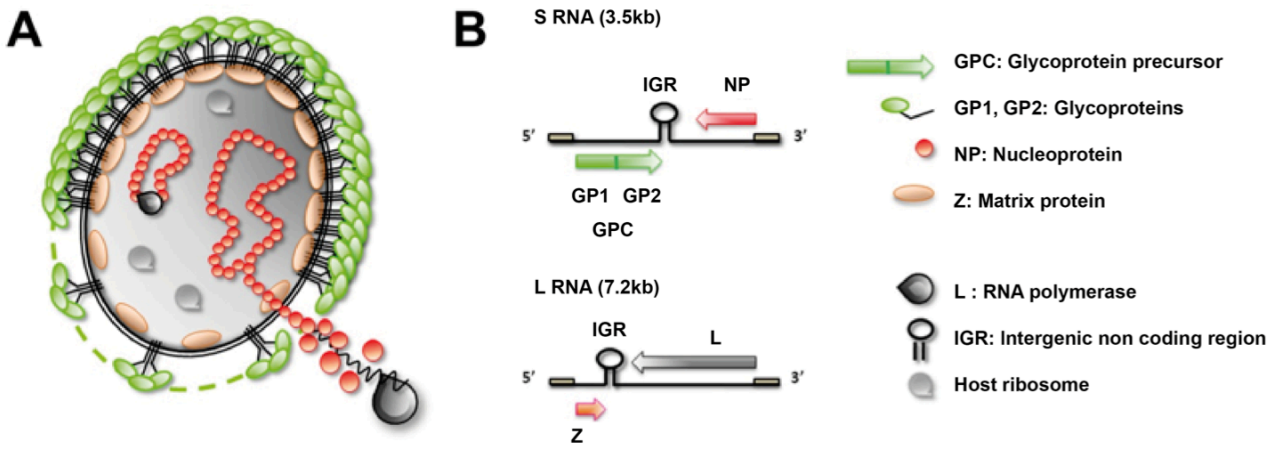

Figure 1–2 Virion structure (A) and genome organization (B) of Arenaviruses *(*Image courtesy of Clara Galan Navarro)

Vaccination with live attenuated pathogens in the zones where LASV is endemic is very improbable, mainly for safety concerns, since a large proportion of the population is immunocompromised due to the incidence of Malaria, HIV/AIDS and Tuberculosis [18]. Despite this, most of the current research towards a LASV vaccine involve live pathogens as antigen carriers [21–23], and most of the safer approaches evaluated such as virus-like particles or DNA vaccines lack the immunogenicity needed for a protective immunity[24–26]. Thus, there is an opportunity and a need to engineer a safe and effective subunit vaccine against LASV.

In order to understand the best strategy to develop a subunit vaccine against Lassa is important to consider the immune response that allows for the control of Lassa virus in subjects that survive the disease.

The recovery of Lassa patients and experimental animals has been mainly associated to CD8 T cell immunity, since antibody levels in serum during the onset of the disease do not correlate with LASV protection. In fact, high antibody titers reflect the uncontrolled levels of viremia, and represent a bad prognosis for infected patients. Moreover, studies from monkeys that recover from the infection demonstrated high levels of activated cytotoxic T lymphocytes (CTLs), compared to the monkeys that died from the disease [27] .

However, there is evidence that after the virus is cleared, neutralizing antibodies (nAbs) against the Lassa glycoprotein can develop, and more importantly, these antibodies can be protective. These antibodies can remain detectable in the blood of convalescent patients, and might prevent from a future infection. Furthermore, some reports indicate that if passive immunization with serum of convalescent patients or animals occurs early during the infection, it can prevent death [28,29]

All together, this data suggests that both arms of the immune system (i.e., cellular and humoral) are able to promote protection against LASV, although at different times, with CD8 T cells being important for controlling the disease, and antibodies preventing from acquiring a

second infection. Thus, a novel subunit vaccine might explore inducing both types of immunity for the development of a novel LASV vaccine candidate.

1.2 ENHANCING THE EFFICACY OF SUBUNIT VACCINES

Lymph node targeting of subunit vaccines to dendritic cells

The first step during an immune response is the antigen uptake by antigen presenting cells (APCs), leading to its presentation to cognate T cells. Macrophages, B cells and dendritic cells (DCs) are recognized as classical APCs, although DCs are unique in that they have the capacity to efficiently present endogenous and exogenous antigen in the context of MHCI and MHCII, thus playing a crucial role in mounting both CD8 and CD4 T cell responses [30–33]. Therefore, targeting subunits vaccines to DCs is an attractive strategy to enhance the potency of vaccines.

DCs are found in high numbers in secondary lymphoid organs (SLO) such as lymph nodes, where they are strategically located in order to maximize their encounter with lymphocytes for the initiation of the immune response [31,34]. Thus, the main events of adaptive immunity such as T cell differentiation and B cell class switching and maturation occur in lymph nodes [35]. A relatively easy method to target subunit vaccines to lymph nodes is by administering subunit vaccines through the intradermal route. In the skin, lymphatic capillaries take up macromolecules from the periphery, which reach afferent lymphatic vessels that drain to local lymph nodes [35–37]. In fact, many infections occur through this route, so the intradermal route of administration of subunit vaccines closely resembles the natural route of such infections.

Subunit vaccines may be transported to lymph nodes by migratory DCs, or may also traffic in a cell independent manner. Within the lymph nodes, subunit components are taken up by diverse DCs with specialized functions. For example, CD8α+ DCs are recognized by their capacity to process exogenous antigens and present them to CD8 T cells, a process known as crosspresentation, which is crucial for defeating intracellular viral infections. Another important subset of DCs is the CD11b+ DCs, which instead are known to promote MHCII presentation, thus enhancing CD4 responses [30,31,38,39]. As such, immune responses cannot only be enhanced by broadly targeting DCs, but can also be tuned to a specific type of immunity by targeting DC subsets using rationally designed antigen delivery systems.

Antigen delivery in Nanoparticulate platforms

Nanoparticulate carriers (<1000nm) have been widely used in the last few decades to enhance the immunogenicity of antigens, such as peptide and proteins (Table1). Nanoparticle platforms have a similar size range to that of pathogens, and are readily taken up by innate immune cells such as DCs, since these cells preferentially internalize particulate shapes. Further, nanoparticle carriers protect the antigen from early degradation, and allow for controlled release of antigen over time. This, in turn, promotes antigen retention in lymphoid organs, enhancing the chances of DCs to uptake protein or peptides and mount an immune response [37,40–42].

Particle	Description	Companies / targeted virus, diseases
LIPOSOMES	Phospholipid vesicles that allow for the encapsulation of antigen within the particle. Introduction of lipids with chemical functionalities allow also for the incorporation of antigens in the liposome surface.	**Vedantra Pharmaceuticals:** Human Papilloma virus
ISCOMs	Cage-like colloidal carriers in which antigen is incorporated. Composed of cholesterol, phospholipids and an in built adjuvant, Quil A (derived from *Quillaia* Saponin)	**CSL Behring**: Human Papilloma virus, Hepatitis C, Influenza
VIRUS-LIKE PARTICLES (VLPs)	VLPs are form from the self-assembly of viral structural proteins, derived for example from Envelope or Capsid. Represent a safer mode of vector since they lack the genetic component of the virus, and thus are not replicative. VLPs offer the advantage to present proteins on the VLP surface in their native conformation.	**Merck:** Human papilloma virus (Gardasil ®) **GSK**: Human papilloma virus (Cervarix ®), Hepatitis B virus (Engerix ®) **Crucell:** Ebola virus, Influenza, Polio, HIV **Pevion Biotech:** HIV, Influenza, Malaria, Herpes Simplex Virus, Respiratory syncytial virus **Novovax:** Respiratory syncytial virus, Influenza, Ebola virus
SYNTHETIC PARTICLES	Colloidal particles usually composed of preformed polymers or by polymerization of monomers. Synthetic particles allow for antigen incorporation within the particle, or on the surface though diverse methods of chemical conjugation.	**Selecta Biosciences**: Nicotine addiction, Malaria, type I diabetes **Liquidia Technologies:** Pneumoniae, Influenza **Vical:** Herpex virus 2,Cytomegalovirus

Table 1 Main nanoparticle based delivery systems in the clinic and preclinical development **(Information from [37,50,51])**

In addition, the design of the nanocarrier also has a drastic impact on the outcome of adaptive immunity. For instance, when particulates are delivered intradermally, the size of the carrier has a marked impact on the uptake by lymphatic capillaries, which in turn affects lymph node targeting. It is generally considered that particles between 10-50nm have an optimal size for entering the lymphatic system instead of the blood, while larger solid particles experience more resistance to lymphatic uptake, and are retained at the injection site for longer periods of time [35–37,43]. Furthermore, particle size will also determine the mechanism of cellular internalization, namely phagocytosis, macropinocytosis or receptor mediated endocytosis, which in turn impacts the type of immune response elicited [42].

The mode of antigen loading offers also another way to manipulate immune responses. Antigen may be encapsulated inside the carrier, or loaded on their surface via degradable or non-degradable covalent bonds [44–48]. For instance, surface coupling is believed to be beneficial for B cell responses, as it allows the recognition of the antigen by the B cell

receptor [44]. However, it requires further modification of the antigen, which could disrupt immunogenic sites crucial for a protective response. In spite of this, it advantageously allows for a more controlled antigen release, since the coupling may be reduction sensitive or acid labile, which allows for antigen release in endosomal compartments inside the cell [42,46,47]. Consequently, a careful selection of the antigen loading technique, particle size, and method of antigen release are factors to take into consideration for the design of particulate subunit vaccines.

Addition of TLR ligands as adjuvants

Activation of T cells not only requires antigen presentation through MHC molecules. In fact, T cells must encounter an APC that displays multiple signals: Signal 1 is the interaction between the cognate TCR receptor with the APC via peptides-MHC complexes, signal 2 is the engagement of costimulatory receptors on T cells by their ligands presented on APCs, and signal 3 is the inflammatory stimulus that instructs T cell behavior [13,14,30,33].

All three signals are strongly modulated by the addition of adjuvants that augment and tune the adaptive immune response. In fact, adjuvants are a crucial components of subunit vaccines, as their activity will direct the immune response towards particular phenotypes, which is highly important since diverse pathogens require different types of immunity [7,37,52–54].

Toll like receptors (TLRs) ligands are compounds that stimulate TLRs, a family of PRRs that sense a broad range of conserved patterns found in pathogens. The stimulation of TLRs initiates a signaling cascade of events that results in a variety of cell responses, including the secretion of pro-inflammatory cytokines that orchestrate adaptive immunity [8,9,55,56.]

Among various TLRs, TLR3, TLR-4, TLR-7/8 and TLR-9 ligands are well-documented and recognized modulators of vaccine efficacy. These ligands are known to promote Th1 biased immune responses, characterized by the presence of cytokines such as IFNγ and TNFα, which are important for the elimination of viruses and intracellular pathogens (Fig1-1) [55].

TLR3 ligands are double stranded RNA that is produced during the replication of viruses within cells, and also during cell damage. Poly I:C are synthetic RNAs that resemble TLR3 ligands, and are potent inducers of IL-12 and type I interferons. Administration of TLR3 ligands in vaccine formulations promotes a strong activation of NK cells, as wells as potent antigen crosspresentation, thus enhancing the generation of cytotoxic CD8 T cells. However, Poly I:C ligands are in general not well tolerated and might promote toxic side effects [55]

The ligands for TLR-4 are bacterial lipopolysaccharides (LPS) that display potent immunostimulatory properties. Monophosphoryl lipid A (MPLA) is a derivative of LPS, which has a much safer profile while still retaining its immunomodulatory properties [55,57]. MPLA is known to be very effective at promoting both CD8 and CD4 T cell responses, as well as inducing long lasting humoral responses [58–61]. Currently, MPLA is used as the adjuvant in two vaccines approved for their use against human papilloma virus (HPV) and HBV (Cervarix® and Fendrix®). MPLA is also studied for use in clinical vaccine candidates against malaria and tuberculosis [2,7].

TLR-9 ligands are synthetic oligonucleotides containing CpG motifs, which mimic bacterial DNA. CpG-B (CpG ODN) is perhaps the most used and best-characterized type of TLR-9 agonist [55,57]. When delivered in combination with soluble antigens or added to standard vaccine formulations, it enhances the magnitude and the quality of immune responses, and promotes long lasting cellular and humoral responses [58,62–65]. CpG-B acts on a broad range APCs, improving antigen uptake and presentation as well as cytokine secretion (IL6, TNF-α, IFN-γ and IL-12) [57,66–69]. Preclinical studies also demonstrate that this adjuvant has a good safety profile, thus marking CpG-B as a very promising immunomodulatory agent [57,69].

TLR-7 and TLR-8 (TLR-7/8) are structurally similar, and play important roles in the response to viral infections. Both receptors recognize single stranded RNA as well as synthetic base analogs [70,71]. In humans, TLR-7/8 are expressed in almost all types of DCs, which make them attractive for their implementation in vaccine formulations [72]. Synthetic agonists of TLR-7/8 such as imidazoquinolines are known for being strong potentiators of antiviral and antitumoral T cell responses [60,73–76] . There are two synthetic activators of TLR-7 and TLR7/8, Imiquimod and Resiquimod, which are approved for topical in use in humans against viral infections and skin cancers[72].

Blockade of tolerogenic signals

In addition to typical APC-mediated routes of antigen presentation, “atypical” modes of antigen presentation by non-hematopoietic cells have recently been described. In LNs, there are four populations described on the basis of CD31 and Podoplanin (gp38) expression. The subclasses are fibroblastic reticular cells (FRCs), lymphatic endothelial cells (LECs), blood endothelial cells (BECs) and a group of double negative cells (DN, CD31-gp38-) that groups perycites and a subset of undefined cells [31,33].

These stromal cell subsets have been demonstrated to upregulate MHCI and MHCII upon exposure to an inflammatory stimuli [77], and are also able to present antigen to T cells. However, the consequences of antigen presentation by these subsets have mainly tolerogenic implications. For this reason, stromal cells are currently acknowledged as one of the main components of peripheral tolerance, as their constant MHCI and MHCII presentation promotes T cell deletion and maintenance of regulatory T cells [78–84].

A potential benefit for enhancing the efficacy of subunit vaccines is to reduce tolerogenic signals that might dampen immunogenic responses. In the field of cancer immunology this concept has been widely studied. For example, co-administering cancer vaccines with blocking antibodies targeted against inhibitory receptors expressed on T cells enhances the anti-tumorigenic immune responses[85]. Therefore, strategies to inhibit or reduce tolerogenic signals derived from stromal cells might serve as a novel stroma-targeting immunotherapy, in order to increase the effectiveness of subunit vaccines. This is a strategy that has been previously suggested, but that is mostly unexplored, although it has the potential to bring novel opportunities to the field of vaccinology.

1.3 AIMS OF THE THESIS

Our group has recently developed two nanocarriers based on Polyethylene glycol (PEG) and propylene sulfide (PPS), called Nanoparticles (NPs) and Polymersomes (PSs), which differ in size, method of antigen loading and method of antigen release (Fig1-3).

In this thesis, we sought to characterize the immune response to the types of particles in order to outline which platform would be beneficial for promoting a cellular response or a humoral response, since both types of immunity are potentially beneficial for a vaccine against LASV. For this purpose, we took advantage of two well-studied antigens, the Lymphochoriomeningitis virus (LCMV) MHCI restricted peptide GP_{33-41} and the protein Chicken Egg Ovalbumin (OVA), in order to better characterize how the types of carriers modulate the magnitude and quality of the adaptive immune response.

We thus aimed at 1) establishing a particle-based vaccine able to promote long lasting memory CD8 T cell responses, 2) evaluating which particulate system promotes a higher magnitude and better quality humoral response and 3) understanding whether modulating the stroma could lead to improvements in the outcome of adaptive immune responses to vaccines employing nanoparticles. Finally, we aimed to apply these findings to develop a subunit vaccine against LASV.

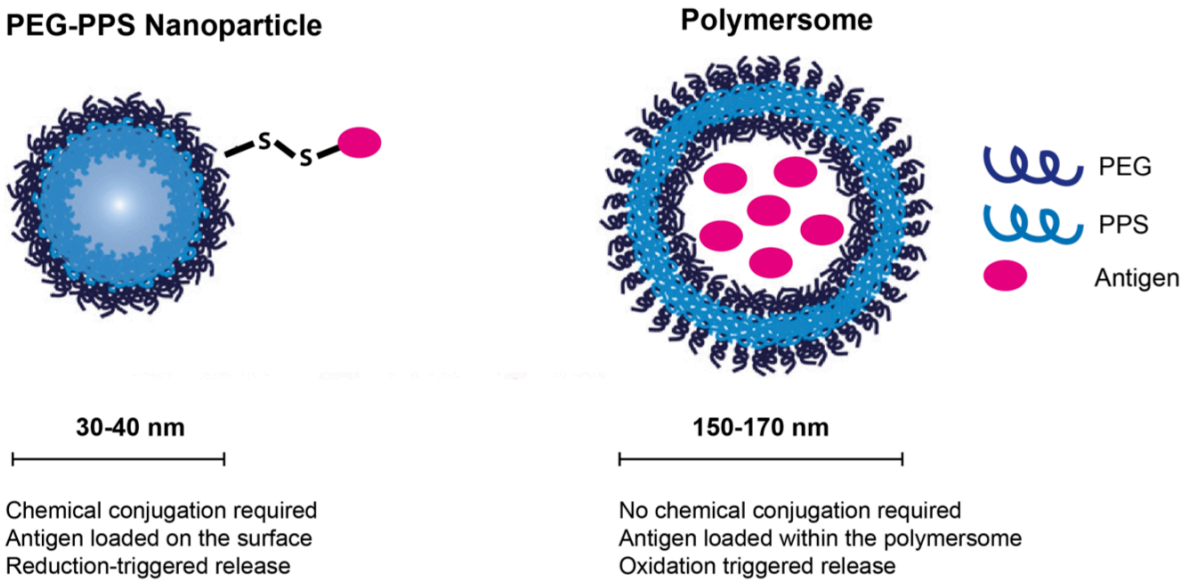

Figure 1–3 Nanoparticle-based carriers based on PEG and PPS. Left, nanoparticles, right, polymersomes. Image adapted from Stano *et al* [86].

1.4 OUTILINE OF THE THESIS

In Chapter 2, we use the nanoparticle (NP) platform for the delivery of the MHCI peptide, GP_{33-41}. We made use of the NPs since this carrier has proven to be very efficient in promoting antigen specific CD8 T cell responses, able to protect against an influenza challenge, as well to significantly enhance tumor regression and host survival in various murine tumor models [63,64,87]. Initially, we described the efficacy of NPs to stimulate CD8 T

cell responses upon intradermal delivery. We demonstrated that coupling of peptide via a reducible bond significantly enhances the number of antigen specific CD8 T cells over free peptide formulation. Furthermore, we demonstrated that the presentation of MHCI peptides in NPs promotes a functional population of memory CD8 T cells. Finally, we showed that nanoparticle loading has a strong impact on the quality of the immune response, skewing the memory CD8 T cells to an effector-like memory phenotype.

In Chapter 3, we wanted to select the platform ideal for the development of protective humoral-based responses. Thus, we compared the ability of NPs and PSs to induce good quality and long lasting CD4 T cell helper cells and antibody responses to the model antigen OVA. Since previous experiments described an enhanced capacity of PSs to promote CD4 T cell responses [86], we initially explored the mechanisms behind these observations. Our results demonstrate that the PSs promoted a distinct intracellular trafficking and a differential organ biodistribution of the antigen, which had significant consequences on the activation of CD4 T cells. Furthermore, we found remarkable differences in the quality of cellular and humoral responses, with PSs enhancing follicular T helper cells over the NPs platform, which translated in an increase in germinal center B cells and plasma cells.

In Chapter 4, we apply our findings from Chapter 3 to develop a subunit vaccine candidate against LASV, employing PSs as particle vectors owed to their capacity to promote cellular T helper responses. We demonstrated the feasibility of producing the Lassa glycoprotein 1 (LASGP1), which is hypothesized to be the target of protective antibodies. Furthermore, we showed that LASVGP1 can be encapsulated into PSs in a reproducible manner. By employing a whole-virus ELISA and a peptide microarray, we demonstrated that encapsulation of LASVGP1 protein within the PSs changes the profile of the epitopes that were recognized by serum antibodies, indicating a qualitatively enhancement of the humoral response.

In Chapter 5, we demonstrated that lymphatic endothelial cells selectively scavenge and process foreign exogenous antigen in inflammatory and non-inflammatory conditions. We also explored the feasibility to intervene with signals from the LEC stromal cell subset to modulate antigen specific CD8 T cell responses. We show that the administration of a monoclonal antibody to block the signaling through VEGFR3, one of the main receptors responsible for proliferation of LECs under inflammatory conditions, has no discernable effect on the magnitude or the quality of the elicited CD8 T cell response.

Finally, I Chapter 6 we summarize our findings, discuss about the implications of our results and present the future prospects of our studies.

1.5 REFERENCES

1. http:// www.who.int/bulletin/volumes/86/2/07-040089/en/
2. Rappuoli, R., Mandl, C. W., Black, S. & Gregorio, E. De. Vaccines for the twenty-first century society. *Nat. Rev. Immunol.* **11,** 865–872 (2012).
3. Hilleman, M. R. Vaccines in historic evolution and perspective: a narrative of vaccine discoveries. *Vaccine* **18,** 1436–1447 (2000).
4. Plotkin, S. a. & Plotkin, S. L. The development of vaccines: how the past led to the future. *Nat. Rev. Microbiol.* **9,** 889–893 (2011).
5. Siegrist, C. Vaccine immunology 2. **22,** 14–32 (2008).
6. Draper, S. J. & Heeney, J. L. Viruses as vaccine vectors for infectious diseases and cancer. *Nat. Rev. Microbiol.* **8,** 62–73 (2010).
7. Pulendran, B. & Ahmed, R. Immunological mechanisms of vaccination. *Nat. Immunol.* **131,** 509–517 (2011).
8. Kawai, T. & Akira, S. Toll-like Receptors and Their Crosstalk with Other Innate Receptors in Infection and Immunity. *Immunity* **34,** 637–650 (2011).
9. Takeuchi, O. & Akira, S. Pattern Recognition Receptors and Inflammation. *Cell* **140,** 805–820 (2010).
10. Querec, T. *et al.* Yellow fever vaccine YF-17D activates multiple dendritic cell subsets via TLR2, 7, 8, and 9 to stimulate polyvalent immunity. *J. Exp. Med.* **203,** 413–424 (2006).
11. Dc, W., Quigley, M., Martinez, J., Huang, X. & Yang, Y. A critical role for direct TLR2-MyD88 signaling in CD8 T-cell clonal expansion and memory formation following vaccinia viral infection. *Blood* **113,** 2256–2264 (2013).
12. Moyle, P. M. & Toth, I. Modern Subunit Vaccines: Development, Components, and Research Opportunities. *ChemMedChem* **8,** 360–376 (2013).
13. Burchill, M. a. *et al.* T cell vaccinology: Exploring the known unknowns. *Vaccine* **31,** 297–305 (2013).
14. Walsh, K. P. & Mills, K. H. G. Dendritic cells and other innate determinants of T helper cell polarisation. *Trends Immunol.* **34,** 521–530 (2013).
15. Clegg, J. C. Current progress towards vaccines for arenavirus-caused diseases. *Vaccine* **10,** 89–95 (1992).
16. Eschli, B. *et al.* Identification of an N-terminal trimeric coiled-coil core within arenavirus glycoprotein 2 permits assignment to class I viral fusion proteins. *J. Virol.* **80,** 5897–907 (2006).
17. Botten, J. *et al.* A multivalent vaccination strategy for the prevention of Old World arenavirus infection in humans. *J. Virol.* **84,** 9947–9956 (2010).
18. Ölschläger, S. & Flatz, L. Vaccination Strategies against Highly Pathogenic Arenaviruses: The Next Steps toward Clinical Trials. *PLoS Pathog.* **9,** e1003212 (2013).
19. Lukashevich, I. S. Advanced vaccine candidates for Lassa Fever. *Viruses* **4,** 2514–2557 (2012).
20. Shaffer, J. G. *et al.* Lassa Fever in Post-Conflict Sierra Leone. *PLoS Negl. Trop. Dis.* **8,** e2748 (2014).
21. Safronetz, D. *et al.* A Recombinant Vesicular Stomatitis Virus-Based Lassa Fever Vaccine Protects Guinea Pigs and Macaques against Challenge with Geographically and Genetically Distinct Lassa Viruses. *PLoS Negl. Trop. Dis.* **9,** e0003736 (2015).

22. Jiang, X. *et al.* Yellow fever 17D-vectored vaccines expressing Lassa virus GP1 and GP2 glycoproteins provide protection against fatal disease in guinea pigs. *Vaccine* **29,** 1248–1257 (2011).
23. Fisher-Hoch, S. P., Hutwagner, L., Brown, B. & McCormick, J. B. Effective vaccine for lassa fever. *J. Virol.* **74,** 6777–6783 (2000).
24. Branco, L. M. *et al.* Lassa virus-like particles displaying all major immunological determinants as a vaccine candidate for Lassa hemorrhagic fever. *Virol. J.* **7,** 279–298 (2010).
25. Rodriguez-Carreno, M. P. *et al.* Evaluating the immunogenicity and protective efficacy of a DNA vaccine encoding Lassa virus nucleoprotein. *Virology* **335,** 87–98 (2005).
26. Mccormick, J. B. Towards a human Lassa fever vaccine. *Rev. Med. Virol.* **11,** 331–341 (2001).
27. Yun, N. E. & Walker, D. H. Pathogenesis of Lassa Fever. *Viruses* **4,** 2031–2048 (2012).
28. Russier, M., Pannetier, D. & Baize, S. Immune responses and Lassa virus infection. *Viruses* **4,** 2766–85 (2012).
29. http://vhfc.org/lassa_fever
30. Mildner, A. & Jung, S. Development and function of dendritic cell subsets. *Immunity* **40,** 642–656 (2014).
31. Turley, S. J., Fletcher, A. L. & Elpek, K. G. The stromal and haematopoietic antigen-presenting cells that reside in secondary lymphoid organs. *Nat. Rev. Immunol.* **10,** 813–825 (2010).
32. Vyas, J. M., Van der Veen, A. G. & Ploegh, H. L. The known unknowns of antigen processing and presentation. *Nat. Rev. Immunol.* **8,** 607–618 (2008).
33. Kambayashi, T. & Laufer, T. M. Atypical MHC class II-expressing antigen-presenting cells: can anything replace a dendritic cell? *Nat. Rev. Immunol.* **14,** 719–730 (2014).
34. Malhotra, D., Fletcher, A. L. & Turley, S. J. Stromal and hematopoietic cells in secondary lymphoid organs: Partners in immunity. *Immunol. Rev.* **251,** 160–176 (2013).
35. Irvine, D. J., Hanson, M. C., Rakhra, K. & Tokatlian, T. Synthetic Nanoparticles for Vaccines and Immunotherapy. *Chem. Rev.* (2015). doi:10.1021/acs.chemrev.5b00109
36. Reddy, S. T. *et al.* Exploiting lymphatic transport and complement activation in nanoparticle vaccines. *Nat. Biotechnol.* **25,** 1159–1164 (2007).
37. Irvine, D. J., Swartz, M. a & Szeto, G. L. Engineering synthetic vaccines using cues from natural immunity. *Nat. Mater.* **12,** 978–990 (2013).
38. Joffre, O. P., Segura, E., Savina, A. & Amigorena, S. Cross-presentation by dendritic cells. *Nat. Rev. Immunol.* **12,** 557–569 (2012).
39. Merad, M., Sathe, P., Helft, J., Miller, J. & Mortha, A. The dendritic cell lineage: ontogeny and function of dendritic cells and their subsets in the steady state and the inflamed setting. *Annu. Rev. Immunol.* **31,** 563–604 (2013).
40. Smith, D. M., Simon, J. K. & Baker, J. R. Applications of nanotechnology for immunology. *Nat. Rev. Immunol.* **13,** 592–605 (2013).
41. Zhao, L. *et al.* Nanoparticle vaccines. *Vaccine* **32,** 327–337 (2014).
42. Petros, R. a & DeSimone, J. M. Strategies in the design of nanoparticles for therapeutic applications. *Nat. Rev. Drug Discov.* **9,** 615–627 (2010).
43. Bachmann, M. F. & Jennings, G. T. Vaccine delivery: a matter of size, geometry, kinetics and molecular patterns. *Nat. Rev. Immunol.* **10,** 787–796 (2010).
44. Moon, J. J. *et al.* Enhancing humoral responses to a malaria antigen with nanoparticle vaccines that expand Tfh cells and promote germinal center induction. *Proceedings of*

the National Academy of Sciences of the United States of America **109,** 1080–1085 (2012).

45. Hirosue, S., Kourtis, I. C., van der Vlies, A. J., Hubbell, J. a & Swartz, M. a. Antigen delivery to dendritic cells by poly(propylene sulfide) nanoparticles with disulfide conjugated peptides: Cross-presentation and T cell activation. *Vaccine* **28,** 7897–906 (2010).
46. Li, H., Li, Y., Jiao, J. & Hu, H.-M. Alpha-alumina nanoparticles induce efficient autophagy-dependent cross-presentation and potent antitumour response. *Nat. Nanotechnol.* **6,** 645–650 (2011).
47. Manolova, V. *et al.* Nanoparticles target distinct dendritic cell populations according to their size. *Eur. J. Immunol.* **38,** 1404–1413 (2008).
48. Mueller, S. N., Tian, S. & DeSimone, J. M. Rapid and Persistent Delivery of Antigen by Lymph Node Targeting PRINT Nanoparticle Vaccine Carrier To Promote Humoral Immunity. *Mol. Pharm.* **12,** 1356–1365 (2015).
49. Cui, L., Cohen, J. a, Broaders, K. E., Beaudette, T. T. & Fréchet, J. M. J. Mannosylated dextran nanoparticles: a pH-sensitive system engineered for immunomodulation through mannose targeting. *Bioconjug. Chem.* **22,** 949–957 (2011).
50. Zhao, Q., Li, S., Yu, H., Xia, N. & Modis, Y. Virus-like particle-based human vaccines: Quality assessment based on structural and functional properties. *Trends Biotechnol.* **31,** 654–663 (2013).
51. Gamvrellis, A. *et al.* Vaccines that facilitate antigen entry into dendritic cells. *Immunol. Cell Biol.* **82,** 506–516 (2004).
52. Swartz, M. a., Hirosue, S. & Hubbell, J. a. Engineering Approaches to Immunotherapy. *Sci. Transl. Med.* **4,** 148rv9–148rv9 (2012).
53. Ahlers, J. D. & Belyakov, I. M. Memories that last forever: Strategies for optimizing vaccine T-cell memory. *Blood* **115,** 1678–1689 (2010).
54. Berzofsky, J. a, Ahlers, J. D. & Belyakov, I. M. Strategies for designing and optimizing new generation vaccines. *Nat. Rev. Immunol.* **1,** 209–219 (2001).
55. Steinhagen, F., Kinjo, T., Bode, C. & Klinman, D. M. TLR-based immune adjuvants. *Vaccine* **29,** 3341–3355 (2011).
56. Wiley, S. R. *et al.* Targeting TLRs expands the antibody repertoire in response to a malaria vaccine. *Sci. Transl. Med.* **3,** 93ra69 (2011).
57. Bode, C., Zhao, G., Steinhagen, F., Kinjo, T. & Klinman, D. M. CpG DNA as a vaccine adjuvant (author manuscript). *Expert Rev. Vaccines* **10,** 499–511 (2011).
58. Orr, M. T. *et al.* A dual TLR agonist adjuvant enhances the immunogenicity and protective efficacy of the tuberculosis vaccine antigen ID93. *PLoS One* **9,** e83884 (2014).
59. Rhee, E. G. *et al.* TLR4 ligands augment antigen-specific CD8+ T lymphocyte responses elicited by a viral vaccine vector. *J. Virol.* **84,** 10413–10419 (2010).
60. Kasturi, S. P. *et al.* Programming the magnitude and persistence of antibody responses with innate immunity. *Nature* **470,** 543–547 (2011).
61. Bershteyn, A. *et al.* Robust IgG responses to nanograms of antigen using a biomimetic lipid-coated particle vaccine. *J. Control. Release* **157,** 354–365 (2011).
62. Lin, L., Gerth, A. J. & Peng, S. L. CpG DNA redirects class-switching towards 'Th1-like' Ig isotype production via TLR9 and MyD88. *Eur. J. Immunol.* **34,** 1483–1487 (2004).
63. De Titta, A. *et al.* Nanoparticle conjugation of CpG enhances adjuvancy for cellular immunity and memory recall at low dose. *Proc. Natl. Acad. Sci. U. S. A.* **110,** 19902–19907 (2013).

64. Jeanbart, L., Ballester, M., Titta, A. De & Swartz, M. Enhancing Efficacy of Anticancer Vaccines by Targeted Delivery to Tumor-Draining Lymph Nodes. *Cancer Immunol Res* **6,** 436–447 (2014).
65. Chakarov, S. & Fazilleau, N. Monocyte-derived dendritic cells promote T follicular helper cell differentiation. *EMBO Mol. Med.* **6,** 590–603 (2014).
66. Bernasconi, N. L., Onai, N. & Lanzavecchia, A. A role for Toll-like receptors in acquired immunity: up-regulation of TLR9 by BCR triggering in naive B cells and constitutive expression in memory B cells. *Blood* **101,** 4500–4504 (2003).
67. Hou, B. *et al.* Selective utilization of toll-like receptor and Myd88 signaling in B cells for enhancement of the antiviral germinal center response. *Immunity* **34,** 375–384 (2011).
68. Gururajan, M., Jacob, J. & Pulendran, B. Toll-like receptor expression and responsiveness of distinct murine splenic and mucosal B-cell subsets. *PLoS One* **2,** e863 (2007).
69. Hennessy, E. J., Parker, A. E. & O'Neill, L. a J. Targeting Toll-like receptors: emerging therapeutics? *Nat. Rev. Drug Discov.* **9,** 293–307 (2010).
70. Schön, M. P. & Schön, M. TLR7 and TLR8 as targets in cancer therapy. *Oncogene* **27,** 190–199 (2008).
71. Diebold, S. S., Kaisho, T., Hemmi, H., Akira, S. & Reis e Sousa, C. Innate antiviral responses by means of TLR7-mediated recognition of single-stranded RNA. *Science* **303,** 1529–1531 (2004).
72. Vasilakos, J. P. & Tomai, M. a. The use of Toll-like receptor 7/8 agonists as vaccine adjuvants. *Expert Rev. Vaccines* **12,** 809–819 (2013).
73. Kastenmüller, K. *et al.* Protective T cell immunity in mice following protein-TLR7/8 agonist-conjugate immunization requires aggregation, type I IFN, and multiple DC subsets. *J. Clin. Invest.* **121,** 1782–1796 (2011).
74. Goldinger, S. M. *et al.* Nano-particle vaccination combined with TLR-7 and -9 ligands triggers memory and effector $CD8^+$ T-cell responses in melanoma patients. *Eur. J. Immunol.* **42,** 3049–3061 (2012).
75. Wille-Reece, U. *et al.* HIV Gag protein conjugated to a Toll-like receptor 7/8 agonist improves the magnitude and quality of Th1 and CD8+ T cell responses in nonhuman primates. *Proc. Natl. Acad. Sci. U. S. A.* **102,** 15190–15194 (2005).
76. Sabado, R. L. *et al.* Resiquimod as an Immunologic Adjuvant for NY-ESO-1 Protein Vaccination in Patients with High-Risk Melanoma. *Cancer Immunol. Res.* **3,** 278–287 (2015).
77. Malhotra, D. *et al.* Transcriptional profiling of stroma from inflamed and resting lymph nodes defines immunological hallmarks. *Nat. Immunol.* **13,** 499–510 (2012).
78. Cohen, J. N. *et al.* Lymph node-resident lymphatic endothelial cells mediate peripheral tolerance via Aire-independent direct antigen presentation. *J. Exp. Med.* **207,** 681–688 (2010).
79. Fletcher, A. L. *et al.* Lymph node fibroblastic reticular cells directly present peripheral tissue antigen under steady-state and inflammatory conditions. *J. Exp. Med.* **207,** 689–697 (2010).
80. Lee, J.-W. *et al.* Peripheral antigen display by lymph node stroma promotes T cell tolerance to intestinal self. *Nat. Immunol.* **8,** 181–190 (2007).
81. Lund, A. W. *et al.* VEGF-C promotes immune tolerance in B16 melanomas and cross-presentation of tumor antigen by lymph node lymphatics. *Cell Rep.* **1,** 191–199 (2012).
82. Hirosue, S. *et al.* Steady-State Antigen Scavenging, Cross-Presentation, and CD8+ T Cell Priming: A New Role for Lymphatic Endothelial Cells. *J. Immunol.* **192,** 5002–5011 (2014).

83. Baptista, a P. *et al.* Lymph node stromal cells constrain immunity via MHC class II self-antigen presentation. *Elife* **3,** 1–18 (2014).
84. Khan, O. *et al.* Regulation of T cell priming by lymphoid stroma. *PLoS One* **6,** e26138 (2011).
85. Nguyen, L. T. & Ohashi, P. S. Clinical blockade of PD1 and LAG3 — potential mechanisms of action. *Nat. Publ. Gr.* **15,** 45–56 (2015).
86. Stano, A., Scott, E. a, Dane, K. Y., Swartz, M. a & Hubbell, J. a. Tunable T cell immunity towards a protein antigen using polymersomes vs. solid-core nanoparticles. *Biomaterials* **34,** 4339–4346 (2013).
87. Nembrini, C. *et al.* Nanoparticle conjugation of antigen enhances cytotoxic T-cell responses in pulmonary vaccination. *Proc. Natl. Acad. Sci. U. S. A.* **108,** E989–E997 (2011).

Chapter 2

Nanoparticle-based vaccination augments cytotoxic T cells responses and promotes memory CD8 T cells with an effector-like phenotype

Marcela RINCON-RESTREPO, Ana Rita GONCALVES-CABECINHAS, Daniel UTZSCHNEIDER, Efhtymia VOKALI, Sachiko HIROSUE, Stefan KUNZ and Melody SWARTZ. *Article in preparation*

2.1 ABSTRACT

The induction of protective T cell mediated immunity is one of the major goals for therapeutic and prophylactic vaccines. Herein, we made use of PEG-PPS nanoparticles (NPs) developed in our group for the delivery of a synthetic peptide representing the MHCI restricted epitope GP_{33-41} derived from the Lymphochoriomeningitis virus (LCMV). We demonstrate that a prime boost homologous immunization promotes a significant increase in the magnitude of CD8 T cell responses when comparing to an unformulated peptide and to a dendritic cell-based vaccine. We show that NPs promoted a robust pool of memory CD8 T cells with an effector-like phenotype, characterized by a high expression of killer cell lectin-like receptor G1 (KLRG1) and low expression of CD43, CD27, CD127 and CD62L. The NP generated memory CD8 T cells exhibited a similar polyfunctional activity *in vivo* compared to those generated via a control dendritic cell vaccine, which displayed a central-memory like phenotype. These studies demonstrate the feasibility to use NPs for inducing robust and long lasting CD8 T cell responses, and emphasize the importance of the antigen carrier for tuning the quality and the magnitude of the immune response.

2.2 INTRODUCTION

A major goal in vaccinology is to promote protective immunity mediated by CD8 T cells. T cell immunity has been associated with pathogen control and clearance during acute viral infections, such as Epstein-Barr virus (EBV) and Influenza [1,2] . Moreover, in the case of established diseases such as human immunodeficiency virus infections (HIV), Hepatitis B (HBV) or cancer, induction of CD8 T cells is necessary for the success of the vaccine [3,4].

In therapeutic and prophylactic vaccines, the magnitude of cellular immunity elicited has been positively correlated with viral clearance and resolution of the infection [5]. Nevertheless, considering uniquely CD8 T cell frequency does not necessarily reflect the functionality of the cellular immune response, as illustrated during chronic infections, where CD8 T cells are present but are dysfunctional and unresponsive [6]. Therefore, to better predict the efficacy of vaccines, phenotypic markers have been described as qualitative correlates of protection. However, there have been discrepancies in the literature about which phenotype is beneficial for a protective immune response.

Earlier studies have described two types of memory T cells, T central memory (Tcm) and T effector memory (Tem). This nomenclature was given depending on the ability of the cells to migrate to lymphoid organs founded on the expression of chemokine receptors such as CCR7 and CD62L. Thus, Tcm cells (CD62L+ CCR7+) mainly have the ability to localize in lymphoid organs, while Tem (CD62L- CCR7-) cells tend to patrol the periphery. Tcm cells also display a higher proliferative potential compared to Tem, while Tem are characterized by a rapid effector function[7]. Joshi et al extended this phenotype to mouse by describing the quality of the immune response based on the expression of killer cell lectin-like receptor G1 (KLRG1) and the interleukin-7 (IL-7) receptor alpha chain (CD127) [8]. Starting from the observation that KLRG1+ cells undergo apoptosis and are present at very low frequencies during the memory phase, they proposed that the quality of the CD8 responses could be predicted early during the CD8 response by defining CD127+ KLRG1- as memory precursors effector cells (MPECs), and CD127-KLRG1+ as short lived effector cells (SLECs).

Therefore, it may appear that for an efficacious response, vaccines that elicit T cells with a Tcm and MPEC phenotype are preferable to those that generate a bias towards Tem, suggesting that KLRG1+ CD62L- memory cells are not involved in mediating long-term protection against pathogens. However, the data on the protective capacity of Tem/SLECs and Tcm/MPECs subsets is contradictory, and there are various reports suggesting that KLRG-1 and CD62L have limited value as biomarkers associating with long-term protection . For instance, Tem cells promoted equally or even better protection than Tcm cells in a model of Malaria and Sendai virus infection [9,10] . Moreover, in the context of cancer, CD62L-KLRG1+ CD8 T cells were the subset that correlated the best with therapeutic vaccine efficacy against established subcutaneous tumors [11] .

Recently Hikono *et al*. reported a new characterization of memory CD8 T cells responses based on the expression of the activation markers CD43 and CD27. In this classification, CD43+/-CD27+ cells resemble Tcm in their capacity to proliferate, but it was the CD43-CD27+ subset that was responsible for controlling a Sendai virus infection in the lungs [12]. However, the accuracy of this classification has been already questioned by a report by

Olson *et al* [13]. Although they found the same subsets as reported by Hikono, in his hands the effector-like memory population (CD43-CD27-) was maintained for a long time after immunization, and by means of a strong cytolitic activity, displayed much higher protective capacity than the other subsets.

Our group has developed an antigen carrier based on propylene sulfide nanoparticles (NPs). The use of this system to deliver antigens has proven to be very efficient in promoting antigen specific CD8 T cell responses, able to protect against an influenza challenge, as well to significantly enhance tumor regression and host survival in various murine tumor models [14–16]. Considering the disagreements of the literature in defining a clear correlate of protection, we wanted to deeply characterize the phenotype of the cellular response elicited upon NP immunization in order to establish in our system how the properties of NP-induced CD8 T cells are associated to the quality of the immune response.

We examined the CD8 T cell responses to the MHCI restricted epitope GP_{33-41} derived from the Lymphochoriomeningitis virus (LCMV) upon delivery in NPs. First, we demonstrate the superiority of this platform over a soluble peptide in enhancing the magnitude of CD8 T cell responses. We showed that NP vaccination also promotes the survival of a robust population of CD8 memory T cells with an effector-like phenotype, characterized by a high expression of KLRG-1, and lack of CD62L, CD43 and CD27 in a dose independent manner. *In vivo,* both DC and NP memory CD8 T cells displayed similar cytokine secretion in response to a viral challenge, although they varied in their proliferative capacity. Our future studies will examine the protection capacity of the effector-like skewed phenotype induced after the NP immunization in models of acute and chronic viral diseases, as well as the efficacy of these CD8 T cells in therapeutic cancer vaccines.

2.3 MATERIALS AND METHODS

Animals

C57BL/6 female mice, age between 8-12 weeks, were purchased from Harlan (France). Thy1.1+ P14 mice, which encode for a T cell receptor that is specific for the LCMV MCHI epitope GP_{33-41}, were obtained from the group of Pedro Romero at CHUV. All animal experiments were performed under the approval from the Veterinary Authority of the Canton of Vaud (Switzerland) according to Swiss Law.

Infections

The LCMV 53b Armstrong virus was obtained from the group of Dietmar Zehn at the CHUV. Mice were infected intraperitoneally (i.p.) with 2.5 $x10^5$ p.f.u., which initiates a systemic infection that is usually cleared during the first week post infection.

Peptide activation

GP_{33-41} (KAVYNFATC) peptide was purchased from Thermo Scientific with a purity of >95%. Peptides were activated by adding a 2-pyridylthiol group to the cysteine residue [17]. Peptide purity and activation was confirmed by analytical HPLC/MS.

Nanoparticle preparation

All chemical reagents were reagent grade and purchased from Sigma-Aldrich unless otherwise stated. Polypropylene sulfide nanoparticle (NP) synthesis was detailed previously [18]. Briefly, Pluronic F127 (surfactant, OH-PEG) and Propylene sulfide (PPS) were mixed in 10 mL of H_2O. The reaction vessel was evacuated and re-equilibrated with inert gas, and incubated for 30 min to form nanoemulsions of Pluronic encapsulating the hydrophobic PPS monomers. Next, 14.8 mg of 4-Arm initiator (synthesized in house), previously activated in 0.5 M $NaOCH_3$ (solution in MeOH), were added to the Pluronic-PPS emulsion and mixed for 15 min, after which, the addition of 60 μL of 1,8-Diazabicyclo[5.4.0]undec-7-ene (DBU) begins the polymerization of the PPS core of the emulsions. This reaction is allowed to proceed for 16 hrs under an inert gas atmosphere, and then crosslinking of the polymers is accomplished by subsequently mixing the reaction under ambient air for 2 hrs . Completed NPs were purified by dialysis against MQ H_2O for 36 hrs at room temperature, and finally filtered through a 0.22 μm membrane (Millipore Corporation). For quantification of the amount of thiols in the NPs, we used a modified Ellman's assay, using as a standard thiomalic acid.

Peptide coupling was achieved by mixing NPs with activated peptide for 16 hrs at room temperature. The reaction was monitored by measuring the absorbance at 340 nm, which represents the release of pyridyl thione from the peptide as the peptide reacts with free thiols on the NPs. NPs-peptide conjugates were purified from free antigen by size exclusion chromatography through a CL-6B Sepharose column equilibrated in physiological saline solution (Braun). Fractions containing the antigen were detected by a BCA assay (Thermo Scientific).

Before and after the coupling, the size of NPs was determined by dynamic light scattering with a Nano Zs Zetasizer (Malvern Instruments). The diameter of NPs varied between 35 nm-40 nm.

Generation of bone marrow derived DCs (BMDCs)

Bone marrow derived CD11c+ dendritic cells (BMDCs) were generated by adapting the protocol described by Lutz et al [19]. Briefly, BM cells were cultured for 8-9 days in the presence of 20ng/mL of GM-CSF, changing the medium every 3 days. After this time, CD11c+ cells constitute the 70-85% of the non-adherent population.

The activation of BMDCs *in vitro* was achieved by stimulating control and LPS treated cells with 1 μg/mL of CpG-B (Microsynth) for 16 hrs. Afterwards, the supernatants were collected and analyzed by ELISA for the quantification of secreted cytokines.

Immunizations

All vaccines were administered intradermally (i.d.) into the 4 limbs. For peptide-loaded NPs and free peptide immunization, a total of 2 μg of antigen and 10 μg of the TLR-9 agonist CpG-B (Microsynth) were injected per mouse. All NPs and peptide batches were tested for endotoxin levels using a TLR activation assay based on HEK-Blue reporter cell lines (Invivogen) before immunization. For DC immunizations, BMDCs from day 8-9 were activated overnight with 20 ng/mL of LPS. Afterwards, cells were washed with full medium and pulsed with 10 μM of peptide for 1 hour at 37°C. To be sure no free peptide remained during the immunization, cells were washed extensively (3x) and finally resuspended in physiological saline solution at the desired concentration. Shortly before the immunization, the cell slurry was mixed with CpG-B. In total, with the exception of the dosing study, each mouse received $2x10^6$ cells, together with 10 μg of CpG-B.

Adoptive transfers and cell sorting

For adoptive transfers of naive antigen specific CD8 T cells, single cell suspensions were prepared from spleens of P14 Thy1.1 mice. CD8 T cells were isolated using the EasySep™ Mouse T Cell Isolation Kit (Stemcell Technologies). Immediately after isolation, $2\text{-}5x10^4$ cells were adoptively transferred i.v. into naïve host mice. For viral challenge experiments, Thy1.1+ P14 CD8 memory T cells were isolated by flow cytometry-assisted cell sorting. $5x10^4$ cells were adoptively transferred into naïve mice.

***In vivo* and *in vitro* cytotoxic assay**

For *in vivo* cytotoxic studies, Thy1.1+ P14 cells were adoptively transferred into wild type naïve mice, and one day after mice were immunized with NPs or BMDCs loaded with peptide, as described above. Four days after the immunization, splenocytes from naïve mice (target cells) were divided in two groups: one group was left untreated, while the second group was pulsed with 10 μM of $GP_{33\text{-}41}$ for 40 min at 37°C, and then washed two times in PBS to remove any free peptide. Following this step, the half that was left untreated was stained with 0.4 μM of CFSE (low), while the half that was pulsed with peptide was stained with 4 μM of CFSE (high). Cells were mixed at 1:1 ratio, and a total of $2x10^7$ cells were injected i.v. into previously immunized mice. The following day, spleens were harvested and

the ratio between the CFSE-low and -high population within each recipient was assessed by flow cytometry as a measure of antigen-specific killing.

ELISAS

Ready-SET-go! ELISA kits for cytokine detection were purchased from eBioscience and used according to the manufacturer's instructions.

Preparation of lymph node and spleen suspensions

For preparing single cell suspensions, lymph nodes were opened with needles and digested in DMEM (1.2mM $CaCl_2$, 2% FBS, Pen/Strep) containing collagenase D (500 μg/mL). After digestion, lymph node cell suspensions were filtered through a 70μm nylon cell strainer. For spleen, single cell suspensions were prepared by mechanical disruption through a 70 μm nylon cell strainer. Splenocytes were further treated with hypotonic ammonium chloride–potassium bicarbonate buffer to lyse red blood cells.

***Ex vivo* restimulation**

Up to $3x10^6$ cells were plated in 96-well plates and cultured in 10%FBS -DMEM medium for 2 hrs at 37°C in the presence 1 μg/mL of GP_{33-41}. Following this step, 5 μg/mL of Brefeldin A were added to the culture and left for 3 additional hrs. For CD107a staining, cells were cultured together with the monoclonal antibody against CD107a and with Monensin at 2 μg/mL for 5 hrs. Finally, cells were washed in PBS prior to staining for flow cytometry.

Flow cytometry.

Up to $3x10^6$ cells were plated in 96 well plated and wash once with HBSS before staining them with a live/dead fixable dye (Life technologies) to assess cell viability. For surface staining, cells were washed once with HBSS supplemented with 0.5% bovine serum albumin (BSA, Sigma) (staining buffer) and resuspended in an antibody cocktail using monoclonal antibodies from Biolegend and eBiosciences. For intracellular staining, cells were fixed and permeabilized with the Foxp3/Transcription Factor Fixation/Permeabilization kit (eBiosciences) according to the manufacturer's instructions. Cells were stained in permeabilization buffer with a cocktail of monoclonal antibodies. After staining, cells were resuspended in staining buffer for analysis by flow cytometry.

Data collection

Flow cytometry was performed using a CyAn™ ADP (Beckman Coulter) and data were analyzed with FlowJo (Tree Star). Because of the small size of the samples, we use the non-parametric Mann-Whitney U test for statistical comparisons. A *P* value of less than 0.05 was used as an indicator of statistical significance. All data were analyzed using the GraphPad Prism 5 Software (GraphPad Software Inc.)

2.4 RESULTS

Nanoparticles-peptide vaccination augments cytotoxic and polyfunctional CD8 T cell responses compared to a soluble antigen

For peptide loading, we activated the cysteine of the GP_{33-41} peptide (GP_{33} hereafter) derived from the LCMV with a pyridyl group, as described previously by Hirosue *et al*. (Fig2-1). The reaction of NPs with thiolate groups with the activated peptide produced nanocarriers with an average concentration of 100 μM of GP_{33} loaded in a reduction-sensitive manner, which is advantageous for driving efficient cross-presentation [17].

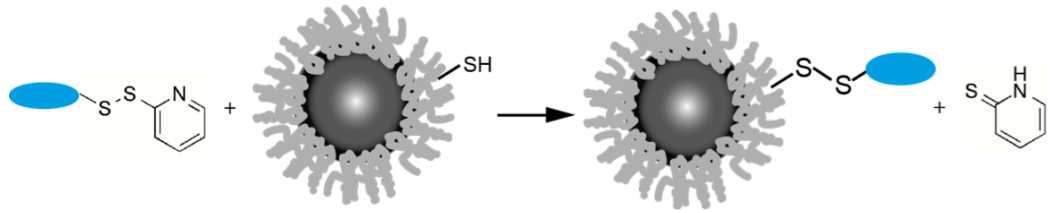

Figure 2–1 Conjugation scheme of nanoparticles to GP_{33-41}. Thiol bearing nanoparticles were incubated with 2-pyridilthiol activated peptides during 16 hours at room temperature. The reaction is followed by measuring the absorbance at 340nm corresponding to the release of the protective group in the form of pyridine thione

To determine the potential of NPs to induce CD8 T cells responses, we followed a prime-boost regime, by immunizing on day 0 and boosting on day 14 intradermally (i.d.) with NP-GP_{33} (2μg) and the unformulated peptide, together with 10μg of the TLR9 agonist CpG-B (Fig2-2, A). We choose the i.d. administration since this route allows for an easy targeting of draining lymph nodes (LNs), enabling the NPs to target various subsets of LN resident DCs [20]. We analyzed the endogenous responses by an *ex vivo* restimulation with the GP_{33} peptide 5 days after the boost, since the peak of the CD8 T cell response to NPs is observed at this time [14–16,21]. In draining LNs, the NP immunization promoted at least 3-fold higher levels of IFNγ and IFNγ TNFα by-functional cells (6.4% and 1.5%) compared to the unformulated peptide (1.9% and 0.5%), while cells secreting IFNγ, TNFα and IL-2 simultaneously were low in both immunizations (Fig 2-2, B and C). In the spleen, the NP immunization also promoted a significant enhancement of polyfunctional T cells, and furthermore, we found a 3-fold higher increase in the frequency of degranulating CD8 T cells, characterized by the expression of CD107a, a cell surface marker associated with cytotoxic activity (Fig2-2, B-D). Finally, we measured the cytokine secretion in the supernatant of cells from LNs and spleen stimulated with the GP_{33} peptide for 3 days. Similar to what we observed by flow cytometry, we found higher amounts of IFNγ and TNFα in all mice vaccinated with the NPs conjugated than those that received the free peptide (Fig2-2, E). All together, this data show that NPs promote a quantitative and qualitative enhancement of antigen specific CD8 T cells than what is obtained with a soluble antigen.

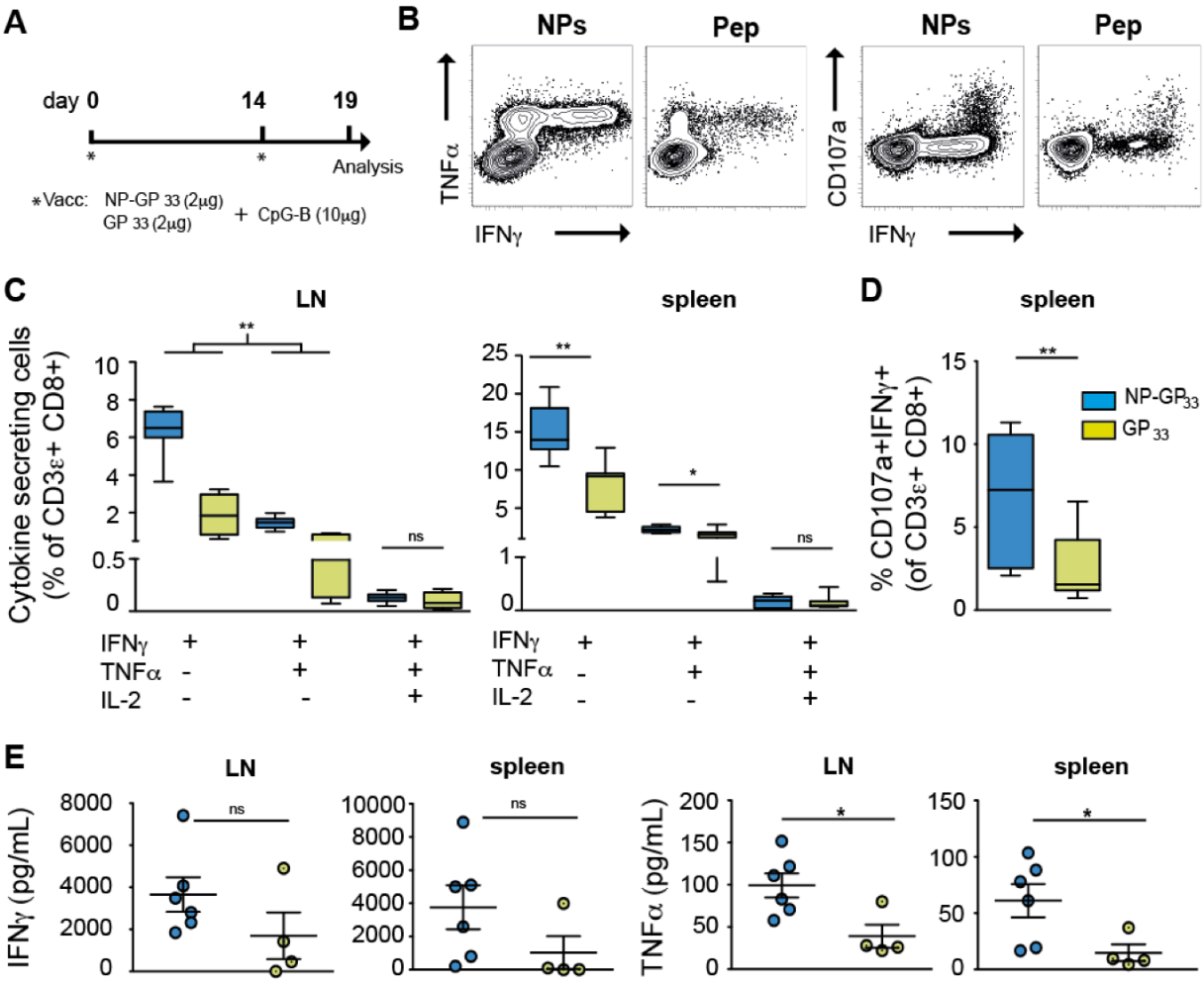

Figure 2–2 Intradermal immunization with nanoparticle-peptide conjugates enhance antigen specific CD8 T cell responses to an unformulated peptide. A) Immunization timeline and vaccination groups. **B)** Representative flow cytometry plots for the detection of polyfunctional (left) and cytotoxic (right) CD8 T cells. **C)** Cytokine-secreting CD8 T cells in spleen and draining lymph nodes five days after a prime-boost immunization with NP-GP_{33} and unformulated $GP_{33,}$ together with CpG-B. Lymphocytes were restimulated *ex vivo* with GP_{33} peptide in the presence of Brefeldin A; cytokine expression was assessed by intracellular staining. **D)** Cytotoxic activity of primed CD8 T cells in the splenocytes indicated by the presence of the degranulation marker CD107a. **E)** Lymph node and spleen lymphocytes were cultured for three days in the presence of $GP_{33;}$ IFNγ and TNFα secretion were determined by ELISA.

Nanoparticle-peptide immunization promotes a strong effector phenotype on CD8 T cells

There is little knowledge of the phenotype of the induced memory CD8 T cells upon PPS NPs immunization. Because this is the first time we characterized memory responses using this platform, we implemented as a control well-established DC vaccination [22–24] protocol. Similar to our platform, DC immunization employs MHCI peptides as antigen and can be administered i.d., together with a selected adjuvant.

DCs were obtained by culturing the bone marrow of naïve mouse for 8 days in the presence of GM-CSF, as described elsewhere [19]. For immunization, bone marrow derived DCs were activated with 20ng of LPS for 12hrs. After this time, DCs expressed high levels of

costimulatory molecules such as MHCII, CD40 and CD86 (Fig2-3,A). However, they no longer secreted detectable levels of inflammatory cytokines. Since we used TLR9 as adjuvant in this study, we evaluated whether these DCs could be reactivated after addition of CpG-B. Indeed, these cells were able to secrete TNFα and IL-6 after the addition of 1μg/mL of CpG-B, although the levels were lower than untreated BMDCs (Fig 2-3,B).

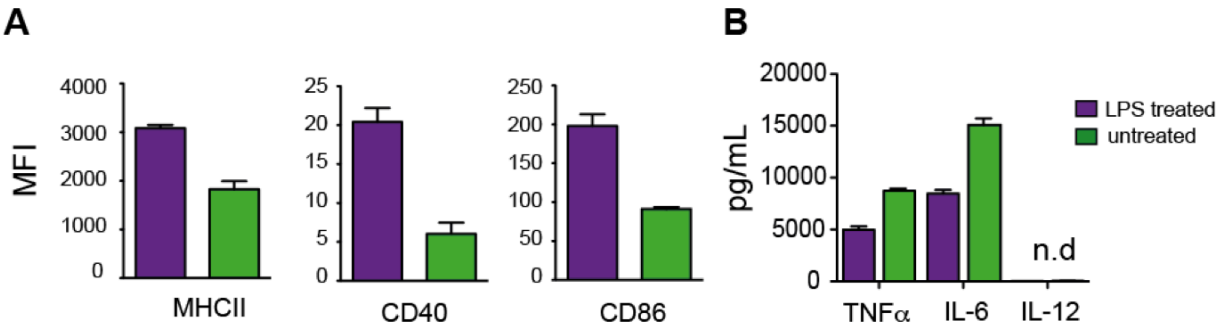

Figure 2–3 Bone marrow derived dendritic cells (BMDCs) activation *in vitro*. A) Expression of MHCII and CD40 and CD86 costimulatory molecules by BMDCs after 12 hours activation with 20ng/mL of LPS. **B)** Secretion of pro-inflammatory cytokines after 12 hours activation with 20ng/mL of LPS is partially restored upon activation with the TLR9 ligand CpG-B.

To facilitate the detection of antigen specific T cells, we transferred Thy1.1^{+} P14 (2-5x10^{4} cells), which recognize the LCMV MCHI epitope GP_{33-41}, into wild type mice. One day after the transfer, mice were immunized i.d. and boosted at day 14 with NP-GP_{33} and DCs pulsed with 10μM of GP_{33}. All formulations were given together with 10 μg of CpG-B, in order to promote the same inflammatory environment in all groups (Fig 2-4, A).

After immunization, we examined the blood, spleen and LNs at different times and compared the frequency of antigen specific cells. In blood, we observed that by day 6 the NP vaccination had promoted almost a 6-fold increase in the frequency of antigen specific CD8 T cells compared to the DC vaccine (31% vs 5.3%). By day 14, these CD8 T cells had notably contracted in both conditions, but the booster immunization generated a relative increase (between day 14 an 19) in the P14 cell frequency of 4.3% and 3.7% for NPs and DCs. This secondary response contracted in a less pronounced way, in agreement with published reports [25], and left a memory pool that made up 24.1 % (NPs) and 2.4% (DCs) of the total circulating CD8 T cell population by day 90 after the first immunization (Fig2-4, B).

To study the effect of both treatments on the CD8 T cell phenotype, we performed a longitudinal analysis in the blood circulating lymphocytes for the expression of KLRG-1 and CD127. To recapitulate, KLRG-1 and CD127 are used to correlate to the formation of terminally differentiated cytotoxic T cells, namely short lived effector cells (SLECs, KLRG1+ and CD127-), and memory precursors cells (MPECs, CD127+KLRG1-) [8]. Between day 6 and day 14, we found that CD8 T cells primed by NPs have a phenotype characterized by a dominant population of SLEC, and a smaller population of MPEC cells. The DC vaccination instead promoted larger frequencies of MPECs, which by day 14 (during the contraction phase) represented the 78.6% of the antigen specific cells. The booster immunization two

weeks after the priming promoted an increase in the SLECs in both groups, consistent with previous reports where a secondary immunization enhanced effector-like phenotype within the memory pool [13,25]. By day 90, the populations displayed similar phenotypes as that observed after the first contraction, with both groups having as the dominant population the KLRG1- CD127+ cells (36.8% and 46.9% for NP and DCs). Interestingly, the NP group had a notable percentage of KLRG1+ CD127- cells, which represented up to 29.9% of the memory pool (Fig2-4, C).

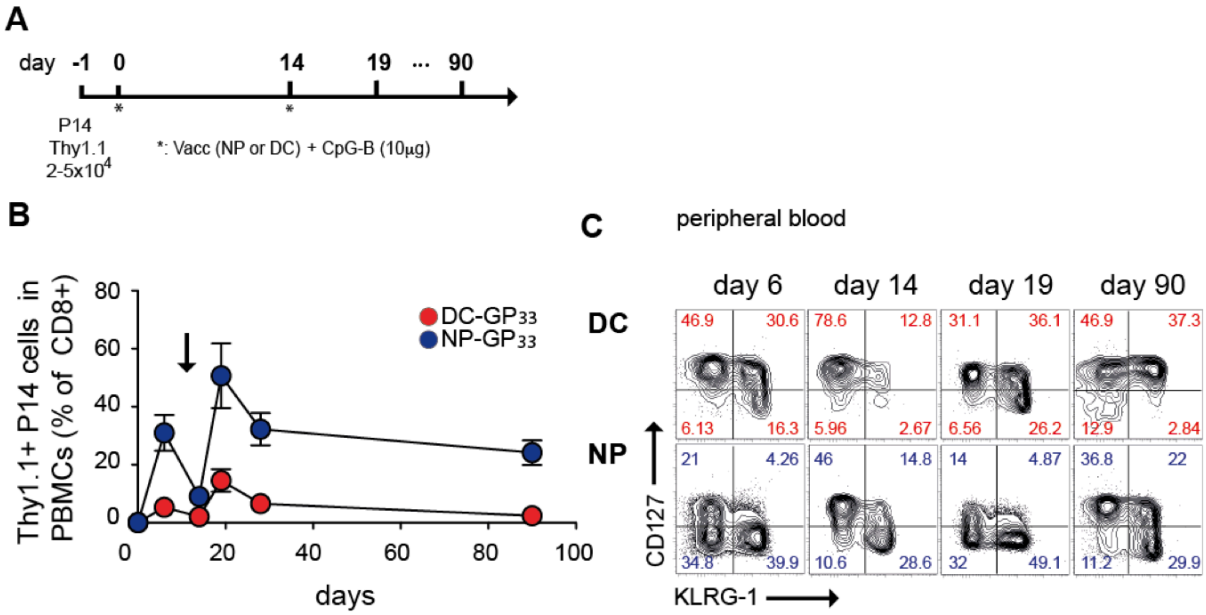

Figure 2–4 Nanoparticle-peptide and DC-peptide vaccination promote stable CD8 T cell memory pools with distinct phenotypic characteristics. **A)** Immunization timeline and vaccination groups. **B)** Frequency of Thy1.1+ P14 cells of total CD8 T cells in peripheral blood after NP-GP_{33} and DC-GP_{33} vaccination, in combination with CpG-B. The arrow indicates the time of the booster immunization. **C)** Longitudinal analysis in peripheral blood of the expression of the phenotypic markers CD127 and KLRG1 in circulating Thy1.1+ P14 cells.

To further understand how the two treatments impact the CD8 T cell response, we also compared the activation and memory differentiation phenotype in the spleen and LNs during the effector phase after the first immunization. First, we analyzed the proliferation of the CD8 T cells locally (in draining LNs) and systemically after the immunization. In LNs, the NP treatment lead to a significant increase in the number of antigen specific CD8 T cells compared to the DC immunization, while in the spleen both immunizations led to the same cell counts (Fig2-5, A).

Examination of the surface markers revealed a comparable downregulation of CD62L, while effector and activation markers such as CD44, CD27, CD43 and KLRG1 were upregulated to similar levels in both groups. Analysis of survival factors showed that IL-2Rβ chain (CD122) was equally expressed in both groups, whereas the IL-2Rα chain (CD25) and CD127 were expressed in lower levels after vaccination with NPs. Surprisingly, we found an increase in the expression of PD-1 in CD8 cells primed by NPs. PD-1 is associated with T cell

exhaustion in various chronic diseases, although it is also associated with T cell activation (Fig2-5, B) [26–28]. However, we did not observe overexpression of other co-inhibitory molecules, such as LAG-3 (data not shown).

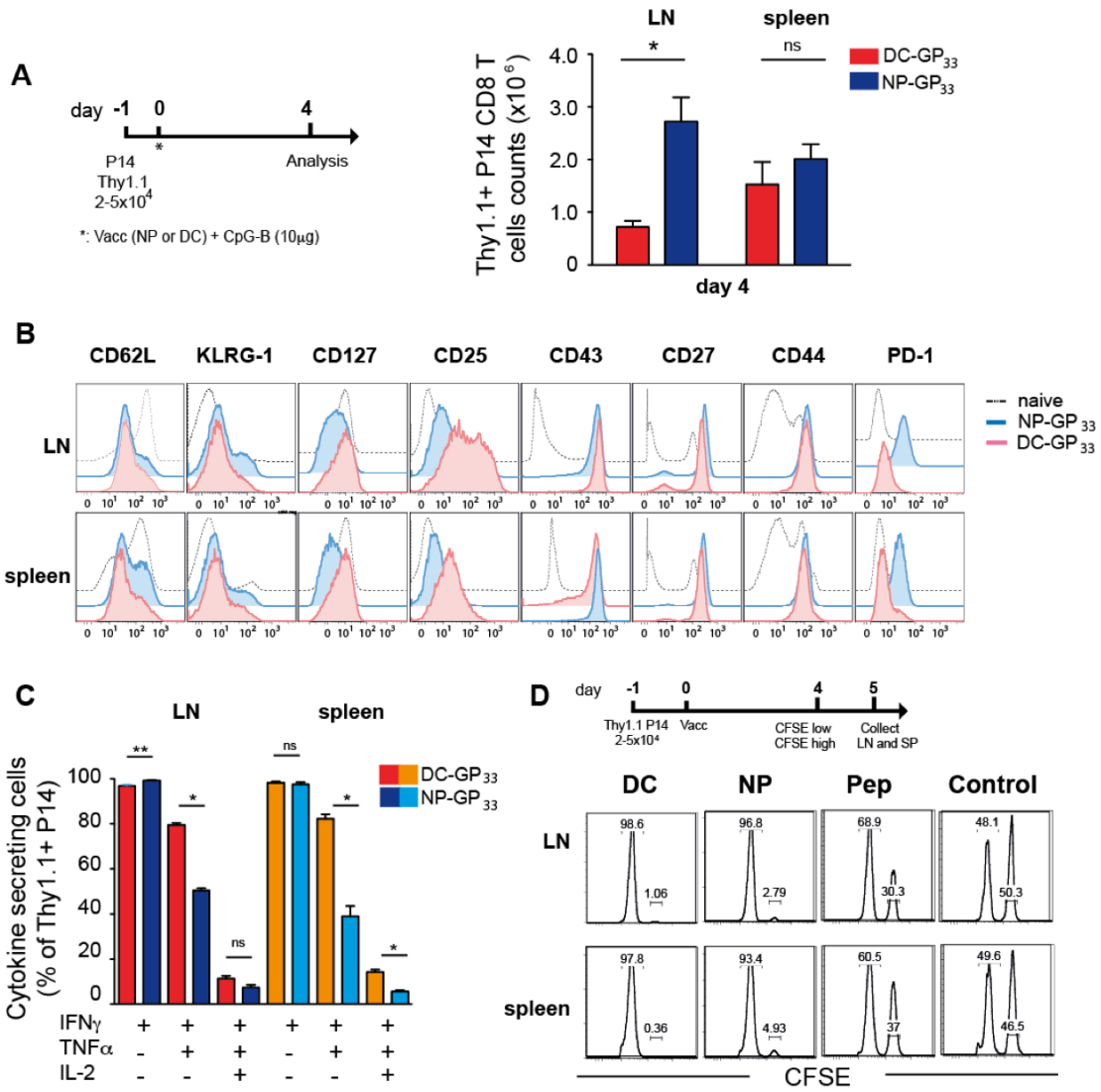

Figure 2–5 Immunization with NP-GP$_{33}$ and DC-GP$_{33}$ immunization differentially regulated effector CD8 T cells. A) Naïve mice were vaccinated on day 0 with NP-GP$_{33}$ and DC-GP$_{33,,}$ together with CpG-B, and CD8 T cell responses were evaluated on day five after immunization. NP-GP$_{33}$ promoted a strong proliferation of Thy1.1+ P14 cells in draining LNs, while DC-GP$_{33}$ promoted a better Th1.1+ P14 expansion in the spleen. **B)** Differences in the expression of markers and survival receptors between NP-GP$_{33}$ and DC-GP$_{33}$ groups at day five after immunization. **C)** Lymphocytes from lymph nodes and spleens were isolated and restimulated *ex vivo* with GP$_{33}$; cytokines were assessed by intracellular staining. **D)** In vivo cytotoxic assay; untreated (CFSE low) and GP$_{33}$ pulsed (CFSE high) splenocytes were administered intravenously (i.v.) into mice vaccinated four days early with NP-GP$_{33}$, DC-GP$_{33}$, soluble GP$_{33}$ or untreated mice. After 9 hours, splenocytes were isolated, and assessed by the presence of CFSE low and CFSE high cells.

To evaluate and compare the functionality of the CD8 T cells induced by the two treatments, we restimulated splenocytes and LNs cells *ex vivo*, and assessed their cytotoxicity and polyfunctional capacity. We observed that almost all the expanded cells secreted IFNγ in both groups, locally and systemically. However, CD8 T cells educated following NP

vaccination were less polyfunctional than those generated following DC vaccination, as observed by a decrease in the percentage of IFNγ and TNFα secreting cells, in both spleen and draining LNs (Fig2-5, C). Moreover, an *in vivo* cytotoxicity assay showed similar killing activity in both groups, as measured by the deletion of target splenocytes labeled with a high concentration of CFSE (Fig2-5, D). In summary, these data indicate that both vaccinations promoted functional CD8 T cells, albeit through distinctive activation pathways that altered their differentiation fate: NP vaccine biased towards a KLRG1+CD127- phenotype, and DC vaccine towards a KLRG1-CD127- phenotype.

Nanoparticles–peptide immunization promotes a stable pool of memory CD8 T cell with an effector-like phenotype

The goal of vaccination is to promote the generation of long-lasting memory CD8 T cells. However, there is contradictory evidence regarding which phenotype correlates the best with protective immunity. Hence, to gain a comprehensive description of the memory CD8 T cells induced by the NPs, we assessed the expression of common "central" vs "peripheral" markers, such as KLRG-1, CD62L, CD44 and CD127 [7,25,29], as well as a new scheme proposed by Hikono *et al,* and reported by others [12,13], where instead of the usual division based on the trafficking patters of the CD8 T cells, the different memory subpopulations are divided based on the expression of the activation marker CD27 and the activated glycoform of CD43.

Following vaccination with a control DC vaccine (as above) or with the NP vaccine, antigen-specific CD8 T cell responses were assessed in several organs known to harbor significant populations of immune cell infiltrates. As expected from the frequency of antigen specific CD8 T cells circulating in blood, the numbers of P14 cells residing in secondary lymphoid organs (LN, spleen) where significantly higher when vaccinating with NPs compared with DCs (Fig2-6, A).

Next, we evaluated the phenotype of P14 cells in LN, spleen, liver and lung. Interestingly, in LNs, the proportion of antigen-specific CD8 T cells expressing CD127 was similar in both groups. Likewise, both treatments promoted CD8 T cells with high expression of CD27, although the NP-primed P14 cells displayed lower frequencies of CD43 than their DC-educated counterparts (Fig2-6, B). In contrast, we found notable differences in the memory phenotype in spleen, liver and lungs. In these organs, the NP group displayed at least a 10-fold increase in the frequencies of $CD127^{low}KLRG\text{-}1^{hi}$ cells, similar to what it is observed in the blood (Fig2-6, C). There were also notable differences in the expression of CD27 and CD43. NP immunization had a memory pool dominated by a $CD43^{-}CD27^{-}$ (DN) population, while the DC vaccination promoted a much higher frequency of CD43+CD27+ (DP) cells. These populations phenotypically resembled those reported by Hikono *et al* and Olson *et al* [12,13], as the DP set express prototypical markers of central memory, and DN cells express low levels of CD62L, CD127 and high levels of KLRG-1 (Fig2-6, B-D). Although not further explored in this thesis, we observed a fourth population characterized by CD27-CD43+, which has not been previously reported in the literature. We do not believe this is an artifact from the experiment, since the population is restricted to the NP group, and was never seen in the DC treatment.

Finally, motivated by the dissimilarities in the PD-1 observed on the T cells following NP vaccination during the effector phase of the response, we evaluated whether the differences are maintained until the memory stage. Notably, almost all NP-primed specific CD8 T cells conserved PD-1 expression in both spleen and LN, while the DCs showed PD-1 levels similar to those on naïve T cells (Fig2-6, F). These results suggest that PD-1 expression was conserved from earlier activation.

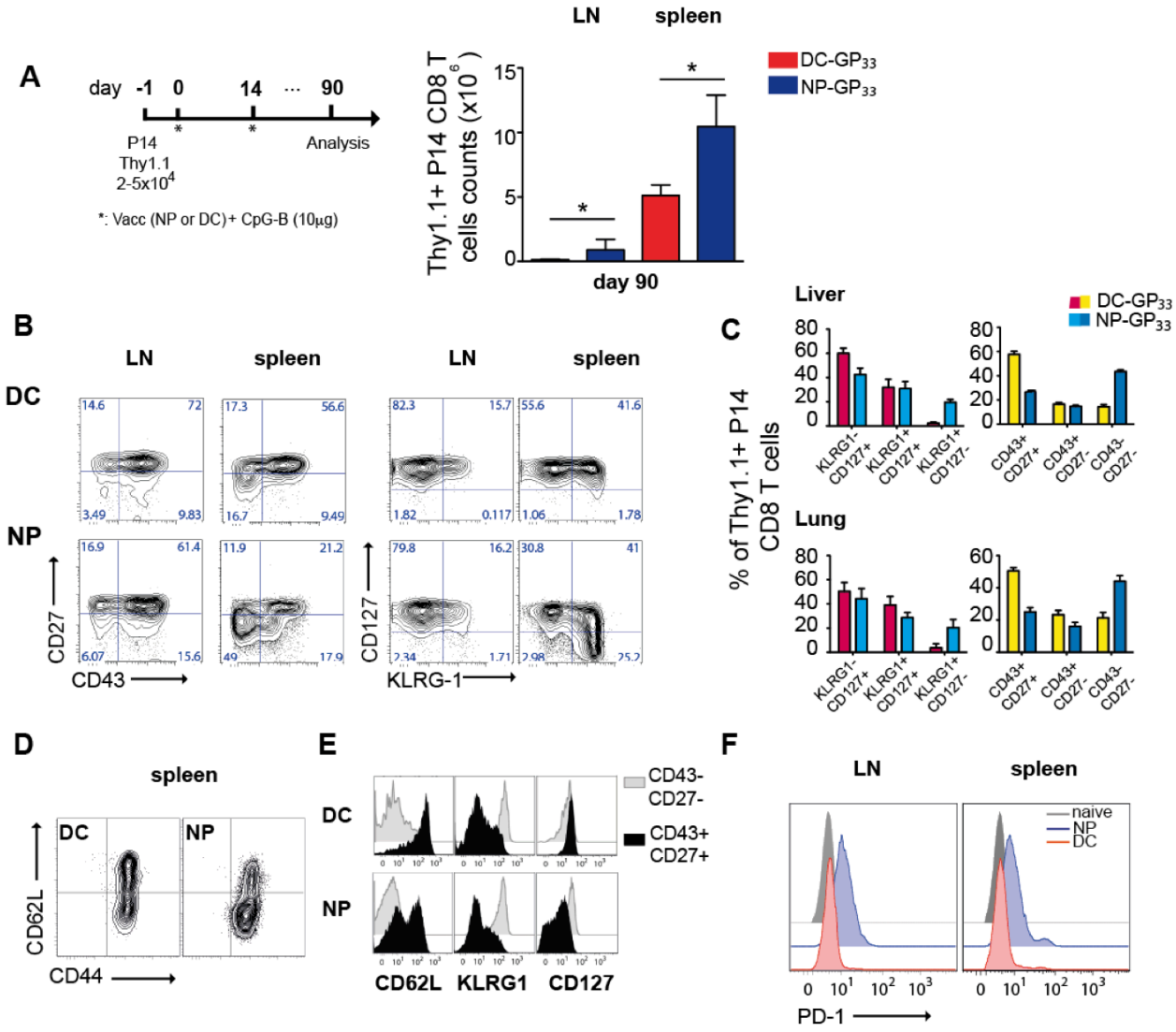

Figure 2–6 NP-GP$_{33}$ promotes an effector like phenotype upon a prime-boost immunization. A) *Left,* Immunization timeline and vaccination groups. *Right,* numbers of Thy1.1+ P14 cells in lymph nodes and spleen at day 90 after the first immunization **B-C)** Phenotype of Thy1.1+ P14 cells in secondary lymphoid organs and peripheral organs at day 90 post immunization, based on the expression of CD27 and CD43; and on the expression of CD127 and KLRG1. **D)** Comparison of the expression of CD44 and CD62L markers in splenocytes. **E)** Characterization of the CD43+CD27+ and CD43-CD27- subsets in Thy1.1+ P14 cells isolated from splenocytes based on the expression of CD62L, KLRG-1 and CD127. **F)** PD-1 expression of memory Thy1.1+ P14 cells in lymph node and spleen.

Phenotype of memory CD8 T cells responses does not depend on the antigen dose

The notable differences in the effector phenotype prompted us to evaluate whether the varying the antigen dose has an effect in instructing the CD8 T cells to adopt a certain phenotype. Therefore, we vaccinated naïve mice (which received P14 cells) with two doses of peptide (0.5μg and 5μg) conjugated onto NPs, and for the DCs we varied a) the concentration of peptide delivered to them *in vitro* or b) the number of DCs used for immunization, keeping constant the amount of pulsing peptide.

For the NP group, the numbers of antigen-specific cells varied according to the amount of antigen administered. For the DC group, the number of CD8 T cells correlated especially with the number of DCs injected, rather than with the concentration of peptide used during pulsing. However, none of the doses tested appeared to have a significant effect on the phenotype. Thus, in our system the dose has an important effect on the magnitude of the response, although it does not impact the phenotype of the CD8 T cells (Fig2-7, A-B).

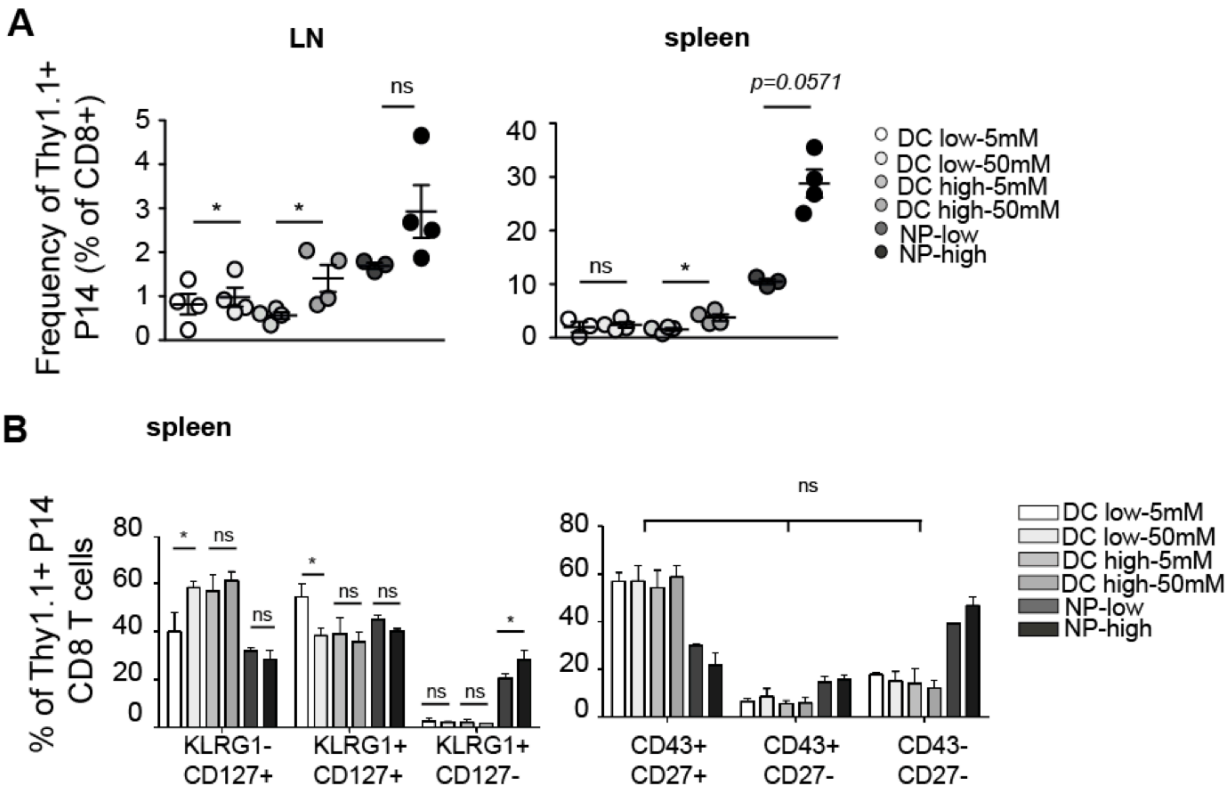

Figure 2–7. Phenotype of memory CD8 T cells upon NP-GP$_{33}$ and DC-GP$_{33}$ immunization is independent of the peptide dose and the DC-cell number administration. A) Frequency of Thy1.1+ P14 cells from total CD8 T cells in lymph nodes and spleen 90 days after the first immunization. **B)** Phenotype of Thy1.1+ P14 cells in lymph nodes and spleen based on the expression of CD27 and CD43; and on the expression of CD127 and KLRG1.

NP-induced memory CD8 T cells with high KLRG1 expression are not senescent, and respond vigorously to an *ex vivo* antigen restimulation and to an *in vivo* viral challenge

To characterize the functional properties of the two different types of memory T cells, we evaluated cytokine secretion in response to restimulation with GP_{33} *ex vivo* at day 90 (Fig2-8, A). Interestingly, in LNs, the proportion of cells with multiple cytokine secretion varied largely between both groups, despite of both memory CD8 T cells displaying a similar phenotype in this organ. NP and DC primed P14 cells were capable of strong IFNγ secretion (89% and 78%), although the NP group generated lower levels of dual-cytokine secreting cells (IFNγ and TNFα) than the DC group (62% vs 37%). In the spleen, instead, both groups displayed a similar cytokine secretion capacity as that observed earlier during the effector phase response with almost all of the cells secreting IFNγ, and a large proportion secreting both, IFNγ and TNFα (62% and 82% for NPs and DCs) (Fig2-8, B).

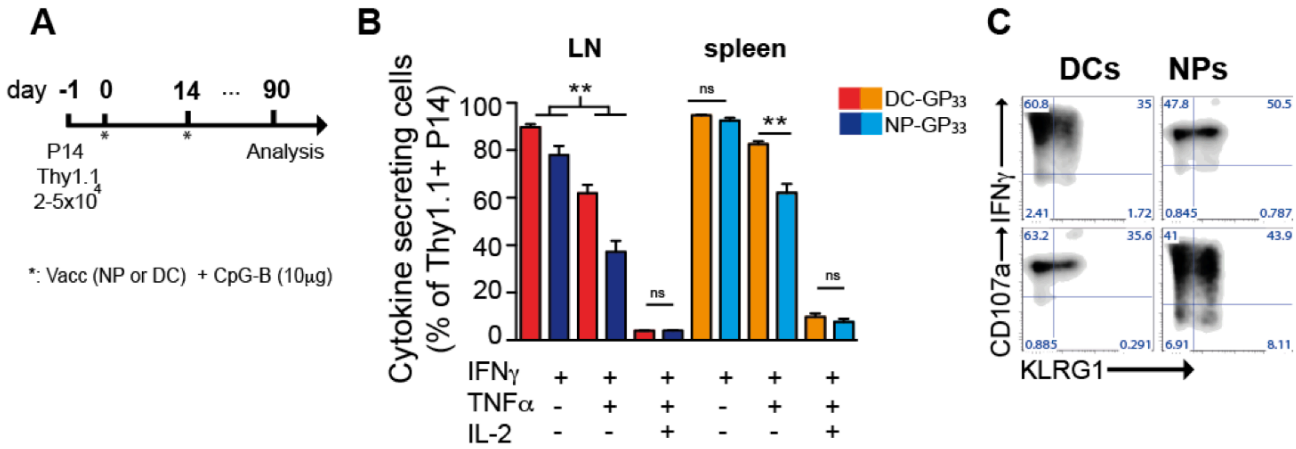

Figure 2–8 Expression of effector molecules by memory CD8 T cells after NP-GP_{33} and DC-GP_{33} immunization. **A)** Lymphocytes isolated from lymph nodes and splenocytes at day 90 after the first immunization were restimulated *ex vivo* with $GP_{33,;}$ cytokine expression was measure by intracellular staining 6 hours after restimulation in the presence of Brefeldin A. **B)** IFNγ and CD107a expression by KLRG-1+ Thy1.1+ P14 cells isolated from splenocytes. **C)** Antigen specific cytotoxicity; memory Thy1.1+ P14 cells were purified by flow-assisted cell sorting and incubated with GP_{33}-targeted splenocytes during 4 hours.

Since KLRG-1 expression has been associated with T cell senescence, we also evaluated IFNγ secretion by KLRG1+ cells, and found that in both groups, these cells can secrete IFNγ and cytokines associated with cytotoxicity equally well to the KLRG1- cell subset (Fig 2-8, C).

We also wanted to explore in a cell-based manner how memory cells in both groups responded to a viral infection. For this, we sorted Thy1.1+ P14 CD8 cells from both, the NP and DCs group, and transferred them ($5x10^4$ cells) into a naïve host. We challenged the mice with $2.5x10^5$ p.f.u. of LCMV-Arm i.p., and five days post infection evaluated the response of P14 cells by assessing proliferation, cytokine secretion and viral titers (Fig2-9,A).

Assuming that 10% of the transferred cells engraft in the spleen after the adoptive transfer [30], we detect more than 7 rounds of division in both groups. There was a two-fold higher cell

number in the cells from the DC immunization over the NPs, as expected given that DC vaccination generated a high proportion of P14 cells that resemble a Tcm- like phenotype [7,9,11–13,31,32] (Fig2-9, B). Nevertheless, we found no differences in the expression of effector molecules such as IFNγ, TNFα or GranzymeB (Fig2-9,C-D). There were also not differences in the viral burden in the kidneys between the DC and NP groups, although very low titers were also detected in the mice that did not received P14 cells (Fig2-9, E). This suggests that the WT mice are inherently capable of generating robust endogenous responses to LCMV, and thus prevented the observation of further improvements in viral clearance due to the transferred cells. It would be perhaps better to use immunodeficient mice in order to assess the protective capacity of the memory cells in the context of an infection with LCMV-Arm

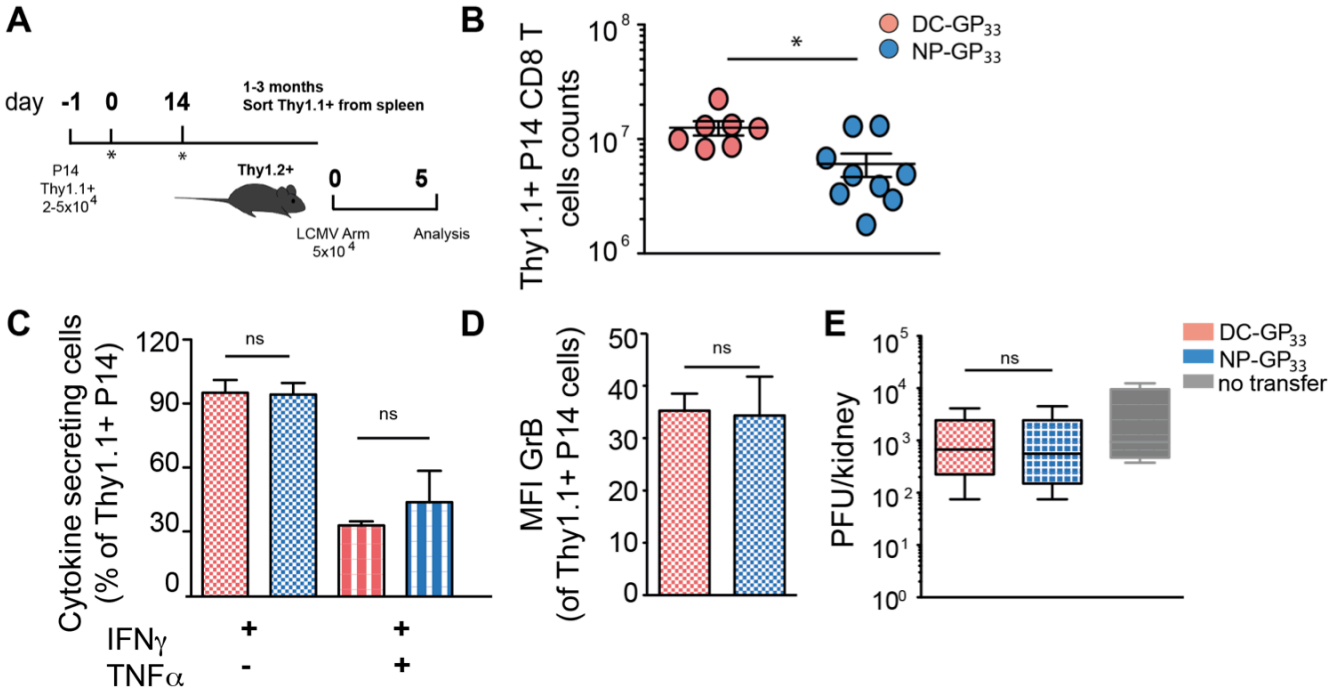

Figure 2–9. Functionality of memory Thy1.1+ P14 cells after viral challenge. A) Memory Thy1.1+ P14 were sorted and $5x10^4$ cells were administered i.v. into naïve mice and challenged with LCMV Arm ($2x10^5$ p.f.u.). **B)** Cell counts of Thy1.1+ P14 cells in splenocytes five days after viral challenge. **C)** Cytokine secretion by adoptively transferred Thy1.1+ P14 cells after viral challenge assessed by intracellular staining after *ex vivo* restimulation with GP_{33}. **D)** MFI of Granzyme B (GrB) expression by adoptively transferred Thy1.1+ P14 cells after viral challenge. **E)** Viral titers in kidneys were determined by a plaque-forming units assay five days after viral challenge

2.5 DISCUSSION

Herein, we have implemented a subunit vaccine based on the PEG-PPS nanoparticle platform for the delivery of the MHCI restricted peptide from LCMV, $GP_{33-41.}$ We have characterized the CD8 T cell response comparing to the unformulated peptide, as well as benchmarking to a well-established DC-based peptide vaccine.

We observed quantitative and qualitative differences in the CD8 T cell response. In terms of quantity, the NPs promoted a significant increase in the frequency of endogenous antigen specific CD8 T cells compared to the soluble peptide. These differences were more evident in draining LNs, which in agreement with previous reports [33–37], suggests that the NPs promote antigen retention in local draining sites, thus enhancing antigen uptake and crosspresentation by professional APCs.

Qualitatively, NPs promoted P14 cells that phenotypically resemble SLECs upon a single immunization, characterized by a strong population of KLRG1+ cells at day 6. In contrary, at this time the DC vaccine displayed a larger population of cells with MPECs characteristics. Various factors could account for these differences. For instance, it has been demonstrated that a strong and prolonged antigen presentation to CD8 T cells induces a differentiation to effector cells [5,8,10,38,39]. Thus, antigen retention, as facilitated by the NP loading, is expected to promote an effector-like phenotype, which is in agreement to what we observed in our studies.

Moreover, we speculate that a dissimilar inflammatory milieu during the T cell priming is also causing the different phenotypes observed following vaccination with NPs or DCs [8,40,41]. Although we did not measure the cytokines after the primary immune response, we infer from the activation phenotype of T cells that both T cells experience different microenvironments. For example, the expression of CD25 (the IL-R2α) is maintained by a positive feedback loop via enhanced IL-2 signals. Although IL-2 has been described to typically peak at day 1 and fade by day 3 (together with the expression of CD25) after viral infection [42], the expression of CD25 on the DC group could be indicating different IL-2 kinetics upon priming in this group. Furthermore, the capacity of NPs to target a broad range of antigen presenting cells APCs is also a factor that might influence the T cell phenotype, since migratory as well as resident DC subsets have different abilities of cross-presentation as well as unique expression of costimulatory and/or inhibitory molecules [43].

Likewise, the lack of CD4 T cell help during the immunization could have influenced the strong effector phenotype after the NP immunization. Studies in MHCII knockout mice or CD4 deficient mice have reported that unhelped memory CD8 T cells display a phenotype consistent to that of the P14 cells reported here following NP vaccination, characterized by the lack of CD62L-, CD127- , CD27-, and high levels of KLRG1 [44,45]. This, however, does not explain why the DC vaccine does not promote the same phenotype. In fact, we have observed during the *ex vivo* restimulation assay IFNγ secretion by CD4 T cells in the DC group (data not shown), while not in the NP immunization. It is likely that CD4 T cell activation could have been prompted by MHCII presentation of bovine serum peptides carried in the DCs, since this is the usual culture medium for BMDC formation.

The NP vaccination also promoted the survival of P14 cells with an effector like phenotype in the memory phase. Based on the CD43 and CD27 expression, up to 49% of the P14 cells in the spleen were CD43-CD27-, which also displayed low CD127 and CD62L levels, but high KLRG-1 expression. The survival of this effector-like memory subset has been reported in various studies that employ diverse immunization models. For instance, Hansen *et al* [39] reported that a vaccine against simian immunodefficient virus (SIV) based on a rhesus cytomegalovirus (RhCMV)- vector induced long-lived memory T cells with effector-like properties. Similarly, Reyes-Sandoval *et al* [10] described that an immunization with an adenovirus based vector encoding Malaria antigens left a memory population of effector CD8 T cells with low CD62L and CD127 expression. Interestingly, in both studies the induction of the effector-like characteristics on CD8 T cells was acknowledged to the ability of the vectors to promote persistent antigen delivery. Moreover, in both immunization models, the protection against their respective pathogen challenges correlated with the presence of the effector memory T cell subset.

We also observed an increase in PD-1 expression on NP-primed memory CD8 T cells, although no other inhibitory receptors, such as LAG-3. PD-1 is often associated with exhausted cells, however in our system, PD-1+ cells were able to respond to a booster immunization. Although the literature is clear in that not all the PD-1+ cells are exhausted, there are very few studies addressing the role of this ligand in memory differentiation [46,47]. Hokey *et al* [47] showed that peptide vaccination in macaques also drives the expression of fully active PD-1+ cells, indicating that rather than being a marker of exhaustion, PD-1 expression defines T cell activation during a primary immune response. PD-1+ cells have also been suggested to be a unique subset derived from chronic infections that have undergone a special differentiation pathway to reach a unique state where viral control is enhanced without excessively damaging the host. Since NPs promote antigen retention in the draining lymph nodes, it is likely that the antigen persistence is causing the PD-1 expression, resembling somehow a chronic infection [48].

We demonstrate that the effector memory P14 cells elicited after NP vaccination were functional and responded vigorously to an *ex vivo* antigen restimulation and a viral challenge by secreting effector molecules (IFNγ, TNFα, GrB) in similar levels to those observed by the Tcm-like memory cells induced after the DC vaccination. Although we could not evaluate which of the two subsets promoted better protection in the context of an acute LCMV infection, we hypothesized that protection against a pathogen would most likely require different types of T cell memory, and this would have to de determined on individual basis. Moreover, we conceive that establishing a correlate of protection would require a comprehensive description of the T cell memory phenotype, the magnitude of the T cell memory pool, the effector capacity of the T cells and their location in lymphoid organs and peripheral tissues.

2.6 REFERENCES

1. Van Braeckel-Budimir, N. & Harty, J. T. CD8 T-cell-mediated protection against liver-stage malaria: Lessons from a mouse model. *Front. Microbiol.* **5,** 1–9 (2014).
2. Slütter, B., Pewe, L. L., Kaech, S. M. & Harty, J. T. Lung airway-surveilling CXCR3hi Memory CD8+ T cells are critical for protection against influenza A virus. *Immunity* **39,** 939–948 (2013).
3. Seder, R. a, Darrah, P. a & Roederer, M. T-cell quality in memory and protection: implications for vaccine design. *Nat. Rev. Immunol.* **8,** 247–258 (2008).
4. Burchill, M. A. *et al.* T cell vaccinology : Exploring the known unknowns. *Vaccine* **31,** 297–305 (2013).
5. Bengsch, B. *et al.* Analysis of CD127 and KLRG1 expression on hepatitis C virus-specific CD8+ T cells reveals the existence of different memory T-cell subsets in the peripheral blood and liver. *J. Virol.* **81,** 945–953 (2007).
6. Koup, R. a, Graham, B. S. & Douek, D. C. The quest for a T cell-based immune correlate of protection against HIV: a story of trials and errors. *Nat. Rev. Immunol.* **11,** 65–70 (2011).
7. Sallusto, F., Lenig, D., Förster, R., Lipp, M. & Lanzavecchia, a. Two subsets of memory T lymphocytes with distinct homing potentials and effector functions. *Nature* **401,** 708–712 (1999).
8. Joshi, N. S. *et al.* Inflammation directs memory precursor and short-lived effector CD8(+) T cell fates via the graded expression of T-bet transcription factor. *Immunity* **27,** 281–95 (2007).
9. Roberts, A. D. & Woodland, D. L. Cutting edge: effector memory CD8+ T cells play a prominent role in recall responses to secondary viral infection in the lung. *J. Immunol.* **172,** 6533–6537 (2004).
10. Reyes-Sandoval, A. *et al.* CD8+ T effector memory cells protect against liver-stage malaria. *J. Immunol.* **187,** 1347–1357 (2011).
11. Van Duikeren, S. *et al.* Vaccine-Induced Effector-Memory CD8+ T Cell Responses Predict Therapeutic Efficacy against Tumors. *J. Immunol.* **189,** 3397–3403 (2012).
12. Hikono, H. *et al.* Activation phenotype, rather than central- or effector-memory phenotype, predicts the recall efficacy of memory CD8+ T cells. *J. Exp. Med.* **204,** 1625–1636 (2007).
13. Olson, J., McDonald-Hyman, C., Jameson, S. & Hamilton, S. Effector-like CD8+ T Cells in the Memory Population Mediate Potent Protective Immunity. *Immunity* **38,** 1250–1260 (2013).
14. Nembrini, C. *et al.* Nanoparticle conjugation of antigen enhances cytotoxic T-cell responses in pulmonary vaccination. *Proc. Natl. Acad. Sci. U. S. A.* **108,** E989–E997 (2011).
15. De Titta, A. *et al.* Nanoparticle conjugation of CpG enhances adjuvancy for cellular immunity and memory recall at low dose. *Proc. Natl. Acad. Sci. U. S. A.* **110,** 19902–19907 (2013).
16. Jeanbart, L., Ballester, M., Titta, A. De & Swartz, M. Enhancing Efficacy of Anticancer Vaccines by Targeted Delivery to Tumor-Draining Lymph Nodes. *Cancer Immunol Res* **6,** 436–447 (2014).
17. Hirosue, S., Kourtis, I. C., van der Vlies, A. J., Hubbell, J. a & Swartz, M. a. Antigen delivery to dendritic cells by poly(propylene sulfide) nanoparticles with disulfide conjugated peptides: Cross-presentation and T cell activation. *Vaccine* **28,** 7897–906 (2010).
18. Rehor, A., Hubbell, J. a. & Tirelli, N. Oxidation-sensitive polymeric nanoparticles. *Langmuir* **21,** 411–417 (2005).

19. Lutz, M. B. *et al.* An advanced culture method for generating large quantities of highly pure dendritic cells from mouse bone marrow. *J. Immunol. Methods* **223,** 77–92 (1999).
20. Kourtis, I. C. *et al.* Peripherally Administered Nanoparticles Target Monocytic Myeloid Cells, Secondary Lymphoid Organs and Tumors in Mice. *PLoS One* **8,** e61646 (2013).
21. Ballester, M. *et al.* Nanoparticle conjugation and pulmonary delivery enhance the protective efficacy of Ag85B and CpG against tuberculosis. *Vaccine* **29,** 6959–6966 (2011).
22. Badovinac, V. P., Messingham, K. a N., Jabbari, A., Haring, J. S. & Harty, J. T. Accelerated CD8+ T-cell memory and prime-boost response after dendritic-cell vaccination. *Nat. Med.* **11,** 748–56 (2005).
23. Cui, W. *et al.* TLR4 Ligands Lipopolysaccharide and Monophosphoryl Lipid A Differentially Regulate Effector and Memory CD8+ T Cell Differentiation. *J. Immunol.* **192,** 4221–4232 (2014).
24. Henrickson, S. E. *et al.* Antigen availability determines CD8+ T cell-dendritic cell interaction kinetics and memory fate decisions. *Immunity* **39,** 496–507 (2013).
25. Masopust, D., Ha, S.-J., Vezys, V. & Ahmed, R. Stimulation history dictates memory CD8 T cell phenotype: implications for prime-boost vaccination. *J. Immunol.* **177,** 831–839 (2006).
26. Wherry, E. J. *et al.* Molecular signature of CD8+ T cell exhaustion during chronic viral infection. *Immunity* **27,** 670–684 (2007).
27. Yi, J. S., Cox, M. a & Zajac, A. J. T-cell exhaustion: characteristics, causes and conversion. *Immunology* **129,** 474–481 (2010).
28. Hong, J. J., Amancha, P. K., Rogers, K., Ansari, A. a. & Villinger, F. Re-Evaluation of PD-1 Expression by T Cells as a Marker for Immune Exhaustion during SIV Infection. *PLoS One* **8,** e60186 (2013).
29. Kaech, S. M., Wherry, E. J. & Ahmed, R. Effector and memory T-cell differentiation: implications for vaccine development. *Nat. Rev. Immunol.* **2,** 251–262 (2002).
30. Blattman, J. N. *et al.* Estimating the precursor frequency of naive antigen-specific CD8 T cells. *J. Exp. Med.* **195,** 657–664 (2002).
31. Wherry, E. J. *et al.* Lineage relationship and protective immunity of memory CD8 T cell subsets. *Nat. Immunol.* **4,** 225–234 (2003).
32. Bachmann, M. F., Wolint, P., Schwarz, K. & Oxenius, A. Recall proliferation potential of memory CD8+ T cells and antiviral protection. *J. Immunol.* **175,** 4677–4685 (2005).
33. Reddy, S. T. *et al.* Exploiting lymphatic transport and complement activation in nanoparticle vaccines. *Nat. Biotechnol.* **25,** 1159–1164 (2007).
34. Reddy, S. T., Swartz, M. a & Hubbell, J. a. Targeting dendritic cells with biomaterials: developing the next generation of vaccines. *Trends Immunol.* **27,** 573–579 (2006).
35. Demento, S. L. *et al.* Biomaterials Role of sustained antigen release from nanoparticle vaccines in shaping the T cell memory phenotype. *Biomaterials* **33,** 4957–4964 (2012).
36. Moon, J. J. *et al.* Enhancing humoral responses to a malaria antigen with nanoparticle vaccines that expand Tfh cells and promote germinal center induction. *Proceedings of the National Academy of Sciences of the United States of America* **109,** 1080–1085 (2012).
37. Li, A. V *et al.* Generation of effector memory T cell-based mucosal and systemic immunity with pulmonary nanoparticle vaccination. *Sci. Transl. Med.* **5,** 204ra130 (2013).
38. Mazzucchelli, R. & Durum, S. K. Interleukin-7 receptor expression: intelligent design. *Nat. Rev. Immunol.* **7,** 144–154 (2007).

39. Hansen, S. G. *et al.* Effector memory T cell responses are associated with protection of rhesus monkeys from mucosal simian immunodeficiency virus challenge. *Nat. Med.* **15,** 293–299 (2009).
40. Obar, J. J. *et al.* Pathogen-induced inflammatory environment controls effector and memory CD8+ T cell differentiation. *J. Immunol.* **187,** 4967–4978 (2011).
41. Mueller, S. N. *et al.* Qualitatively different memory CD8+ T cells are generated after lymphocytic choriomeningitis virus and influenza virus infections. *J. Immunol.* **185,** 2182–2190 (2010).
42. Kalia, V. *et al.* Prolonged Interleukin-2R?? Expression on Virus-Specific CD8+ T Cells Favors Terminal-Effector Differentiation In Vivo. *Immunity* **32,** 91–103 (2010).
43. Joffre, O. P., Segura, E., Savina, A. & Amigorena, S. Cross-presentation by dendritic cells. *Nat. Rev. Immunol.* **12,** 557–569 (2012).
44. Intlekofer, A. M. *et al.* Requirement for T-bet in the aberrant differentiation of unhelped memory CD8+ T cells. *J. Exp. Med.* **204,** 2015–2021 (2007).
45. Edwards, L. E., Haluszczak, C. & Kedl, R. M. Phenotype and function of protective, CD4-independent CD8 T cell memory. *Immunol. Res.* **55,** 135–145 (2013).
46. Charlton, J. J. *et al.* Programmed death-1 shapes memory phenotype CD8 T cell subsets in a cell-intrinsic manner. *J. Immunol.* **190,** 6104–6114 (2013).
47. Hokey, D. a *et al.* Proliferation and Following Lentiviral Infection in Macaques. *Eur. J. Immunol.* **38,** 1435–1445 (2010).
48. Utzschneider, D. T. *et al.* T cells maintain an exhausted phenotype after antigen withdrawal and population reexpansion. *Nat. Immunol.* **14,** 603–610 (2013).

Chapter 3

Implications for the quality of cellular and humoral responses after antigen delivery on Nanoparticles and Polymersomes

Marcela RINCON RESTREPO, Aaron MAYER, Sylvie HAUERT, Sachiko HIROSUE, and Melody SWARTZ. *Article in Preparation*

3.1 ABSTRACT

Nanoparticle-based delivery systems are known to enhance the immune response to soluble antigens, thus standing as a promising tool for the development of new vaccines. In our group, we have engineered two different particulate systems in which antigen is either encapsulated in the core (polymersomes, PSs) or decorated onto the surface of nanoparticles (NPs). Previous studies demonstrated that PSs are better enhancing CD4 T cell responses, while NPs preferentially augment cytotoxic CD8 T cell responses. Herein, we demonstrated that the distinct activation of the T cell immunity reflects two modes of intracellular trafficking, as well as a differential biodistribution of the antigen in lymphoid organs, which is promoted by the properties of the nanocarriers.

Furthermore, we found that PSs promoted a better CD4 T cell activation, and induced a higher frequency of CD4 T follicular helper cells (Tfh). The differences in CD4 Tfh cell responses correlated with changes in germinal center B cells and plasma cell formation. Moreover, when evaluating the long-term antibody response, we demonstrated that both vectors promoted comparable levels of serum antigen specific IgG titers. Nevertheless, the humoral responses to both vectors varied qualitatively, with PSs skewing the antibodies towards a Th1-like phenotype, and NPs towards a Th2-like phenotype.

Taken together, these results demonstrate that nanocarriers have a deep impact on the quality of the adaptive immune response. It also suggests that PSs are a promising vector for the delivery of antigens for B cell vaccine development, since PSs promote robust CD4 Tfh cells responses and corresponding GC B cells. Additionally, it removes the need to chemically modify the antigen, which simplifies the development of new subunit vaccines.

3.2 INTRODUCTION

Vaccination is undoubtedly a major success in modern medicine, and stands as an affordable and safe technology that has allowed the control and eradication of life threatening diseases [1,2]. Yet, today there are pathogens that account for more than a million deaths annually, for which no licensed or fully protective vaccines have been created [3,4].

Development of vaccines based on subunit components has proven to be a safe and cost effective method for eliciting protection against pathogenic infections. It erases safety concern related to immunization with live attenuated viruses, and it offers the flexibility to target an specific antigen as well as to tune the quality of the response by selecting a precise immunostimulatory compound [5]. Still, the ability of subunit vaccines to stimulate an immune response is usually weaker than traditional preparations with whole-attenuated pathogens. One of the approaches used to enhance immunogenicity of subunit vaccines is antigen loading or presentation by biomaterial-based carriers, especially in particulate shapes [6–9]. Various studies have demonstrated that antigen loading into synthetic particles enhances uptake and presentation by professional presenting cells, such as dendritic cells (DCs), as well as increases antigen bioavailability by promoting antigen retention in lymphoid organs [10–16].

Our group has recently developed two nanocarriers, nanoparticles (NPs) [17,18] and polymersomes (PSs) [11,19], composed by the hydrophobic polymer Propylene sulfide (PPS), and by the hydrophilic polymer polyethylene glycol (PEG). Despite of having the same building units, both systems differ considerably between each other in their physical and chemical properties. NPs are carriers of 30-50 nm in diameter, and consist of a rubbery hydrophobic core of PPS, covered by a corona of PEG where antigen is loaded through diverse chemical ligations. Usually, proteins are attached through a disulfide bond (-ss-), as our lab has shown that a reducible bond favors crosspresentation to CD8 T cells [7]. PSs instead are formed to a minimum diameter of 150-170 nm, and constitute a vesicle surrounded by a polymeric bilayer of PEG-PPS. In such a conformation, hydrophobic compounds are loaded into the amphiphilic bilayer, while hydrophilic compounds are encapsulated into the aqueous core. This platform allows for antigen release *in vitro* in an oxidative dependent manner, which is likely happening in harsh condition inside DCs, such as those found in the lysosomes [11].

Interestingly, the difference in design between the two particulates significantly affects innate and adaptive immune responses. Recently, Stano *et al* [20] demonstrated that PSs are better at enhancing CD4 responses, while nanoparticles preferentially enhanced the induction of cytotoxic CD8 T cells. The exact mechanisms by which a particulate enhanced a specific type of response are still unknown. Based on the way antigen is presented and released to professional presenting cells, it is probable that differences in antigen processing at the cellular level account for the distinct immune responses [21]. Particle size should also impacts the lymphatic transport, as well as the nanocarrier distribution in lymphoid organs, and therefore targeting to specific DCs populations.

In this study we investigated how the model antigen chicken egg ovalbumin (OVA) formulated in NPs (NP-ss-OVA) and PSs (PS(OVA)) differ at the cellular and at the organ

level in terms of intracellular trafficking and cellular uptake. Our data demonstrates that antigen in PSs is delivered preferentially to lysosomes, while a fraction of the antigens on NPs undergo endosomal escape. At the organ level, NP-ss-OVA and PS(OVA) have a differential lymphoid organ distribution and uptake by DCs. Furthermore, we show that PS(OVA) enhanced the formation of T follicular helper CD4 responses, which correlated with an increase in germinal center cells (GCs) and plasma cell formation. These differences where reflected in the quality of the humoral response, with PS(OVA) skewing the antibodies towards a Th1-like-phenotype and NP-ss-OVA towards a Th2-like phenotype.

3.3 MATERIALS AND METHODS

Animals

C57BL/6 female mice, age between 8-12 weeks, were purchased from Harlan (France). Thy1.1+ OTII mice were obtained from an in house colony. All animal experiments were performed under the approval from the Veterinary Authority of the Canton of Vaud (Switzerland) according to Swiss Law.

Nanoparticle preparation

All chemical reagents were reagent grade and purchased from Sigma-Aldrich unless otherwise stated. Nanoparticles (NPs) were prepared as described in chapter 2, with some modifications to allow for protein loading into the PEG corona [22]. Briefly, a mixture of 1:3 COOH-PEG / OH-PEG was used to prepared the emulsion polymerization to form NPs. After exposure to air for 2 hours, the remaining thiolates were quenched by the addition of 45 mg of iodoacetamide and stirred for 15min. To functionalize the COOH groups in the NP surface, sulfo-NHS (Life Technologies), Pyridyl disulfide cysteamine (synthesized in house) and 1-Ethyl-3-(3-dimethylaminopropyl) (EDC) were added to the mixture and let to react for 24 hr. For purification, NPs were dialyzed against MQ H_20 for 36 hour at room temperature by replacing the water every 6 hrs, and passed through a filter with a 0.22 μm pore size (Millipore Corporation). The concentration of the loaded pyridyl disulfide was determined by measuring the absorbance at 340 nm after adding TCEP (ThemoScientific) to the NPs solution.

For Ovalbumin (OVA) loading, 500 μL of NPs were mixed with 286.6 mg of guanidine hydrochloride (GndHCl) to achieve a final concentration of 6M of GndHCl. The solution was filtered through a 0.22 μm membrane (Millipore Corporation) and mix with 50μL of OVA at 40 mg/mL. The mixture was left overnight at room temperature, and then purified by size exclusion chromatography through a Sepharose CL-6B column equilibrated in 50mM sodium phosphate. The concentration of OVA in the fractions obtained after purification was determined by a BCA assay following the manufacture's instructions (ThermoScientific).

Before and after the coupling, the size of NPs was determined by dynamic light scattering with a Nano Zs Zetasizer (Malvern Instruments). The diameter of NPs varied between 35 nm-40 nm.

Block-copolymer synthesis and polymersomes preparation

All chemical reagents were reagent grade and purchased from Sigma-Aldrich unless otherwise stated. Polymersomes (PSs) were prepared following the original description in [23]. Block-copolymers were synthesized using benzyl mercaptan to start the living polymerization of propylene sulfide. The terminal thiolates were capped with PEG-mesylate. For purification, the co-polymers were precipitated two times in cold methanol. The purity and length of the PPS chain were confirmed by gel chromatography and by NMR. Usually, chains of PEG_{17}-bl-$PPS_{x,}$ containing between 26-32 PPS units were used to form PSs. An amount of 30-50mg resuspended in DCM was placed in piranha-etched glass vials and desiccated overnight. For the formation of PSs, the formed thin-film of copolymer was rehydrated with a solution of 5 mg/mL of OVA or fluorescently labeled OVA in 50 mM phosphate buffer, and let

rotating for 48 hrs at room temperature. Afterwards, the solution was extruded at least 4 times through a 0.2 μm nucleopore track-etched membranes (Whatman) to obtain PSs ranging between 150 nm-170 nm, with polydispersity values lower than 0.2. Purification of the unloaded molecules was achieved by size exclusion chromatography trough a Sepharose CL-6B column. Fractions containing PSs were pull together and further concentrated though an Ultra-centrifugal filter (Millipore Corporation) with a cutoff of 100kDa. Final OVA loading was quantified by a sandwich ELISA as described by Stano *et al* [20].

The size of PSs was determined by dynamic light scattering with a Nano Zs Zetasizer (Malvern Instruments).

Immunizations and adoptive transfers

All vaccines were administered intradermally (i.d.) into the 4 limbs. 10 μg of OVA were injected per mouse for all formulations, unless otherwise stated, together with 10 μg of CpG-B (Microsynth). Before the immunizations, OVA was filtered through a 0.22μm membrane (Millipore Corporation) to remove aggregates. Furthermore, all formulations were tested for LPS contamination using a TLR activation HEK-Blue LPS detection assay (Invivogen).

For adoptive transfers of naive TCR transgenic CD4 T cells, single cell suspensions were prepared from spleens of OTII Thy1.1+ mice. CD4 T cells were isolated using the EasySep™ Mouse CD4 T Cell Isolation Kit (Stemcell Technologies). Immediately after isolation, $2x10^6$ cells were adoptively transferred i.v. into naïve host mice.

ELISAS

For the detection of antigen specific antibodies, 96-well Nunc MaxiSorp® plates were coated with 5μg/mL of OVA overnight at 4°C. Plates were washed 3 times with PBS / 0.02% Tween-20 and block using a 2.5% casein solution in PBS for 2 hours at room temperature. Serial dilutions of serum in casein were added to the blocked plates for 2h at room temperature. Plates were washed 4 times and mixed with detection antibodies against IgG1, IgG2, IgG3 or total IgG (Southern Biotech). All secondary antibodies were conjugated to horse radish peroxidase. After 1h incubation; plates were washed 4 times and developed using 50 μL of TMB (eBiosciences). Signal was stopped by adding 20μL of 2N H_2SO_4. Plates were analyzed using a plate reader spectrophotometer (Tecan) by measuring the absorbance at 450nm with correction at 570nm.

Generation of bone marrow derived DCs (BMDCs)

Bone marrow derived CD11c+ dendritic cells (BMDCs) were generated by adapting the protocol described by Lutz *et al* [24]. Briefly, BM cells were cultured for 8-9 days in the presence of 20 ng/mL of GM-CSF, changing the medium every 3 days. After this time, CD11c+ cells constitute the 70-85% of the non-adherent population.

Preparation of lymph node and spleen suspensions

For the biodistribution study, lymph nodes were opened with needles and first digested in DMEM (1.2mM $CaCl_2$, 2% FBS, Pen/Strep) containing collagenase IV (1mg/mL) and DNAse I (40 μg/ml) to isolate lymphocytes. In a second digestion step with DMEM with collagenase D (1mg/mL) and DNAse I (40 μg/ml), stromal lymph node cells were isolated for further

analysis. In the remaining experiments, lymph nodes were opened with needles and digested in DMEM (1.2mM $CaCl_2$, 2% FBS, Pen/Strep) containing collagenase D (500 μg/mL). After digestion, lymph node cell suspensions were filtered through a 70 μm nylon cell strainer. For spleen, single cell suspensions were prepared by mechanical disruption through a 70μm nylon cell strainer. Splenocytes were further treated with hypotonic ammonium chloride–potassium bicarbonate buffer to lyse red blood cells.

***Ex vivo* reestimulation**

Up to $3x10^6$ cells were plated in 96-well plates and cultured in 10%FBS -DMEM medium for 2 hours at 37°C in the presence 200 μg/mL of OVA. Afterwards, 5 μg/mL of Brefeldin A were added to the culture and left for 3 extra hours.

Flow cytometry

Up to $3x10^6$ cells were plated in 96 well plated and wash once with HBSS for staining with live/dead fixable cell viability reagent (Life technologies). For surface staining, cells were washed once with HBSS supplemented with 0.5% bovine serum albumin (BSA, Sigma) (staining buffer) and resuspended in an antibody cocktail using monoclonal antibodies.

Detection of follicular helper cells T cells was achieved in a 2-step process. First, cells were incubated with CXCR5-biotin (eBiosciences) in staining buffer for 30 min, washed once and then incubated with an antibody cocktail with Streptavidin-647 (Biolegend) and the remaining antibodies. For intracellular staining, cells were fixed and permeabilized with the Foxp3 / Transcription Factor Fixation/Permeabilization kit (eBiosciences) according to the manufacturer's instructions. After staining, cells were resuspended in staining buffer for analysis by flow cytometry.

Data collection

Flow cytometry was performed using a CyAn^{TM} ADP (Beckman Coulter) and data were analyzed with FlowJo (Tree Star). We used the non-parametric Mann-Whitney U test or 1-way ANOVA, followed by a Bonferroni post-test to find differences between the groups. A *P* value of less than 0.05 was used as an indicator of statistical significance. All data was analyzed using the GraphPad Prism 5 Software (GraphPad Software Inc., La Jolla, CA).

3.4 RESULTS

Nanoparticles and Polymersomes promote a distinct intracellular antigen trafficking in dendritic cells

The intracellular route of antigen is known to play a role in driving CD4 or CD8 T cell responses [25,26]. Therefore, to understand if intracellular trafficking takes part in differential T cell activation by the two particulate carriers, we incubated bone marrow derived dendritic cells (BMDCs) together with PSs and NPs loaded with fluorescently labeled OVA, and evaluated their colocalization with markers associated with endosomal or lysosomal compartments, such as the early endosome antigen 1 (EEA1), and the lysosomal-associated membrane protein 1 (LAMP1).

After incubation of NP-ss-OVA and PS(OVA) with BMDCs for 2hrs, we began to observe a high colocalization of PS(OVA) within LAMP1+ vesicles in the perinuclear space, but a much lower association with EEA1 (Fig3-1, A, left; Fig3-1, B). Instead, NP-ss-OVA colocalized more with EEA1+ endosomes compared to PS(OVA) (Fig3-1, B). Although the percentage of colocalization with LAMP-1 compartments for the NP group was similar to that one found for the PSs, qualitatively we noticed than the antigen was more dispersed throughout the cell rather than located in proximity of the perinuclear space in association with LAMP1+ vesicles (Fig 3-1 A, right; Fig3-1, B).

Early work in our group [7] showed that the vehicle alone (NPs, no antigen) aggregated in the perinuclear space and exhibited a high degree of LAMP1+ colocalization. Thus, our finding that NP-ss-OVA colocalized with early endosomes suggests that when the antigen is incorporated into the carrier, a fraction of it is cleaved during intracellular trafficking, allowing for endosomal escape into the cytoplasm.

Subsequently, we calculated the ratio of colocalization between LAMP1 and EEA1, and found that the distribution of OVA when delivered through NPs exhibited an approximate 1:1 ratio between late and early endosomal compartments whereas the OVA inside PSs displayed a nearly 6:1 ratio of LAMP1+ to EEA1+ vesicular colocalization (Fig 3-1, C).

Taken together, this data demonstrates that OVA loading into nanocarriers impact the final location of the antigen. It suggests that antigen loaded within PSs carriers may be precluded from early endosomal escape and subsequent early cytosolic processing, and thus traffics through LAMP1+ late endosomal or lysosomal compartments. This intracellular route is typical of exogenous antigen processing and has been shown to lead to MHCII presentation [27]. Meanwhile, the differences in the relative distribution of NP-ss-OVA and NP delivery vehicle alone observed in earlier work suggests that a fraction of antigen escapes into the cytoplasm, where it is processed by the machinery associated with MHCI presentation.

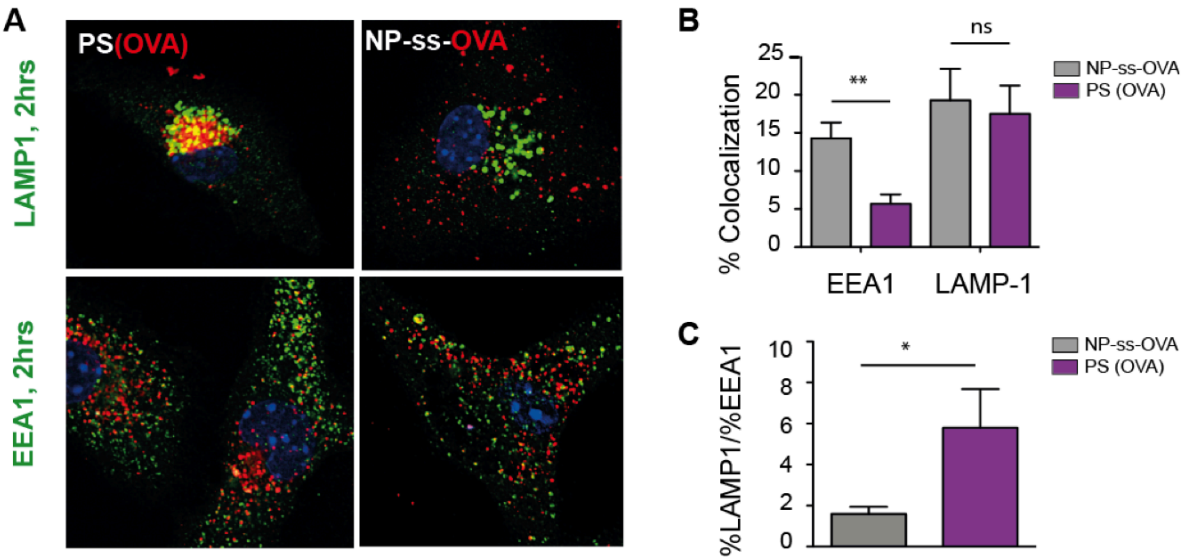

Figure 3–1. Intracellular trafficking of OVA-64 after loading into Nanoparticles (NPs) or encapsulated within polymersomes (PSs). A) NP-ss-OVA and PS(OVA) were incubated with BMDCs during 2h at 37°C. Cells were stained for the early endosome antigen 1 (EEA1) and for lysosomal-associated membrane protein 1 (LAMP1) to evaluate the intracellular trafficking of OVA. **B)** Percentage of colocalization of NP-ss-OVA or PS(OVA) with either EEA1 or LAMP1. **C)** Ratio of the percentage of colocalization with LAMP1 o EEA1 reveals the relative distribution of OVA within these intracellular compartments. Data courtesy of Aaron Mayer.

NP-ss-OVA are associated preferentially with CD8+ DCs and migratory DCs, while PS(OVA) are preferentially associated with lymph node resident CD11b+CD11c+ cells

We wanted to evaluate whether the differences observed in cellular responses were also attributed to a differential organ distribution and cellular uptake by dendritic cells (DCs).

DCs are crucial for the initiation of T cell responses in the lymph node (LN) [28]. Several subsets of DCs have been identified, including lymphoid tissue resident DCs, which locate in their majority in close contact with the LN conduit system to rapidly take up draining antigens [29–33]; and the migratory DCs, which travel from peripheral tissues via afferent lymphatics, and carry antigen from distal sites for its transfer to resident DCs or for its presentation to lymphocytes [28,31,33–38].

To investigate the early events of antigen acquisition by DCs, we labeled OVA with a fluorescent dye, and immunized mice together with CpG-B. We collected draining LNs at 2 and 36 hours (hrs) after immunization, and analyzed by flow cytometry the distribution of cells positive for antigen at both time points (Fig3-2, A). After 2 hrs, we observed a frequency of OVA+ cells of 6% in the NP group, compared to a 1% in the PSs group. By 36 hrs, the level of OVA+ cells in LNs was similar in both conditions, displaying a drastic reduction for NPs, while a modest increase for the PSs group (Fig3-2, B).

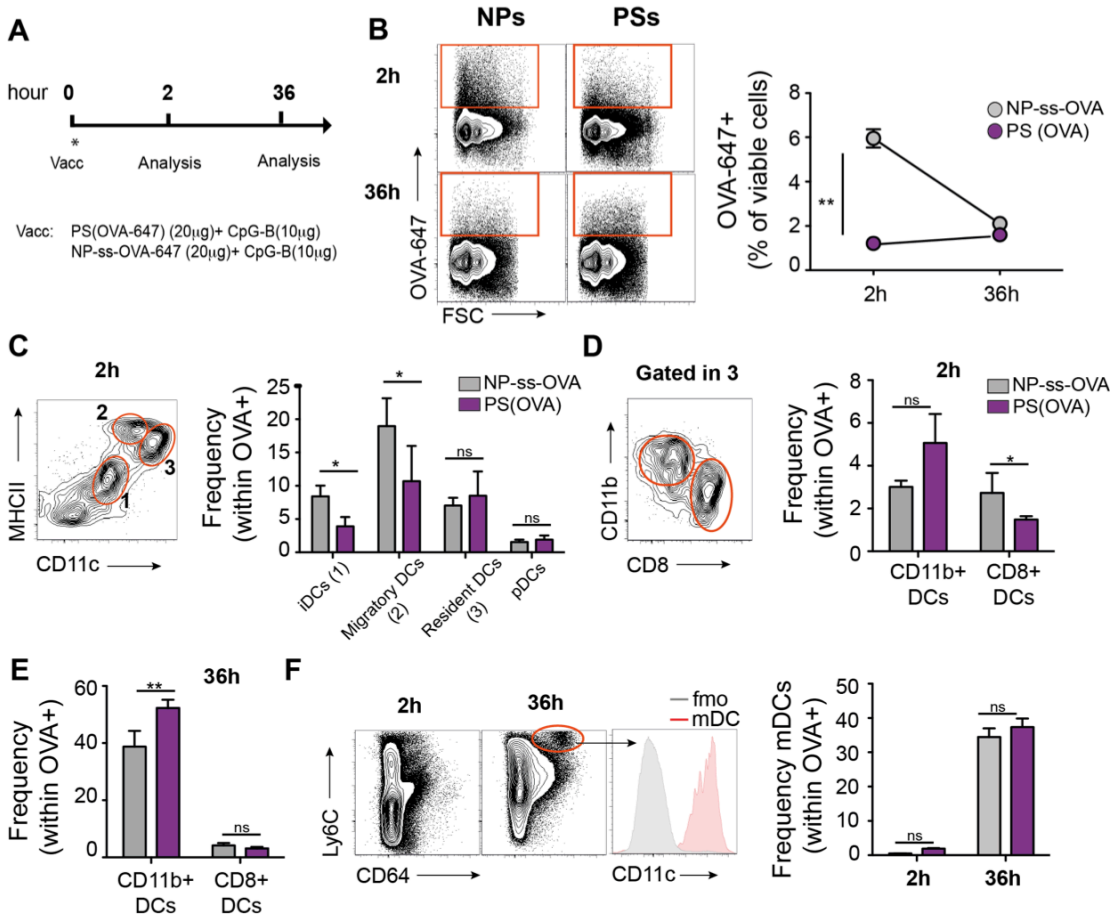

Figure 3–2. **Lymph node biodistribution of NP-ss-OVA and PS(OVA) after intradermal (i.d.) administration with CpG-B. A)** Immunization timeline and vaccination groups. **B)** *Left,* representative flow cytometry plot of OVA+ cells in the viable cell population. *Right,* frequency of OVA+ cells within the viable cell population after 2 and 36 hrs immunization. **C)** *Left,* gating strategy of dendritic cell (DC) subsets. The flow cytometry plot of MHCII vas CD11c was generated after exclusion of B cells and pDCs. *Right,* frequency of DCs within the OVA+ population at 2 hrs post immunization. **D)** *Left,* gating strategy of the lymph node resident DC subsets CD11b+CD11c+ and CD8+CD11c+. *Right,* frequency of lymph node resident DC subsets within the OVA+ population at 2 hrs post immunization. **E)** Frequency of CD11b+ CD11c+ and CD8+ CD11c+ within the OVA+ population at 36 hrs post immunization. **F)** *Left,* Identification of myeloid derived DCs based on the expression of Ly6C, CD64 and CD11c. *Right,* frequency of myeloid derived DCs within the OVA+ population at 2 hrs and 36 hrs post immunization.

Afterwards, we analyzed the various DCs subsets within the OVA+ cells. For the 2 hrs timepoint, we first excluded B cells and identified plasmocytoid DCs (pDCs) based on B220 and CD11c expression, with B cells as B220+CD11c- and B220+CD11c^{mid} cells as pDCs. We also excluded monocytes and macrophages as CD11b+CD11c- [39], and on the remaining cells distinguished the migratory and resident DC subsets based in the CD11c and MHCII expression [33,40,41]. The migratory cells DCs were classified as CD11c^{mid}MHCII^{hi} and resident DCs as CD11c^{hi}MHCII^{mid}. We also found a MHCII^{mid}CD11c^{mid} population, that we called intermediate DCs (iDCs). This subset was a quite heterogeneous population containing CD103+, CD8+, CD4+, as well as Ly6C monocytes and Ly6G+ cells. This last population may potentially be neutrophils that upregulated CD11c expression early after the immunization (Fig3-2, C).

By 2 hrs, migratory cells present in the LN were the main DCs associated with PS(OVA) and NP-ss-OVA (18% and 10%). For the NP group, the iDCs were the second population taking up antigen (8%), followed by the resident DCs (7%). For PS(OVA), instead, the resident DCs cells display the second highest association (8%), followed by the iDCs (4%). Finally, we found very low association with pDCs, consistent with previous description of these cells being less efficient APCs [40] (Fig3-2 C, right).

We were also interested in analyzing the diverse subsets of resident DCs. There is increasing evidence that the CD11b+ CD11c+ LN DCs, which reside in close contact with cortical and medullary sinuses in draining LNs, are one of the main subset associated with MHCII presentation to CD4 T cells [29–31,33,36]. CD8+ DCs, on the contrary, are mainly responsible of crosspresentation of exogenous antigens to CD8 T cells [37]. Therefore, we separate the resident subset into CD11b+ DCs and CD8+ DCs. Notably, we found a higher association of PS(OVA) with CD11b+ cells (5% for PSs, and 3% for NPs), while NP-ss-OVA were observed in higher frequencies in CD8+ DCs (3% vs 1.5%, Fig3-2, D).

For the 36hrs timepoint, we analyzed LNs solely based on the expression of CD8+ and CD11b+, since the classification used at 2 hrs was not longer possible, as most of the DCs have matured and upregulated MHCII and CD11c [42] (Fig 3-2, E). Overall, we found much lower OVA+ CD8+ DCs at this time, and a significant association of PS(OVA) and NP-ss-OVA with CD11b+ DCs. We analyzed whether the CD11b+ were monocyte derived DC, which were recently acknowledged to have enhanced MHCII presentation to CD4 T cells [43] (Fig 3-2, F). Distinction of mDCs from conventional DCs was assessed by the expression of CD64, Ly6C and CD11c. Indeed, a prominent population of mDCs was observed after 36 hrs post-immunization, which corresponded to the majority of CD11b+ cells at this timepoint. However, we did not observe large differences in antigen uptake between NP-ss-OVA and PS(OVA) for this population (28% for NPs and 30% for PSs).

PS(OVA) and NP-ss-OVA display a differential lymph node biodistribution

During the last decade, there has been increasing evidence of the role of non-hematopoietic cells in antigen presentation to T cells [32,44]. Herein, we wanted to evaluate whether antigen was associated with LN stromal cells after vaccination with NPs and PSs.

LN stromal cells are negative for the CD45 antigen. Therefore, we examined CD45- cells at 2 and 36 hrs after immunization. Within the OVA+ fraction, we observed that PSs and NPs displayed a similar frequency of CD45- cells at both timepoints. As expected, the frequencies of CD45- at 36 hrs were much lower than the earlier time (Fig 3-3, A).

We also examined the main LN stromal subsets based on the expression of gp38 and CD31. We classified the CD45- cells as blood endothelial cells (BECs, CD31+gp38-), fibroblastic reticular cells (FRCs, CD31+gp38+), lymphatic endothelial cells (LECs, CD31+gp38-) and double negative cells (DN, CD31-gp38-) (Fig3-3, B). We performed this analysis only for the 2hrs time, since the frequencies of CD45- cells at 36hrs were to low to obtains a nice differentiation of the four stromal subsets.

Interestingly, there was a significant difference in the distribution of OVA between both carriers. When the antigen was delivered by NPs, it was mainly associated with FRCs (54%)

and BECs (27%), and in a lesser extent with LECs (7%). There was also a significant fraction of DN cells (12%), although to date it is not clear the location or role of these cells within LNs. Conversely, OVA within PSs was found in higher frequencies in LECs (72%), and much lower in FRCs (14%) and BECs (7%), as well as DN cells (7%) (Fig3-3, C).

It is known that soluble molecules with a molecular radius higher than 5-8nm are excluded from the reticular conduits found in the LN cortex [45,46]. Thus, finding PS(OVA) mainly in LECs, while little in FRCs, suggests that this carrier is hold in the subcapsular sinus, and that its entry into reticular fibers deep in the lymph cortex is limited due to the larger PSs molecular weight [46]. However, it is puzzling to find that NP-ss-OVA are so poorly in LECS, and strongly associated with FRCs, as well as BECs, which are in connection with the reticular fibers in the LN cortex [46]. A potential explanation is that a fraction of OVA is cleaved from the NPs surface before being internalized, thus allowing for its entry into the reticular system.

Overall, this set of data indicates that each delivery platform has a distinct intranodal antigen distribution signature. This differential location inside the LN may promote acquisition of antigen by diverse subsets of DCs that reside in specific LN locations, thus contributing to the differential cellular responses observed in previous studies.

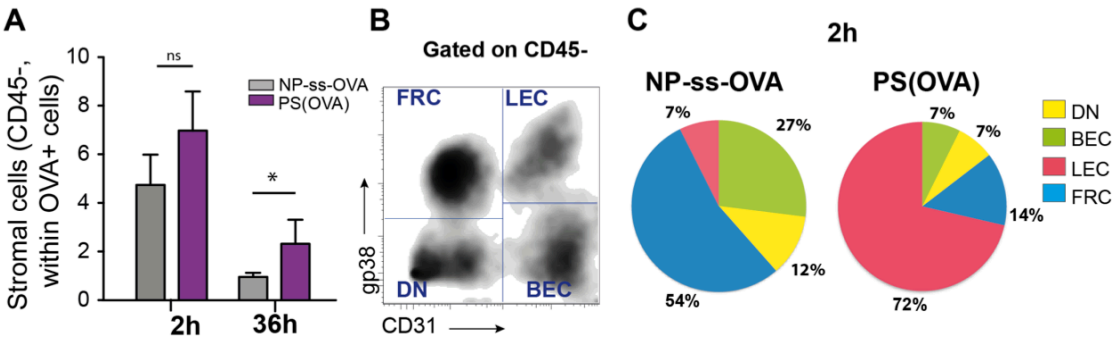

Figure 3–3 Association of NP-ss-OVA and PS(OVA)with lymph node stromal cells populations after intradermal (i.d.) immunization with CpG-B A) Frequency of CD45- stromal cell subsets within the OVA+ population at 2 and 36 hrs post immunization. **B)** Identification of stromal cell subsets based on the expression of podoplanin (gp38) and CD31. **C)** Pie charts displaying the frequency of each stromal cell subsets within the OVA+ population after 2 hrs immunization with NP-ss-OVA and PS(OVA).

Encapsulation of antigen in PSs enhances T follicular helper CD4 cell responses and promotes the generation of germinal center B cells and plasma cells

Considering the distinct profile of PS(OVA) and NP-ss-OVA in intracellular trafficking, as well as cell targeting, and knowing from Stano *et al* that Th1-like antigen specific CD4 responses were higher in mice immunized with PSs, we asked ourselves whether humoral responses where also enhanced upon immunization with PSs. First, we evaluated whether vaccination with PS(OVA) enhances T follicular helper (Tfh) cell responses. Tfh cells represent a unique CD4 T cell subset that specializes in providing help to B cells within germinal centers (GCs)

[47], where B cells undergo affinity maturation, class switch recombination, plasma cell differentiation, and memory B cell differentiation [47].

To analyze the induction of Tfh cell responses, we immunized mice i.d. with PS(OVA), NP-ss-OVA and free OVA, together with 10 μg CpG-B, and at day 9, collected draining LNs and spleen. In order to facilitate the detection of Tfh cells, we adoptively transfer $2x10^6$ congenic CD4 OT-II cells, which have a MHCII-restricted TCR transgene specific for OVA (Fig3-4, A).

At this timepoint, PS(OVA) and NP-ss-OVA induced similar OT-II CD4 T cell expansion, displaying similar counts in both draining LNs and spleen, while only OVA displayed almost 100-fold less expansion than the nanocarriers (Fig3-4, B). We then analyzed the phenotype of all CD4 T cells (endogenous and adoptively transferred) after NP and PS immunization. We found that CD4 T cells primed with PS(OVA) had an enhanced activation phenotype, described by a higher frequency of CD44+CD62L- cells. NP-ss-OVA and soluble OVA displayed instead similar frequencies of activated CD4 T cells (Fig 3-4, C).

Subsequently, we quantified the frequency of OTII-CD4 T cells that have adopted a Tfh cell phenotype (CXCR5+PD-1+Bcl6+) (Fig3-4, D-E). In LNs, up to 15% of the OT-IIs in the PS(OVA) group were Tfh cells, compared to 3% for NP-ss-OVA and 1.8% for soluble OVA. A similar trend was seen in the spleen, although the overall frequencies were much lower (6.5%, 1.4%, 1.2% for PS, NPs and OVA) (Fig3-4, E). Considering that Tfh cells are positively correlated with GCs [48], we analyzed the phenotype of B cells during the same experiment. In agreement with previous publications [14,48], we found higher frequencies of GC B cells in PS(OVA) immunized mice, with a 2-fold increase over the NP-ss-OVA counterpart (Fig3-4, F-H). We also assessed the frequency of plasma cells, which should be in their peak of the response in LNs and spleen [49]. Once again, the PS group showed an enhancement in the frequencies of plasma cells (IgD- CD138+) when compared to the other immunization regimes (Fig3-4, G-H).

All together, these data suggest that the delivery of antigen within PSs results in enhancement of Tfh CD4 T cells positively impact important aspects of the humoral responses, promoting B cell differentiation into GCs and antibody secreting plasma cells.

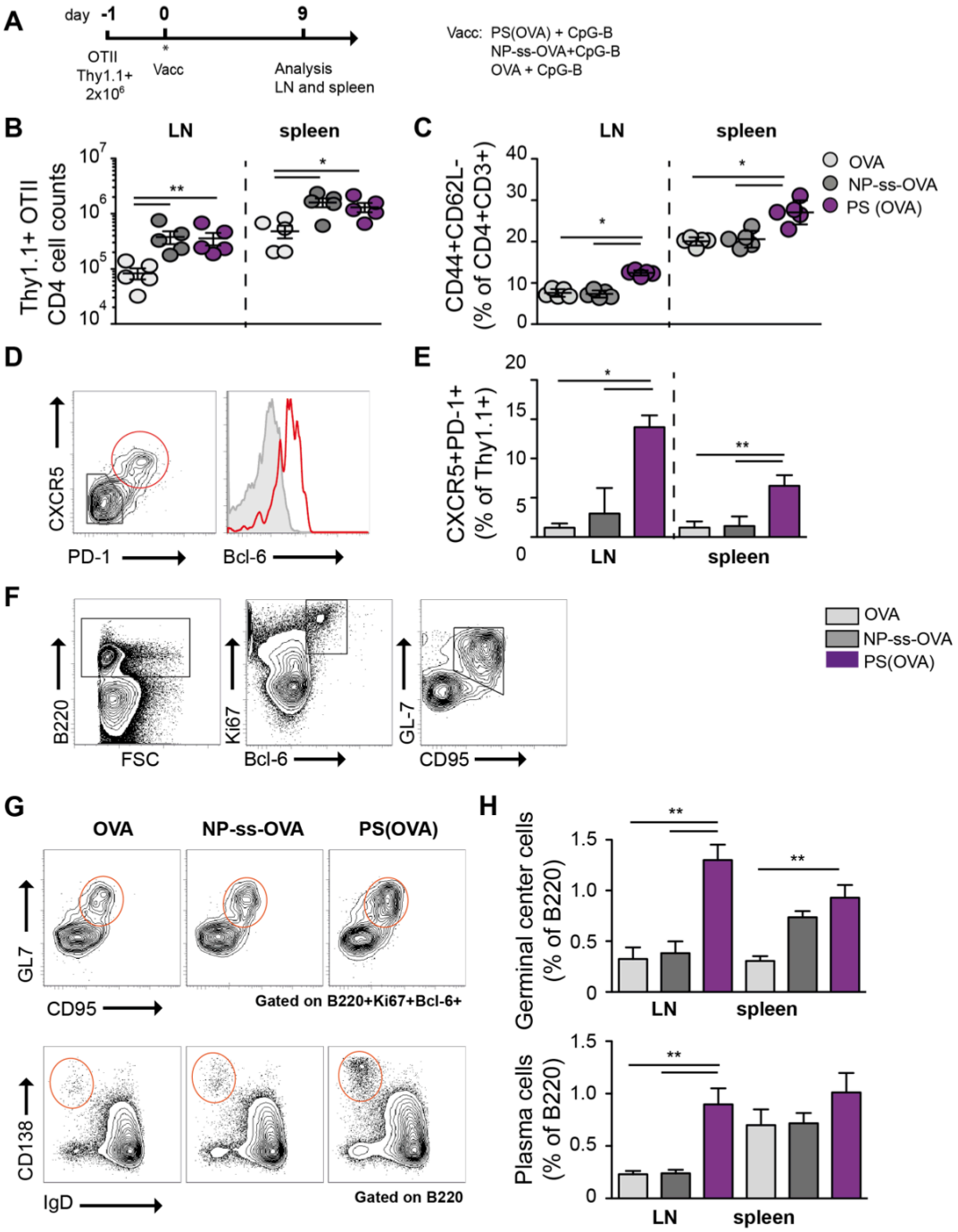

Figure 3–4. **PS(OVA) immunization enhances the induction of T follicular helper (Tfh) CD4 T cells A)** Immunization timeline and vaccination groups. **B)** Cell counts of Thy1.1+ OTII cells in lymph nodes and splenocytes 9 days after i.d. immunization with PS(OVA), NP-ss-OVA and soluble OVA. **C)** Activation phenotype of all CD4 T cells (endogenous + adoptively transfered CD4 T cells) in draining lymph nodes and spleen. **D)** Identification of Tfh CD4 T cells by flow cytometry ; flow cytometry plots were gated on Thy1.1+ OTII cells**. E)** Frequency of Tfh withing the Thy1.1+ OTII CD4 population after immunization in draining lymph nodes and spleen. **F)** Gating strategy of germinal center (GC) B cells; B220+ B cells cells were previously gated from viable cells. **G)** Representative flow cytometry plots displaying GC B cells (up) and plasma cells(down) 9 days after immnunization with PS (OVA), NP-ss-OVA and soluble OVA. **H)** Quantification of **G**, frequency of GCs and plasma cells withing the B220+ B cell population. When not indicated, differences between groups were not significant. * *p* 0.05 ; ***p* , 0.01

Polymersomes and nanoparticles promote long-lasting antibody responses

Based on the observations that GCs and Tfh cells were enhanced with PSs, we sought to evaluate the antibody titers upon a prime boost immunization regime, as described by Stano *et al* [20]. However, we slightly modified the vaccination regime, by boosting at day 21 instead of day 14, since longer intervals between prime and booster immunization has been associated with an enhancement of the boosting effect [50] (Fig 3-5, A).

Mice were immunized with 10μg of OVA as free OVA, PS(OVA), and NP-ss-OVA, together with 10μg of CpG-B. Consistent with the previous studies[20], a prime boost immunization with PS(OVA) enhanced CD4 T cell responses over NP-ss-OVA and free antigen vaccination (Fig3-5, B).

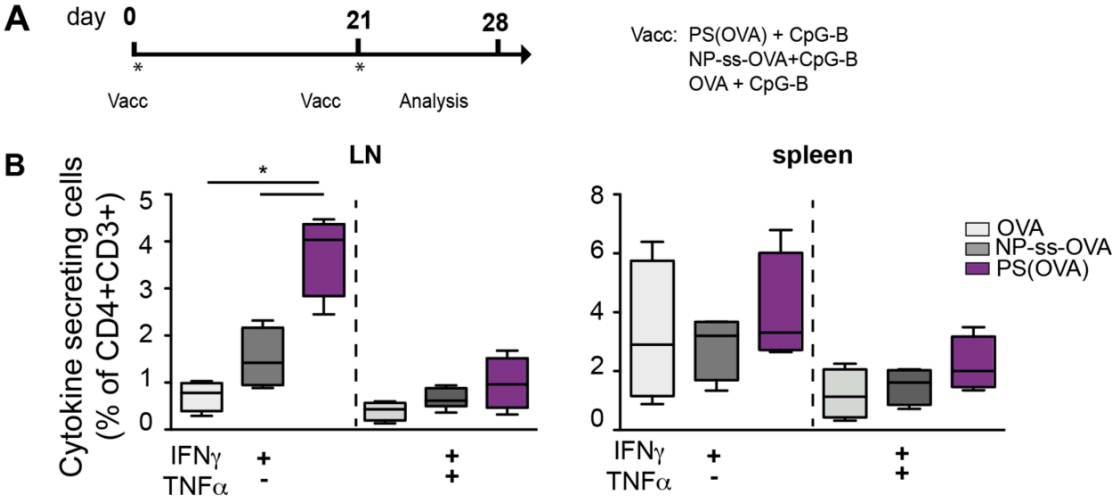

Figure 3–5 PS(OVA) enhance polyfunctional CD4 T cell responses compared to NP-ss-OVA and unformulated protein. A) Immunization timeline and vaccination groups. **B)** Cytokine secreting CD4 T cells in draining lymph nodes and spleen 7 days after a prime-boost immunization with PS(OVA), NP-ss-OVA and unformulated OVA, together with CpG-B. Lymphocytes were restimulated *ex vivo* with OVA protein in the presence of Brefeldin A; cytokine expression was assessed by intracellular staining**.**

Afterwards, we evaluated the antibody responses to the vaccination with the diverse platforms. Notably, by 3 weeks after a single immunization, the NP group displayed the highest levels of IgG antigen-specific antibody titers in serum (Fig 3-6 A, left). This observation was quite surprising, considering that this carrier displayed a significantly lower CD4 response after an *ex vivo* restimulation with the full protein, as well as lower frequencies of Tfh CD4 cells and GC B cells. A booster immunization using the same formulation three weeks later markedly increase the titers in all the groups, and by day 28 the NP and PS groups displayed similar levels of OVA specific IgGs. Free antigen, as expected, promoted lower antibody titers than the particulate regimes (Fig 3-6 A, middle). We also evaluated antibody levels at >30 days after the booster vaccination, and found that both NP-ss-OVA and PS(OVA) had stable levels of IgG serum antibodies, displaying similar levels to those observed by day 28 (Fig 3-6 A, right).

Evaluation of the antibody subtypes displays a markedly different response between the two carriers. While IgG2c was very high in all immunizations, as expected from the strong Th1 skewing capacity of the adjuvant CpG-B [51,52], we also found that the NP group display much higher IgG1 and IgG3 than PS(OVA) (Fig3-6, B). Analysis of the IgG2/IgG1 and the IgG1/IgG2 ratios indicates that in the absence of a carrier, the response is strongly driven to a Th1 response. Antigen encapsulated within PSs promotes a more balanced Th1/Th2 response, but antigen in the surface of NPs promotes a Th2-like skewed response (Fig3-6,C). Overall, the data demonstrates that particle-based carriers have a strong impact on the quality of humoral responses.

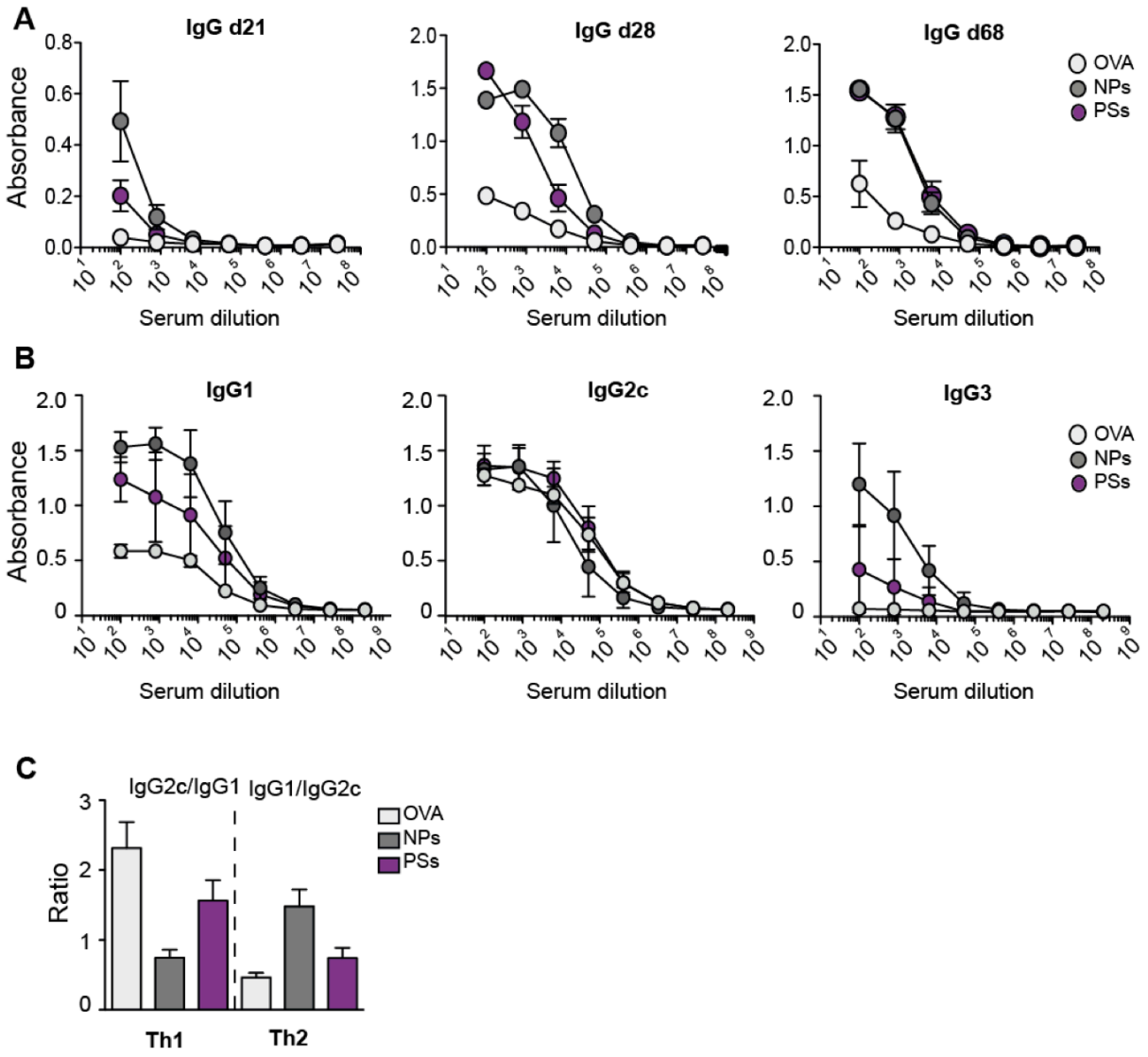

Figure 3–6 Nanoparticles and Polymersomes qualitatively modify the humoral response to OVA. A) Total IgG OVA-specific serum antibody titers at day 21, 28 and 68 post immunization. **B)** OVA-specific IgG antibody subtypes at day 28, one week after the booster immunization. **C)** Ratio of IgG2c/ IgG1 and IgG1/IgG2c at day 28 after prime/boost immunization.

3.5 DISCUSSION

Particulate-antigen carrier systems are of great interest for the development of subunit vaccines. Understanding their mechanisms in cellular targeting and processing as well as implications in adaptive immunity is important for vaccine design, as this information would be crucial in the decision making process of which carrier would be ideal for an specific vaccine application. Previous studies have demonstrated that immunization with PSs enhanced CD4 responses, while NPs enhance cytotoxic CD8 T cells. Here, we demonstrated that various mechanisms at the cellular and organ level synergize to give rise to the opposing responses observed between the two nanocarriers.

We showed that OVA loaded in NPs upon internalization is partially cleaved in early endosomes, allowing for its escape into the cytoplasm and increasing the likelihood of proteasome processing and MHCI loading [53,54]. Instead, OVA within PSs displayed higher association with lysosomes, where the oxidative environment allows for antigen release and loading into the MHCII presentation pathway (Fig 3-7) [55]. Such a differential intracellular localization might be owed to different modalities of cellular internalization. NPs are known to enter the cells through more than one pathway, including macropinocytosis and clathrin-mediated endocytosis [7]. PSs, because of their larger size, are likely being internalized mainly by macropinocytosis [25]. Interestingly, various studies demonstrated that antigen taken up by macropinocytosis is targeted to late endosomal/lysosomal compartments, that are known to be specialized for antigen loading in MHCII [26,56–58], which might account for the enhanced CD4 responses observed in our experiments.

At the organ level, we observed a higher amount of antigen draining to local LNs after immunization with NPs, when compared to the PSs group. This data suggests that PSs have a lower lymphatic uptake rate than NPs, which could be associated to an increase interstitial resistance associated to the larger size and molecular weight of PSs [59]. Furthermore, we found a differential distribution of the NPs and PSs within the DC populations at earlier timepoints after immunization. NPs associated more with migratory DCs, which were likely present in the LN (since DC trafficking takes 18h, so it is unlikely they capture the antigen on the periphery); and also with LN resident CD8+ DCs. PSs instead were more associated with LN resident CD11b+ DCs, and in a lesser extend with migratory DCs. Notably, the CD8+ DCs are mainly associated with the crosspresentation of exogenous antigen, while the CD11b+ DCs are related with an enhanced MHCII presentation [29–31,33,36,37].

Despite of the differences in overall distribution, the higher frequency of OVA+ cell in the NP group implies that, in terms of cell numbers, the NPs excel in targeting all DC population subsets, including the CD11b+ DCs. Given these observations, albeit the differential biodistribution, we believe that it is likely that the intracellular processing of antigen plays a more important role in directing the T cell response towards CD4 or CD8. Indeed, it has been suggested that crosspresentation is not a specialization of DC subsets, rather a process that is triggered depending on the way the antigen is presented.

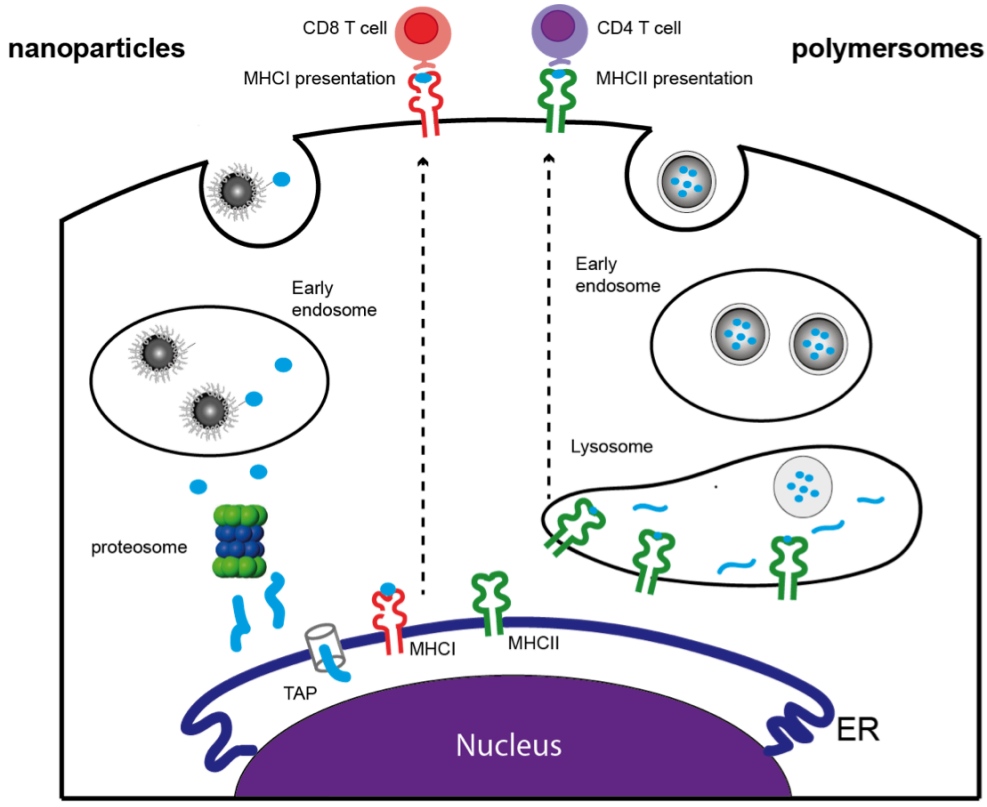

Figure 3–7 Intracellular distribution of antigen after coupling to Nanoparticles and encapsulation within Polymersomes. Nanoparticles allow for the endosomal release of antigen, leading to antigen processing in the cytoplasm by the MHCI presentation machinery. Polymersomes, instead, protect the antigen until it reaches the lysosomes, where it is released and loaded into MHCII molecules.

By instance, targeting of antigens through the DEC205 presentation pathway in both, CD8+ and CD8- DCs leads to potent crosspresentation to CD8 T cells [60]. Similar results were observed with human DCs, were targeting of the antigen to early endosomes through CD40 or CD11c leads to levels of crosspresentation in BDCA1+ cells (CD8- DCs in mouse) similar to those observed in BDCA3+ cells (CD8+ DCs in mouse) [61]. Nevertheless, we do not disregard the fact that differential uptake of antigen in the LN by migratory DCs as well as LN resident DCs contribute to the differential T cell activation.

Concerning the stromal cell subsets, we observed that antigen in PSs is mainly associated with LECs, while antigen in NPs is found mainly in FRCs. The results might suggest a distinct micro-anatomical localization of the antigen, with PS(OVA) associated mainly in lymphatic sinuses, while NP-ss-OVA, surprisingly, reaching the LN cortex in association of FRCs (Fig 3-8). These observations could also explain the differential uptake observed by migratory and resident APCs. Migratory DCs are known to express high levels of CCR7[62], that bind to CCL21 bound to the reticular fiber deep in the T cell area. Therefore, migratory DCs are expected to locate mainly in the LN cortex, in close association with FRCs and reticular conduits[29]. Therefore, it is likely mDCs have more access to the antigen that is found in FRCs upon delivery in NPs, thus explaining their enhancement of CD8 T cell responses. Conversely, PSs are retain in the lymphatic sinuses, where CD11b+ resident

DCs sample antigen, as observed by 2-photon in vivo studies [29,30] . This subset, importantly, is acknowledged by several studies to enhance CD4 responses [29,30,36].

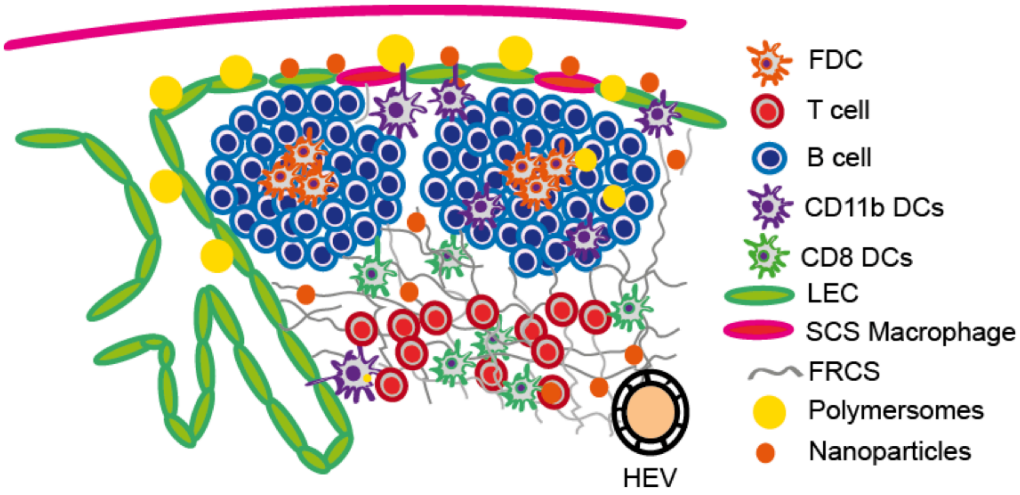

Figure 3–8 Lymph node biodistribution of Polymersomes and Nanoparticles. Antigen loaded into nanoparticles can reach the FRC network, where it interacts with LN resident cells such as CD11c+ CD8+ DCs. Meanwhile, antigen within PSs is hold on the subcapsular sinus where it is sampled by specialized DCs such as CD11b+ CD11c+ cells.

Two questions arise from these results. First, it is unknown whether the antigens found associated in LECs and FRCs are being presented to CD4 or CD8 T cells, and whether this has implications on the overall vaccine response. There is strong evidence that these two subsets present antigen in both, the MHCI and the MHCII context [32,44,63,64]. However, these subsets are strongly tolerogenic, and there is little evidence that indicate that they initiate an immune response. Secondly, it is still unclear if antigen inside LECs is processed [32,65], or if it is transferred intact to other APCs for presentation, similar to what is observed in follicular dendritic cells [66].

We also demonstrated that PS encapsulated antigen promoted better Tfh CD4 responses, and increased the formation of GCs and plasma cells early during the immune response. There is evidence that the initiation of Tfh CD4 response relies on DC presentation of the antigen [67]. From the vaccine engineering perspective, it would be exciting to understand whether the targeting of a particular intracellular trafficking pathway on DCs enhances the formation of Tfh CD4 T cells. This information would be a major contribution to engineering principles in vaccine design. Furthermore, it would become conceivable to target antigen to specific receptors known to enhance MHCII presentation.

Conversely, the data obtained for NPs does not fit the classical picture. Despite lower Tfh CD4 cells and less GC B cells, this immunization promoted high antibody titers, although the quality of the response was considerably different to that observed with PSs. However, humoral responses could also develop through the extrafollicualr pathway or in a T independent mode, which might be initiated in the absence of GCs and also lead to the generation of long lived plasma cells [68,69] . Interestingly, NPs promoted higher titers of the IgG3 antibody subtype, which is one of the main IgG subtypes in T independent type 2

responses (TI). Therefore, our previous observations may suggest that the NPs could also enhance an extrafollicular route or a TI response. However, this is only a hypothesis, and its validation will require further experiments.

It is clear that antigen formulations have a strong impact on the quality of the elicited immune response. Consequently, for particulate vaccine design, consideration of factors such as the route of uptake of the antigen, method of antigen release, intracellular trafficking of the antigen, size of the carrier and lymphoid organ distribution of the conjugate should be taken into account to target a specific immune response.

In summary, NPs and PSs carriers differ in their immune response to OVA. We conclude that modifying the antigen delivery method, i.e, tuning the carrier size and antigen conjugation chemistry, has important implications in the quality and quantity of the cellular and humoral responses. For vaccine design considerations, the data suggest that enhancing lysosomal targeting of particulate carrier is important in order to enhance CD4 responses. Concerning the platforms developed in our group, we conclude that antigen encapsulation in PSs is a promising way to deliver antigens for vaccine targeting humoral responses, since it promotes robust CD4 responses and corresponding GCs responses without the need to chemically modify antigen for loading into delivery vehicles, which simplifies the development of new subunit vaccines.

3.6 REFERENCES

1. Plotkin, S. a. & Plotkin, S. L. The development of vaccines: how the past led to the future. *Nat. Rev. Microbiol.* **9,** 889–893 (2011).
2. Rappuoli, R., Mandl, C. W., Black, S. & Gregorio, E. De. Vaccines for the twenty-first century society. *Nat. Rev. Immunol.* **11,** 865–872 (2012).
3. Todryk, S. M. & Hill, A. V. S. Malaria vaccines: the stage we are at. *Nat. Rev. Microbiol.* **5,** 487–489 (2007).
4. Andersen, P. & Woodworth, J. S. Tuberculosis vaccines--rethinking the current paradigm. *Trends Immunol.* **35,** 387–395 (2014).
5. Moyle, P. M. & Toth, I. Modern Subunit Vaccines: Development, Components, and Research Opportunities. *ChemMedChem* **8,** 360–376 (2013).
6. Reddy, S. T., Swartz, M. a & Hubbell, J. a. Targeting dendritic cells with biomaterials: developing the next generation of vaccines. *Trends Immunol.* **27,** 573–579 (2006).
7. Hirosue, S., Kourtis, I. C., van der Vlies, A. J., Hubbell, J. a & Swartz, M. A. Antigen delivery to dendritic cells by poly(propylene sulfide) nanoparticles with disulfide conjugated peptides: Cross-presentation and T cell activation. *Vaccine* **28,** 7897–906 (2010).
8. Swartz, M. a., Hirosue, S. & Hubbell, J. a. Engineering Approaches to Immunotherapy. *Sci. Transl. Med.* **4,** 148rv9–148rv9 (2012).
9. Gregory, A. E., Titball, R. & Williamson, D. Vaccine delivery using nanoparticles. *Front. Cell. Infect. Microbiol.* **3,** 13 (2013).
10. Bershteyn, A. *et al.* Robust IgG responses to nanograms of antigen using a biomimetic lipid-coated particle vaccine. *J. Control. Release* **157,** 354–365 (2011).
11. Scott, E. A. *et al.* Dendritic cell activation and T cell priming with adjuvant- and antigen-loaded oxidation-sensitive polymersomes. *Biomaterials* **33,** 6211–6219 (2012).
12. Stano, A. *et al.* PPS nanoparticles as versatile delivery system to induce systemic and broad mucosal immunity after intranasal administration. *Vaccine* **29,** 804–812 (2011).
13. Nembrini, C. *et al.* Nanoparticle conjugation of antigen enhances cytotoxic T-cell responses in pulmonary vaccination. *Proc. Natl. Acad. Sci. U. S. A.* **108,** E989–E997 (2011).
14. Moon, J. J. *et al.* Enhancing humoral responses to a malaria antigen with nanoparticle vaccines that expand Tfh cells and promote germinal center induction. *Proc. Natl. Acad. Sci. U. S. A.* **109,** 1080–1085 (2012).
15. Li, A. V *et al.* Generation of effector memory T cell-based mucosal and systemic immunity with pulmonary nanoparticle vaccination. *Sci. Transl. Med.* **5,** 204ra130 (2013).
16. Irvine, D. J., Hanson, M. C., Rakhra, K. & Tokatlian, T. Synthetic Nanoparticles for Vaccines and Immunotherapy. *Chem. Rev.* (2015). doi:10.1021/acs.chemrev.5b00109
17. Rehor, A., Hubbell, J. a. & Tirelli, N. Oxidation-sensitive polymeric nanoparticles. *Langmuir* **21,** 411–417 (2005).
18. Reddy, S. T., Rehor, A., Schmoekel, H. G., Hubbell, J. a. & Swartz, M. A. In vivo targeting of dendritic cells in lymph nodes with poly(propylene sulfide) nanoparticles. *J. Control. Release* **112,** 26–34 (2006).
19. O'Neil, C. P., Suzuki, T., Demurtas, D., Finka, A. & Hubbell, J. A. A novel method for the encapsulation of biomolecules into polymersomes via direct hydration. *Langmuir* **25,** 9025–9029 (2009).
20. Stano, A., Scott, E. a, Dane, K. Y., Swartz, M. A & Hubbell, J. A. Tunable T cell immunity towards a protein antigen using polymersomes vs. solid-core nanoparticles. *Biomaterials* **34,** 4339–4346 (2013).

21. Burgdorf, S., Kautz, A., Böhnert, V., Knolle, P. a & Kurts, C. Distinct pathways of antigen uptake and intracellular routing in CD4 and CD8 T cell activation. *Science* **316,** 612–617 (2010).
22. Van der Vlies, A. J., O'Neil, C. P., Hasegawa, U., Hammond, N. & Hubbell, J. A. Synthesis of pyridyl disulfide-functionalized nanoparticles for conjugating thiol-containing small molecules, peptides, and proteins. *Bioconjug. Chem.* **21,** 653–62 (2010).
23. Cerritelli, S. *et al.* Aggregation behavior of poly(ethylene glycol-bl-propylene sulfide) di- and triblock copolymers in aqueous solution. *Langmuir* **25,** 11328–11335 (2009).
24. Lutz, M. B. *et al.* An advanced culture method for generating large quantities of highly pure dendritic cells from mouse bone marrow. *J. Immunol. Methods* **223,** 77–92 (1999).
25. Petros, R. a & DeSimone, J. M. Strategies in the design of nanoparticles for therapeutic applications. *Nat. Rev. Drug Discov.* **9,** 615–627 (2010).
26. Burgdorf, S., Lukacs-kornek, V. & Kurts, C. The mannose receptor mediates uptake of soluble but not of cell-associated antigen for crosspresentation. *J. Immunol.* **176,** 6770–6776 (2006).
27. Vyas, J. M., Van der Veen, A. G. & Ploegh, H. L. The known unknowns of antigen processing and presentation. *Nat. Rev. Immunol.* **8,** 607–618 (2008).
28. Mildner, A. & Jung, S. Development and function of dendritic cell subsets. *Immunity* **40,** 642–656 (2014).
29. Sixt, M. *et al.* The conduit system transports soluble antigens from the afferent lymph to resident dendritic cells in the T cell area of the lymph node. *Immunity* **22,** 19–29 (2005).
30. Gerner, M. Y., Torabi-Parizi, P. & Germain, R. N. Strategically Localized Dendritic Cells Promote Rapid T Cell Responses to Lymph-Borne Particulate Antigens. *Immunity* **42,** 172–185 (2015).
31. Allenspach, E. J., Lemos, M. P., Porrett, P. M., Turka, L. a. & Laufer, T. M. Migratory and Lymphoid-Resident Dendritic Cells Cooperate to Efficiently Prime Naive CD4 T cells. *Immunity* **29,** 795–806 (2008).
32. Turley, S. J., Fletcher, A. L. & Elpek, K. G. The stromal and haematopoietic antigen-presenting cells that reside in secondary lymphoid organs. *Nat. Rev. Immunol.* **10,** 813–825 (2010).
33. Gerner, M. Y., Kastenmuller, W., Ifrim, I., Kabat, J. & Germain, R. N. Histo-cytometry: A method for highly multiplex quantitative tissue imaging analysis applied to dendritic cell subset microanatomy in lymph nodes. *Immunity* **37,** 364–376 (2012).
34. Allan, R. S. *et al.* Migratory dendritic cells transfer antigen to a lymph node-resident dendritic cell population for efficient CTL priming. *Immunity* **25,** 153–162 (2006).
35. Itano, A. a. *et al.* Distinct dendritic cell populations sequentially present antigen to CD4 T cells and stimulate different aspects of cell-mediated immunity. *Immunity* **19,** 47–57 (2003).
36. Iezzi, G. *et al.* Lymph node resident rather than skin-derived dendritic cells initiate specific T cell responses after Leishmania major infection. *J. Immunol.* **177,** 1250–1256 (2006).
37. Shortman, K. & Heath, W. R. The CD8+ dendritic cell subset. *Immunol. Rev.* **234,** 18–31 (2010).
38. Cerovic, V. *et al.* Lymph-borne CD8α(+) dendritic cells are uniquely able to cross-prime CD8(+) T cells with antigen acquired from intestinal epithelial cells. *Mucosal Immunol.* **8,** 1–11 (2014).
39. Jakubzick, C. *et al.* Lymph-migrating, tissue-derived dendritic cells are minor constituents within steady-state lymph nodes. *J. Exp. Med.* **205,** 2839–2850 (2008).

40. Heath, W. R. & Carbone, F. R. The skin-resident and migratory immune system in steady state and memory: innate lymphocytes, dendritic cells and T cells. *Nat. Immunol.* **14,** 978–985 (2013).
41. Heath, W. R. & Carbone, F. R. Dendritic cell subsets in primary and secondary T cell responses at body surfaces. *Nat. Immunol.* **10,** 1237–1244 (2009).
42. Merad, M., Sathe, P., Helft, J., Miller, J. & Mortha, A. The dendritic cell lineage: ontogeny and function of dendritic cells and their subsets in the steady state and the inflamed setting. *Annu. Rev. Immunol.* **31,** 563–604 (2013).
43. Chakarov, S. & Fazilleau, N. Monocyte-derived dendritic cells promote T follicular helper cell differentiation. *EMBO Mol. Med.* **6,** 590–603 (2014).
44. Hirosue, S. *et al.* Steady-State Antigen Scavenging, Cross-Presentation, and CD8+ T Cell Priming: A New Role for Lymphatic Endothelial Cells. *J. Immunol.* **192,** 5002–5011 (2014).
45. Gonzalez, S. F. *et al.* Trafficking of B cell antigen in lymph nodes. *Annu. Rev. Immunol.* **29,** 215–233 (2011).
46. Gretz, J. E., Norbury, C. C., Anderson, a O., Proudfoot, a E. & Shaw, S. Lymph-borne chemokines and other low molecular weight molecules reach high endothelial venules via specialized conduits while a functional barrier limits access to the lymphocyte microenvironments in lymph node cortex. *J. Exp. Med.* **192,** 1425–1440 (2000).
47. Crotty, S. Follicular helper CD4 T cells (TFH). *Annu. Rev. Immunol.* **29,** 621–663 (2011).
48. Baumjohann, D. *et al.* Persistent antigen and germinal center B cells sustain T follicular helper cell responses and phenotype. *Immunity* **38,** 596–605 (2013).
49. Slifka, M. K., Antia, R., Whitmire, J. K. & Ahmed, R. Humoral immunity due to long-lived plasma cells. *Immunity* **8,** 363–372 (1998).
50. Flatz, L. *et al.* Gene-Based Vaccination with a Mismatched Envelope Protects against Simian Immunodeficiency Virus Infection in Nonhuman Primates. *J. Virol.* **86,** 7760–7770 (2012).
51. Lin, L., Gerth, A. J. & Peng, S. L. CpG DNA redirects class-switching towards 'Th1-like' Ig isotype production via TLR9 and MyD88. *Eur. J. Immunol.* **34,** 1483–1487 (2004).
52. Netea, M. G., Meer, J. W. M. Van Der, Sutmuller, R. P., Adema, G. J. & Kullberg, B. From the Th1 / Th2 Paradigm towards a Toll-Like Receptr/T-Helper Bias. *Antimicrob. Agents Chemother.* **49,** 3991–3996 (2005).
53. Cresswell, P., Ackerman, A. L., Giodini, A., Peaper, D. R. & Wearsch, P. a. Mechanisms of MHC class I-restricted antigen processing and cross-presentation. *Immunol. Rev.* **207,** 145–157 (2005).
54. Joffre, O. P., Segura, E., Savina, A. & Amigorena, S. Cross-presentation by dendritic cells. *Nat. Rev. Immunol.* **12,** 557–569 (2012).
55. Austin, C. D. *et al.* Oxidizing potential of endosomes and lysosomes limits intracellular cleavage of disulfide-based antibody-drug conjugates. *Proc. Natl. Acad. Sci. U. S. A.* **102,** 17987–17992 (2005).
56. Liu, Z. & Roche, P. a. Macropinocytosis in phagocytes: regulation of MHC class-II-restricted antigen presentation in dendritic cells. *Front. Physiol.* **6,** 1–6 (2015).
57. Yameen, B. *et al.* Insight into nanoparticle cellular uptake and intracellular targeting. *J. Control. Release* **190,** 485–499 (2014).
58. Sallusto, B. F. & Lanzavecchia, A. Dendritic cells use macropinocytosis and the mannose receptor to concentrate macromolecules in the major histocompatibility complex class II compartment: Downregulation by cytokines and bacterial products. *J. Exp. Med.* **182,** 389–400 (1995).

59. Irvine, D. J., Swartz, M. a & Szeto, G. L. Engineering synthetic vaccines using cues from natural immunity. *Nat. Mater.* **12,** 978–990 (2013).
60. Kamphorst, A. O., Guermonprez, P., Dudziak, D. & Nussenzweig, M. C. Route of antigen uptake differentially impacts presentation by dendritic cells and activated monocytes. *J. Immunol.* **185,** 3426–3435 (2010).
61. Cohn, L. *et al.* Antigen delivery to early endosomes eliminates the superiority of human blood BDCA3+ dendritic cells at cross presentation. *J. Exp. Med.* **210,** 1049–1063 (2013).
62. Ohl, L. *et al.* CCR7 governs skin dendritic cell migration under inflammatory and steady-state conditions. *Immunity* **21,** 279–288 (2004).
63. Dubrot, J. *et al.* Lymph node stromal cells acquire peptide-MHCII complexes from dendritic cells and induce antigen-specific CD4+ T cell tolerance. *J. Exp. Med.* **211,** 1153–1166 (2014).
64. Fletcher, A. L. *et al.* Lymph node fibroblastic reticular cells directly present peripheral tissue antigen under steady-state and inflammatory conditions. *J. Exp. Med.* **207,** 689–697 (2010).
65. Tamburini, B. a, Burchill, M. a & Kedl, R. M. Antigen capture and archiving by lymphatic endothelial cells following vaccination or viral infection. *Nat. Commun.* **5,** 3989 (2014).
66. Gonzalez, S. F. *et al.* Trafficking of B cell antigen in lymph nodes. *Annu. Rev. Immunol.* **29,** 215–233 (2011).
67. Barnett, L. G. *et al.* B cell antigen presentation in the initiation of follicular helper T cell and germinal center differentiation. *J. Immunol.* **192,** 3607–3617 (2014).
68. MacLennan, I. C. M. *et al.* Extrafollicular antibody responses. *Immunol. Rev.* **194,** 8–18 (2003).
69. Vinuesa, C. G. & Chang, P.-P. Innate B cell helpers reveal novel types of antibody responses. *Nat. Immunol.* **14,** 119–126 (2013).

Chapter 4

Polymersomes enhance the qualitative humoral response to Lassa glycoprotein 1: Implications for a vaccine against Lassa Virus

Marcela RINCON-RESTREPO, Clara GALAN-NAVARRO, Sachiko HIROSUE, Stefan KUNZ and Melody SWARTZ

4.1 ABSTRACT

Lassa hemorrhagic fever is caused by the Lassa virus (LASV), which kills approximately 5,000-10,000 people yearly. To date, there is single treatment available, Ribavirin, although it only has a therapeutic effect when administered early during the infection, Therefore, there is clear need of a vaccine or an effective treatment against LASV. In this chapter, we explore the feasibility of developing a LASV vaccine targeted to the Lassa glycoprotein 1 (LASV-GP1), which is believed to be the main target of protective antibodies. We used the Polymersomes (PS) platform, based on the capacity of this nanocarrier to enhance antigen specific CD4 responses, as well as to promote T follicular helper T cells and germinal center B cells. We demonstrated that encapsulation of LASV-GP1 into PSs promotes an enhancement of the quality of the elicited antibodies, which had an increased binding to LASV-GP1 when displayed in its native conformation and moreover, displayed a broader epitope targeting. In summary, our data underscores the effectiveness of nanoparticle-based carriers in enhancing qualitatively the immune response to soluble antigens, and suggests that a synthetic subunit vaccine against the Lassa fever is feasible.

4.2 INTRODUCTION

Arenaviruses merit significant attention as causative agents of severe hemorrhagic fevers in humans. Old world arenaviruses such as Lassa virus (LASV) in Africa and New world arenaviruses, such as the South American hemorrhagic fever viruses Junin (JUNV), Machupo (MACV), and Guanarito (GTOV) have emerged as important human pathogens and represent serious public health problems in their respective endemic areas [1].

Treatment options for patients infected with pathogenic arenaviruses are very limited. There is just a single licensed drug for the treatment of human arenavirus infection, Ribavirin, (1-β-D-ribofuranosyl-1,2,4-triazole-3-carboxamide), which is effective when administered at an early time during the disease (< 6 days). Since early diagnosis is proven to be a major challenge in the endemic locations where the viruses are found (since the symptoms might be usually mistaken with other diseases), it is important to develop prophylactic measures to reduce the mortality rate of arenavirus-related diseases, which can reach up to 60% during epidemic times [2,3]. Nevertheless, to date, there is only one licensed vaccine against arenaviruses, specifically JUNV, named Candid No. 1. However, it does not cross-protect against important pathogens such as LASV, which of the arenavirus infections, affects the most people annually with an estimated of 5000-10000 people dying per year in Africa [4].

There is little research on developing a LASV vaccine based on humoral responses. Protection against Lassa is believed to be mediated mainly by CD8 T cell responses, since neutralizing antibodies in surviving patients appear very late after the resolution of the infection [2]. Furthermore, the information on the protective role of antibodies is controversial. For instance, studies in monkey and guinea pigs showed that the passive transfer of neutralizing serum from convalescent patients was protective against a lethal LASV challenge [5]. However, in humans, the passive transfer of antibodies had no effect on the control of the disease [6,7]. This could be attributed to the difficulty of obtaining high antibodies titers for transfer, and also due to the timing of administration, since protection only occurs if the transfer happens at the onset of the disease.

Likewise, the importance of neutralizing antibodies as a mechanism of protection upon vaccination is not clear, mainly because of the difficulty to induce protective antibodies against LASV. Studies with gamma ray-inactivated Lassa virus failed to promote protection despite high levels of antibody titers in the serum of animals [8]. Similarly, the majority of reports using homologous and heterologous prime-boost vaccinations with viral vectors expressing the GP1 and GP2 LASV glycoproteins found low titer antibodies in immunized mice with no neutralizing activity [9]. However, it is worth noting that several studies did not assess the contribution of humoral immunity upon immunizations, as cellular responses were considered the main mechanisms of protection [10–12].

The reasons for the lack of protective humoral responses against glycoproteins of LASV are currently unknown. One possibility may be lack of antigenicity of LASV glycoprotein (GP) due to extensive shielding by glycans, which is similar to the mechanism of evasion proposed for human immunodeficiency virus (HIV) [13]. Alternatively, the weak neutralizing antibody response against LASV may be caused by hidden immunogenic epitopes within the native

trimeric glycoprotein. In this situation, presentation of monomeric components of the surface proteins to the immune system could be beneficial for induction of neutralizing antibodies.

Our group has recently developed a polymeric vesicle composed of copolymers of propylene sulfide (PPS) and polyethylene glycol (PEG), namely polymersomes (PSs) that allow for the encapsulation of native proteins without the need for any chemical modification. We made use of this platform for the development of a vaccine against LASV, focusing our efforts towards the development of humoral immunity. We have chosen as a target the viral glycoprotein 1 (LASV-GP1), as it is generally accepted that the GP1 of arenaviruses such as LASV might be the target of neutralizing antibodies, since it contains the host receptor binding site [14].

We demonstrated that production and loading of LASV-GP1 is feasible, and furthermore we showed that humoral responses against this pathogen are elicited in naïve mice. Quantitatively, we observed no differences in the antibody response between formulations; however, we showed that PSs encapsulation of LASV-GP1 promoted enhanced recognition of the virus GP1 when displayed in its native conformation. Furthermore, by employing a peptide array we demonstrated that encapsulation broadens the epitope targeting by serum antibodies against LASV. These results support the feasibility of the development of a pure synthetic subunit LASV vaccine using PSs, offering a safer alternative in immunization.

4.3 MATERIALS AND METHODS

Animals

C57BL/6 female mice, between 8-12 weeks of age, were purchased from Harlan (France). All animal experiments were performed under the approval from the Veterinary Authority of the Canton of Vaud (Switzerland) according to Swiss Law.

LASV-GP1 encapsulation

PEG-bl-PPS block-copolymers were produced as described in Chapter 3. For the formation of PSs with Lassa antigens, a thin-film of copolymer was rehydrated with a solution of 500μl at 2 mg/mL of LASV-GP1 or fluorescently labeled LASV-GP1 in 50mM phosphate buffer, and rotated for 48hrs at 4°C. Afterwards, the solution was extruded at least 4 times through 0.2 μm nucleopore track-etched membranes (Whatman) to obtain PSs ranging between 150 nm-170 nm, with polydispersity values lower than 0.2. Purification of the PS-loaded from the unloaded protein was achieved by size exclusion chromatography through a Sepharose CL-6B column. Fractions containing PSs were pooled together and further concentrated though an Ultra-centrifugal filter (Amicon) with a cutoff of 100 kDa. Final LASV loading was estimated by subtracting the amount of the unloaded protein to the starting LASV-GP1 used. Using this method, we calculated an average concentration of 432 μg/mL of LASV in the PSs solution. The size of PSs was determined by dynamic light scattering with a Nano Zs Zetasizer (Malvern Instruments).

MPLA labelling

The adjuvant MPLA was labeled on its primary 6'- hydroxyl position by reaction with the pentafluorophenol pyrene active ester (PfPy) using pyridine both as base and solution. The reaction mixture was heated to 50°C and stirred for 18h. The solvent was then removed under reduced pressure, and the product purified from the non-reactive dye by precipitation in acetone.

Immunizations

All vaccines were administered intradermally (i.d.) into the 4 limbs. 10 μg of LASV-GP1 was injected per mouse for all formulations, together with 10 μg of CpG-B (Microsynth), 10 μg of MPLA (*Salmonella minnesota* R595, AvantiLipids) or 50 μg of R848 (Invivogen). Before the immunizations, free LASV-GP1 was filtered through a 0.22 μm membrane (Millipore Corporation) to remove aggregates. All PSs and proteins batches were tested for endotoxin levels using a TLR activation assay based on HEK-Blue reporter cell lines (Invivogen) before immunization.

ELISAS

For the detection of antigen specific antibodies, 96-well Nunc MaxiSorp® 96-well maxisorp plates were coated with 5 μg/mL of LASV-GP1 overnight at 4°C. For the ELISA with the purified virus, VSV pseudotypes expressing the Lassa glycoprotein were used for the plate coating. Plates were washed 3 times with PBS/ 0.02% Tween-20 and blocked using a 2.5% casein solution in PBS for 2 hours at room temperature (RT). Serial dilutions of serum in casein were added to the blocked plates for 2 hrs at RT. Plates were washed 4 times and

mixed with detection antibodies against IgG1, IgG2c, IgG3 or total IgG (Southern Biotech). All secondary antibodies were conjugated to horseradish peroxidase (HRP). After incubation of 1h at RT, plates were washed 4 times and developed using 50 μL of TMB (eBiosciences). The signal was stopped by adding 20μL of 2N H_2SO_4. Plates were analyzed using a plate reader spectrophotometer (Tecan) by measuring the absorbance at 450nm with correction at 570nm.

Preparation of lymph node and spleen suspensions

Lymph nodes were opened with needles and digested in DMEM (1.2mM $CaCl_2$, 2% FBS, Pen/Strep) containing collagenase D (500μg/mL). After digestion, lymph node cell suspensions were filtered through a 70 μm nylon cell strainer. For spleen, single cell suspensions were prepared by mechanical disruption through a 70μm nylon cell strainer. Splenocytes were further treated with hypotonic ammonium chloride–potassium bicarbonate buffer to lyse red blood cells.

***Ex vivo* restimulation**

Up to $3x10^6$ cells were plated in 96-well plates and cultured in 10% FBS -DMEM medium for 2 hours at 37°C in the presence of 200 μg/mL of LASV-GP1. As a negative control, we restimulated with the Fc portion of the human IgG antibody, in order to make sure that no remaining Fc was present in the protein. For retention of intracellular cytokines, 5 μg/mL of Brefeldin A was added to the culture and left for 3 hours. Finally, cells were washed in PBS to proceed with staining for flow cytometry.

Flow cytometry

Up to $3x10^6$ cells were plated in 96 well plates and washed once with HBSS for staining with live/dead fixable cell viability reagent (Life technologies). For surface staining, cells were washed once with HBSS supplemented with 0.5% bovine serum albumin (BSA, Sigma) (staining buffer) and resuspended in an antibody cocktail using monoclonal antibodies. For intracellular staining, cells were fixed and permeabilized with the Foxp3 / Transcription Factor Fixation/Permeabilization kit (eBiosciences) according to the manufacturer's instructions. Cells were stained in permeabilization buffer with a cocktail of monoclonal antibodies. After staining, cells were resuspended in staining buffer for analysis by flow cytometry.

Peptide array (Celluspots™)

Celluspots™ (Intavis) slides were blocked with PBS-Tween 0.02% containing 5% milk for 1h, followed by 2h incubation at room temperature with mice sera (1/200 dilution in PBS-Tween 0.02% containing 5% milk). Slides were further washed 3 times (5 min each) with PBS-Tween 0.02% and incubated with an anti-IgG HRP-conjugated antibody (diluted 1/2000 in PBS Tween 0.02%, and 5% milk) for 1h. Finally slides were washed 3 times for 5 min each with Tween 0.02% containing and 5% milk. The epitopes were revealed by further incubation with SuperSignal™ West Pico Chemiluminescent Substrate (LifeTechnologies) and transferred on an X-ray film.

Data collection

Flow cytometry was performed using a CyAn^{TM} ADP (Beckman Coulter) and data were analyzed with FlowJo (Tree Star). We used 1-way ANOVA, followed by a Bonferroni post-test to find differences between the groups. A *P* value of less than 0.05 was used as an indicator of statistical significance. All data was analyzed using the GraphPad Prism 5 Software (GraphPad Software Inc., La Jolla, CA). All data presented as bar graphs represent the mean ± standard deviation.

4.4 RESULTS

LASV-GP1-Fc fragment production

Induction of antibodies targeted against surface receptor binding proteins in viruses is particularly attractive as it prevents host cell receptor binding and entry.

The LASV-GP1 construct was generated by fusing a cDNA fragment containing the codon optimized LASV-GP1 sequence (provided by Prof. Erica Ollman Saphire, Scripps Research Institute, La Jolla) with human IgG1 Fc by PCR cloning in order to allow for better expression in mammalian cells, and also to allow purification via Protein A affinity chromatography from cell culture supernatants. The constructs contained an enterokinase (EK) cleavage site sequence to allow for the removal of the Fc portion during protein purification (Fig4-1,A).

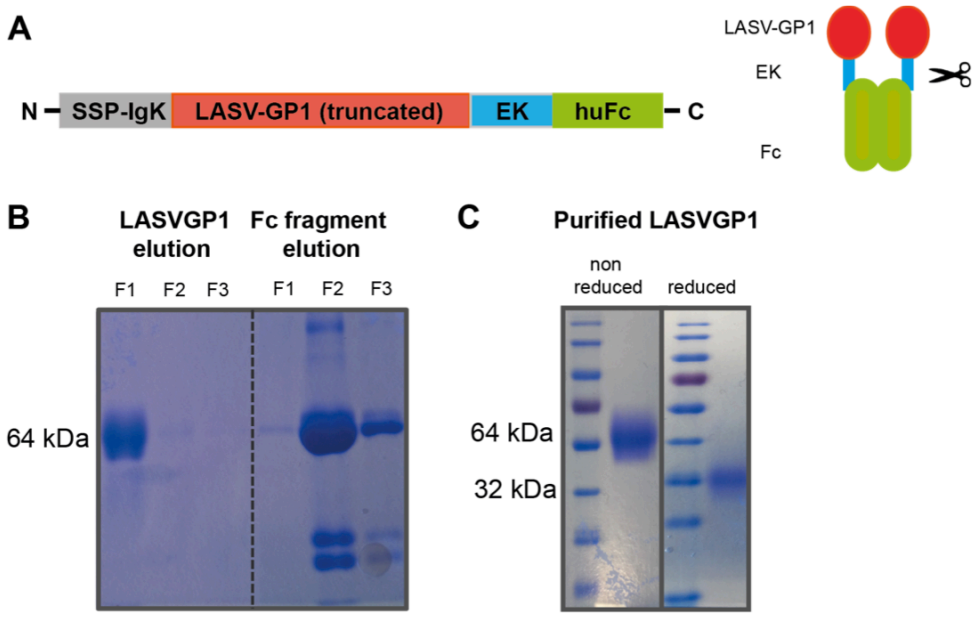

Figure 4–1 Production of the recombinant LASV-GP1. A) Schematic of the LASVGP1-EK-Fc construct. **B)** Purification of LASVGP1-EK-Fc. Supernatants of transfected HEK293T cells were subjected to protein A purification. Elution was performed by EK cleavage of LASV GP1-EK-Fc bound to the protein A column under neutral pH. The gel shows the Coomassie staining of three eluate fractions of LASVGP1 protein after EK cleavage (LASV GP1 F1-3) and three fractions of the Fc fragment retained on the protein A column, after acidic elution (Fc fragment F1-3). The LASV GP1 elutes as a single broad band of 60-65 kDa. **C).** SDS-PAGE under non-reducing (non reduced) and reducing (reduced) conditions of the purified LASV-GP. The extrapolated apparent molecular masses are indicated.

Large-scale production of the resulting LASV-GP1-EK-Fc construct was achieved by expression in HEK293T cells. After 5 days of culture, the crude supernatants were passed though a protein A column for binding to the Fc portion of the protein. After extensive washing, the LASV-GP1 was cleaved by adding EK and eluted under neutral pH and physiological ionic strength. The EK binding site allowed for the elution of the purified LASV-GP1 directly from the protein-A column, without the requirement of acidic elution procedures, which could have interfered with the native LASV-GP1 conformation. The eluted LASV GP1

was generally > 95% pure, as assessed by SDS-PAGE and Commassie blue staining (Fig4-1, B). Next, the LASV GP1 was subjected to ion exchange chromatography (IEC) to eliminate further impurities and to remove the remaining EK. IEC-purified LASV GP1 was then dialyzed against PBS to remove the salts contained in the buffer and concentrated it to 2 mg/ml for further encapsulation into PSs.

During the IEC we observed that the purified LASV-GP1 had a molecular weight (MW) between 62-64kDa, indicating that the protein exists mainly as a dimer. We corroborated this dimeric form by running the protein in reducing versus non-reducing conditions, where a band representing the LASV monomer appeared at approximately 34 KDa under reducing conditions (Fig4-1, C). The dimerization likely occurs as a consequence of an unpaired cysteine residue present at the N-terminus of the protein.

LASVGP1 loads efficiently into Polymersomes

Our first goal was to determine if LASV-GP1 (LASVGP1 hereafter) could be loaded into PSs. For this purpose, we fluorescently labeled LASVGP1 with the AF-594 dye, and mixed 1 mg of the labeled protein with 30 mg of the dried PEG-PPS copolymer. After a 48hr incubation time at 4°C, we extruded and purified the PSs by gel filtration chromatography. The collected fractions revealed that the signal from LASVGP1 was localized in the same fractions where PSs routinely elute, indicating antigen loading (Fig4-2, A). To assess that the loaded protein was not degraded or damaged during the loading, we dissociated the PSs with PBS/0.5% Triton-X100, and analyzed the solution by gel electrophoresis. The protein released from the PSs displayed the same MW, close to 70kDa, as the free counterpart (Fig4-2, B). The data suggests that no damage has been caused to LASVGP1 during the PSs encapsulation, and furthermore, indicates that LASVGP1 encapsulates as a dimer within PSs.

We measured the size of the PSs loaded with LASVGP1, and found that, on average, PSs had a size of 163nm ±7 nm, with a polydispersity index of 0.1 ± 0.05. Thus, we successfully formed carriers loaded with the glycoprotein1 from LASVGP1.

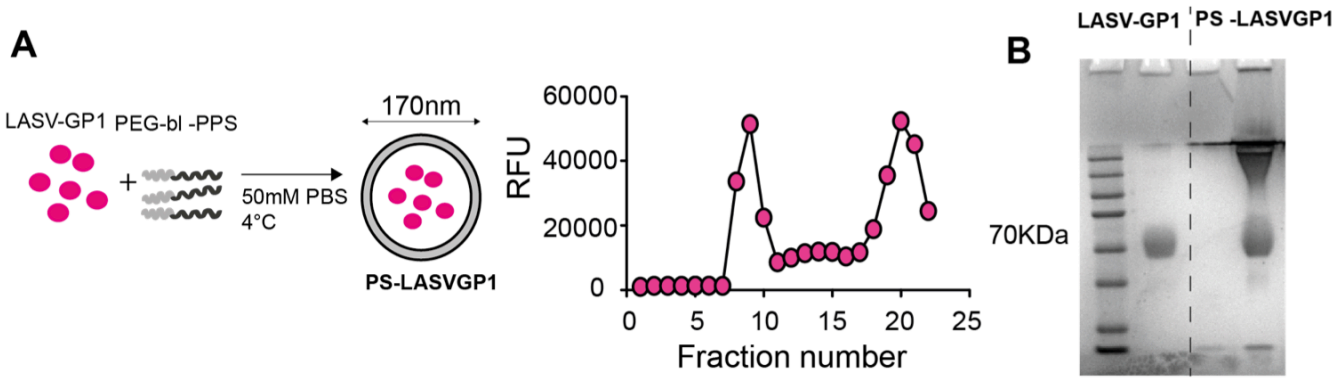

Figure 4–2 Loading of LASVGP1 glycoproteins into Polymersomes (PSs). A) Left, Schematic of the protein encapsulation into PSs. Right, Elution of fluorescently labeled LASVGP1 protein after mixing with the PEG-PPS block-copolymers. Signal from the loaded protein appears at earlier fractions (8-10), while non encapsulated protein is retained for a longer time in the column, and appears at fractions >17. **B)** SDS-PAGE gel under non-reducing conditions. *Right*, the purified LASVGP1, *left*; PS (LASVGP1) after disruption of the vesicles with a solution of Triton X-100.

Polymersomes loading enhances CD4 T cell responses and humoral responses to LASV-GP1

Several groups have demonstrated that particle-loading both antigen and adjuvant synergistically enhances the immune response, since both components drain at similar rates and can be targeted to DCs residing at similar locations [15–17].

We therefore took advantage of the amphiphilic nature of the TLR-4 ligand MPLA for entrapping in the PSs during the rehydration of the PEG-PPS polymer. To measure the amount of MPLA loaded into PSs, we fluorescently labeled the lipidic molecule as described in Fig 4-3. After extrusion and purification, we calculated the amount of MPLA loaded based on the fluorescent signal, and found an average of 400µg/mL of MPLA in the PSs. With this formulation, we then evaluated the immunogenicity of the LASVGP1 proteins when encapsulated in PSs, co-delivered with MPLA formulated or as a soluble compound.

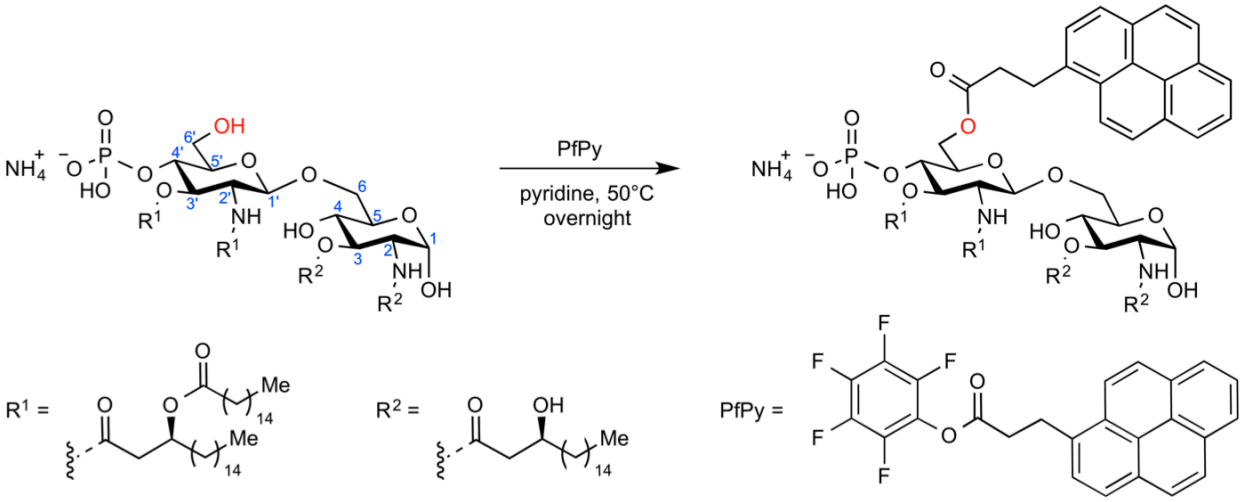

Figure 4–3 Labeling strategy of MPLA. MPLA was labeled with pentafluorophenol pyrene active ester (PfPy) for its detection upon loading into PSs.

Mice were immunized two times in three weeks intervals with unformulated LASV or PSs containing 10µg of LASV (LASV or PS-LASVGP1, respectively), both in combination with 10µg of MPLA unformulated or loaded into PSs (MPLA or PS(MPLA)) (Fig4-4, A). After 5 days, we collected the spleen and draining lymph nodes (LNs), and evaluated the CD4 responses by an *ex vivo* restimulation assay, using the purified LASVGP1 as stimulant. As a control, we used the human Fc portion, in order to make sure that the CD4 T cell responses are indeed targeted to the viral protein, and not to immunogenic Fc fragments that might have not be removed by the enterokinase treatment.

There was an enhancement of the CD4 T cell immune response in LNs and spleen in the groups where the LASVGP1 was encapsulated, indicating that the immunogenicity of the glycoprotein was augmented upon formulation into PSs. As expected, no response was produced upon human-Fc restimulation. In the LNs and spleen, PS-LASVGP1 groups promoted a 3-fold and 7-fold higher secretion of IFNγ and TNFα by CD4 T cells over the

LASVGP1+PS(MPLA) group, and a prominent 20-fold and 10-fold change when either the protein or the adjuvant were encapsulated (Fig4-4, B).

While free LASVGP1 administered with PS-MPLA displayed an enhanced CD4 cellular response over the soluble protein and MPLA, the effect was much lower than that observed with the encapsulation of the protein. It was also interesting that between the groups where LASVGP1 was encapsulated there were no major differences in the immune response. It is possible that MPLA also incorporated or adsorbed to the PSs surface after their formation. Indeed, when fluorescently labeled MPLA and pre-formed PS were mixed together and eluted in a size exclusion column, both components ran together, while MPLA alone without PSs displayed a higher retention time in the column (data not shown).

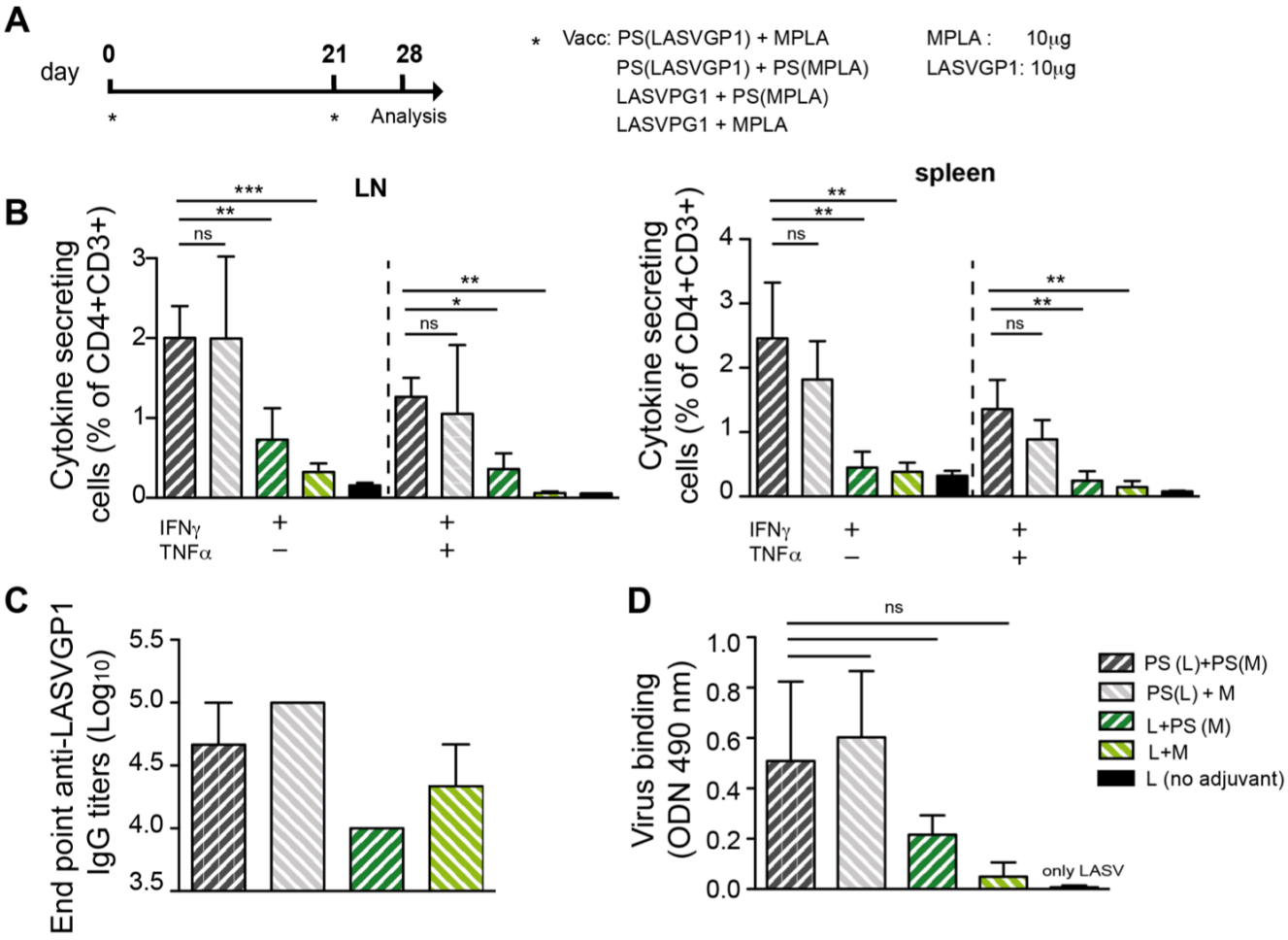

Figure 4–4 Intradermal (i.d.) immunization with PS(LASVGP1) conjugates enhance antigen specific CD4 T cell responses A) Immunization timeline **B)** Cytokine secreting CD4 T cells in spleen and draining lymph nodes five days after a prime-boost immunization. Lymphocytes were restimulated *ex vivo* with LASVGP1 protein or with the human Fc fragment as a control in the presence of Brefeldin A; cytokine expression was assessed by intracellular staining **C)** LASVGP1 serum antigen-specific antibody titers at day 28, one week after the booster immunization. **D)** Virus binding of serum antibodies at day 28, as a control, we included the serum of mice that received only LASVGP1 protein, without adjuvant. L, LASVGP1; M, MPLA. * < *p* 0.05 ; ***p* < 0.01 ; *** *p* < 0.001

We also evaluated the humoral responses, and found robust antibody titers in all the immunizations (Fig4-4, C). There was a modest increase in the total IgG antibody titer when antigen was delivered in the PSs. Notably, we found a 3-10 times greater IgG antibody binding between the PS-LASVG1 and the soluble protein groups when instead of the purified protein we used a purified whole virus as antigen during the ELISA assay (Fig4-4, D), indicating a better recognition of the LASVGP1 in its native conformation by antibodies induced upon protein encapsulation. Overall, the data suggest that antigen formulation has a positive impact on cellular responses, as well as in the quality of humoral responses.

Effect of adding multiple TLR adjuvants on the humoral response against LASVGP1

It has been widely reported that multiple TLR ligation actuates synergistically the outcome of an immune response[16,18–20]. We wanted to evaluate the effect of co-administration of MPLA with TLR-7 and TLR-9 agonists on the antibodies against LASVGP1. Therefore, groups of mice were immunized with PS-LASVGP1 together with a) 10μg MPLA, b) 10μg MPLA + 10μg CpG-B, c) 10μg MPLA + 50μg R848 and finally, d) 10μg MPLA+10μgCpG-B+50μg R484 (Fig 4-5, A).

By day 28, one week after the booster immunization, we looked at serum for LASVGP1 specific IgG antibody titers and IgG antibody isotypes. Compared with our previous immunization, this time the free LASV group displayed an enhancement of total IgG titers over the PS-LASVGP1. When looking at the effect of the multiple TLR adjuvant formulation, we observed that groups containing CpG-B exhibited the highest enhancement in antibody titers. In contrast, in the PS-LASVGP1 group, the incorporation of R848 had almost no effect on the humoral response (Fig 4-5, B).

Analysis of the antibody subtypes displayed similar trends to those observed with total IgG, although the differences between the free antigen and PS-loaded antigen in the groups with two or three adjuvants were more noticeable (Fig 4-5, C). All the groups displayed high IgG2c antibodies, as expected from the Th1-skewing capacity of the chosen TLRs. Interestingly, we observed that groups that contained CpG-B had increased IgG3 antibodies, although the serum levels of this antibody subclass were generally low.

We then analyzed the capacity of the serum IgG to recognize the LASVGP1 in its native conformation using the whole virus ELISA assay. As observed earlier, the PS loading enhanced the recognition of the native glycoprotein over unformulated LASVGP1 (Fig 4-6, A). Notably, the only class subtypes able to recognize the LASVGP1 were the IgG2c and IgG3 isotypes, while no signal was observed with IgG1 (Fig 4-6, B).

Finally, in order to determine which regions over the entire LASVGP1 protein were recognized by the elicited antibodies, we incubated the immunized serum with a peptide array displaying 20mer peptides spanning the LASVGP1 antigen with an offset of 1 aminoacid. We studied mainly the PS(LASVGP1) immunization adjuvanted with MPLA. Antibodies induced upon free LASVGP1 immunization recognized mainly the C terminus of the protein. Moreover, PSs promoted that various regions within the LASVGP1 were recognized, suggesting that PS loading promoted a broadening of the antibody targeting

Overall, the data ratifies that PSs enhanced the quality of the immune response to LASVGP1.

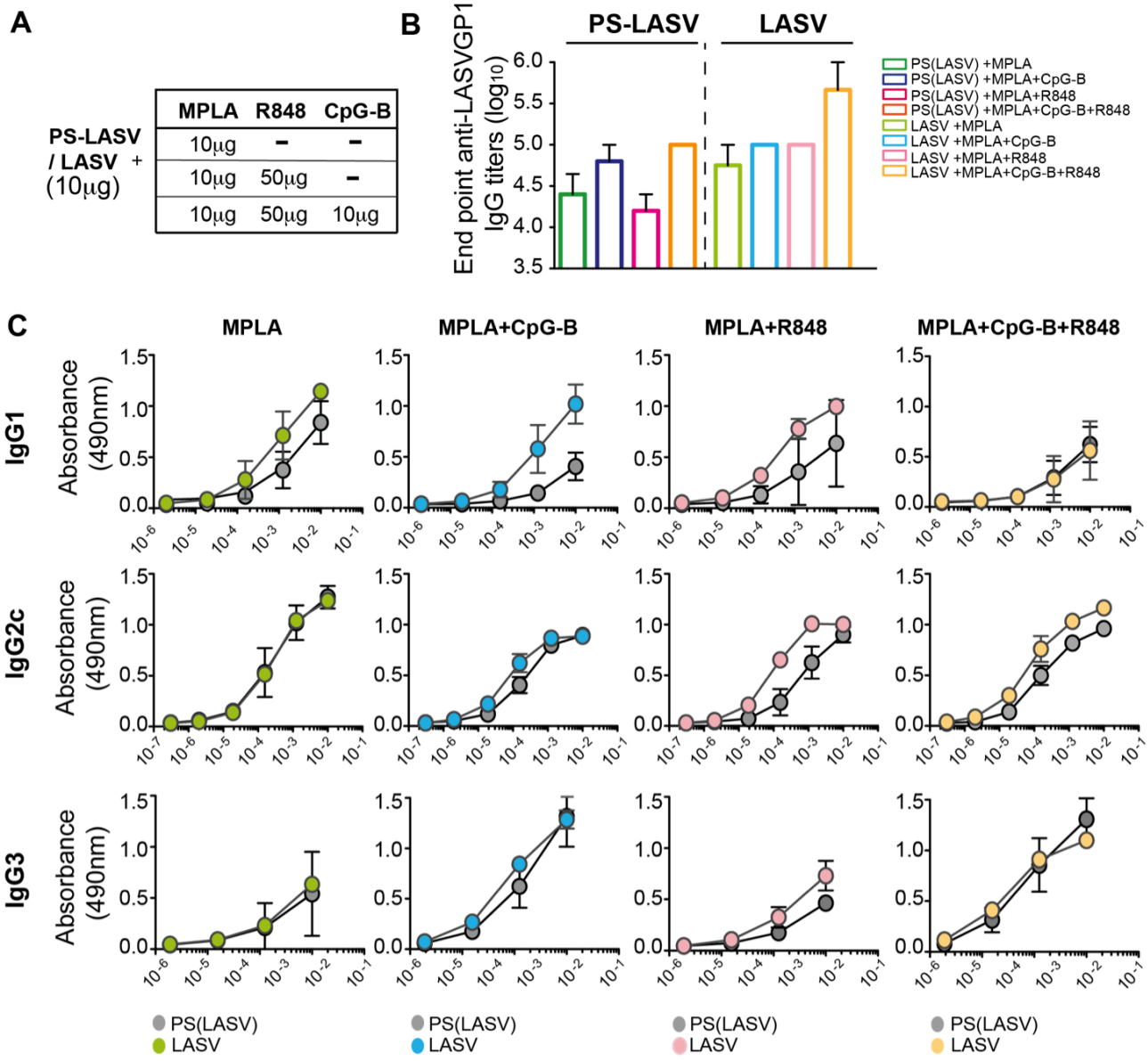

Figure 4–5 Addition of the unformulated TLR adjuvants to the PS(LASV)-MPLA immunization does not enhance the magnitude of the humoral response. A) Adjuvants (doses) used in the study. **B)** End point titers by day 28, one week after the booster immunization. **C)** LASV-specific IgG antibody subtypes at day 28, one week after the booster immunization.

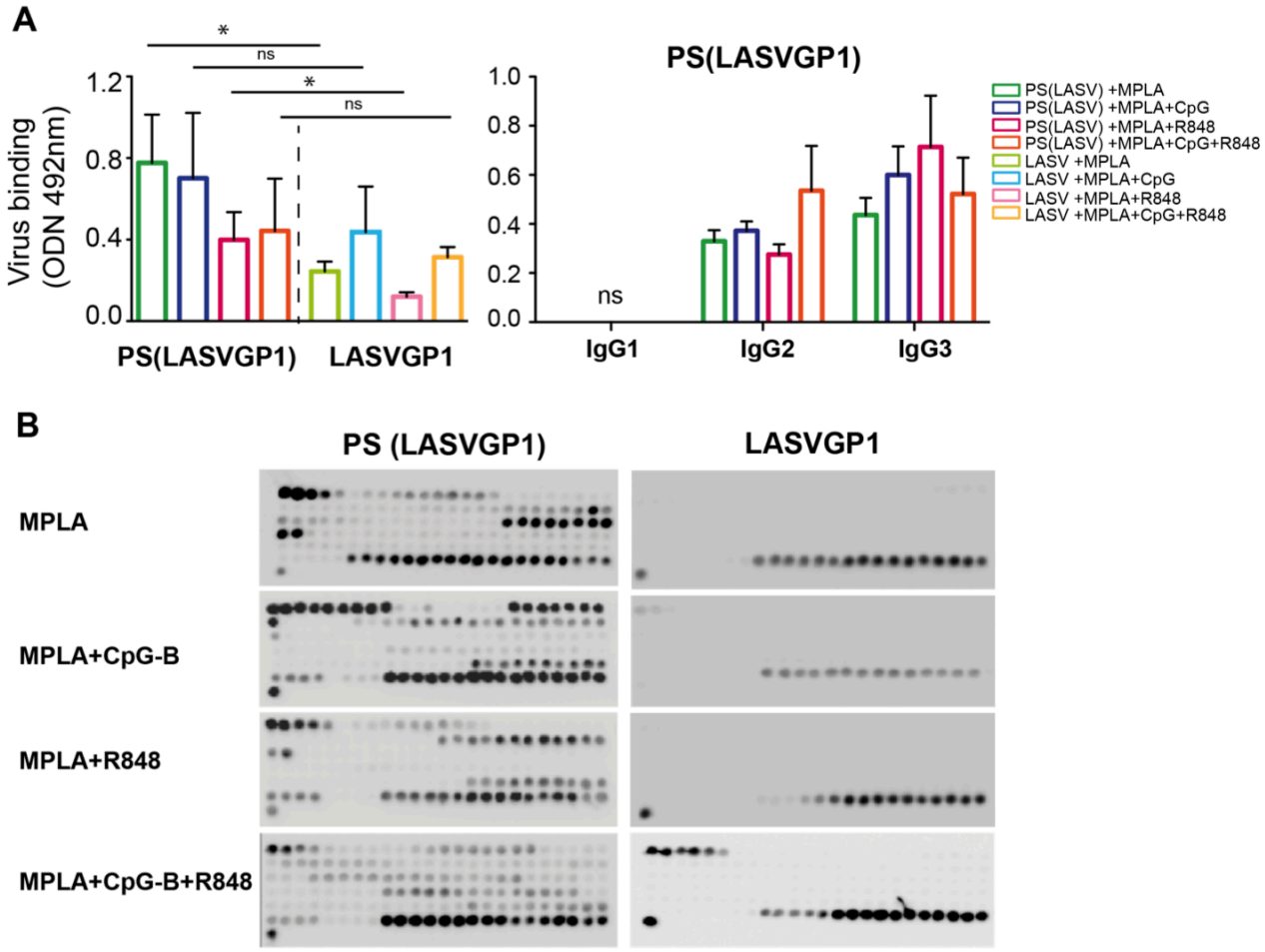

Figure 4–6 Virus binding and epitope recognition by serum antibodies elicited after LASVGP1 and PS(LASVGP1) immunization. A) Total LASVGP1 specific IgG serum antibodies (left) and IgG subtypes (right) binding to the virus-ELISA assay. **B)** Epitope array displaying the regions recognized by serum antibodies after administration with single or multiple TLR ligands.

4.5 DISCUSSION

Live attenuated vaccines have been used successfully during the last few decades as vaccine platforms [21,22]. However, their use in regions where endemic diseases, such as HIV, prevail is highly debated since the risk of the vector reverting to a virulent form defeats the benefits of vaccination. On the contrary, protein subunit vaccines are a great and safe alternative to standard methods of immunization [23]. Loading proteins and adjuvants into nanocarriers can further increase the effectiveness of subunit vaccines. These carriers drive the antigen to lymphoid tissue, enhance DC uptake and increase antigen presentation [24–27]. Moreover, particulates offer the advantage of homologous prime-boost regime immunizations, which is not desired with viral vectors because of the host immune response to the proteins of the carrier, which diminishes their effectiveness [28].

Herein, we demonstrated that the preparation of a stable LASV glycoprotein1 protein is feasible. Furthermore, we investigated the impact on the immunogenicity of LASVGP1 after loading into PSs. We optimized the vaccine formulation with the TLR-4 adjuvant MPLA, and demonstrated that loading into PSs elicited antigen specific CD4 T cellular responses as well as robust humoral responses.

In terms of antibody titers, the PSs encapsulation does not surpass the response induced by the soluble protein when administered with MPLA. However, the most important finding is that the antigen encapsulated in the PSs platform qualitatively changed the immune response in two ways: one, by enhancing the recognition of the LASVGP1 when presented in its native conformation; and two, by broadening the serum antibody targeting regions, as seen by the increase in peptides recognized by the PS-LASVGP1 serum. Similarly to our previous results, the PSs drove a Th1-like response, characterized by a strong induction of serum IgG2c antibodies, and enhanced secretion of IFNγ and TNFα by antigen specific CD4 T cells. Furthermore, we showed that the antibody subclasses responsible for virus binding were the IgG2c and IgG3, which underscore the importance of inducing a Th1-like humoral response for a LASV vaccine.

While the precise mechanism underlying the quality of the humoral response is unknown, we speculate that the capacity of the PSs carriers to promote T follicular helper CD4 responses, as detailed in our previous chapter, is partially responsible for the observed results. This CD4 T cell subset provides critical signals to B cells in order to initiate somatic hypermutation and affinity maturation, therefore their increased number could augment survival signals for B cells and thus sustain their differentiation into long lived plasma cells or memory B cells [29] . Instead, in the soluble protein the Tfh cell numbers could have been a limiting factor, thus only few B cell clones could survive.

Interestingly, in our system the addition of TLRs had little effect on the total serum IgG titers in the groups when LASV was delivered within PSs, while modestly enhanced serum titers in the LASV free group. However, it is important to note that CpG-B and R848 were not formulated into particulates for these experiments, and thus it is likely that the antigen and the adjuvant did not target the same antigen presenting cells simultaneously when LASVGP1 was encapsulated. For instance, Kasturi *et al.* [15] reported that a dual TLR vaccine enhanced memory B cell responses due to signaling through TLR receptors on the same B cells, which

is likely not happening in our system, since all the adjuvants used varied in their molecular weights and thus, in their lymphatic drainage and cell targeting. Nevertheless, we observed that the addition of TLRs further diversifies the antibody repertoire, in agreement with previous reports [30], although it happened uniquely when LASVGP1 was delivered within PSs. These results suggest that the antigen encapsulation is a crucial parameter for enhancing the quality of humoral responses, and also indicates that the response can be further improved by formulating additional adjuvants into PSs.

In summary, we have demonstrated the feasibility of developing a safer subunit vaccine based on the PS platform against a neglected disease as Lassa fever. We are currently evaluating the protective capacity of our vaccination by employing a pseudotyped viral challenge, using the LCMV-Lassa glycoprotein chimeras described recently by Sommerstain *et al.* [31]. Furthermore, we are trying to formulate novel TLR7 agonists into PSs in order to determine if adjuvant formulations allow for further amplification of the immune response.

4.6 REFERENCES

1. Charrel, R. N., de Lamballerie, X. & Emonet, S. Phylogeny of the genus Arenavirus. *Curr. Opin. Microbiol.* **11,** 362–368 (2008).
2. Ölschläger, S. & Flatz, L. Vaccination Strategies against Highly Pathogenic Arenaviruses: The Next Steps toward Clinical Trials. *PLoS Pathog.* **9,** e1003212 (2013).
3. Shaffer, J. G. *et al.* Lassa Fever in Post-Conflict Sierra Leone. *PLoS Negl. Trop. Dis.* **8,** e2748 (2014).
4. Flatz, L. *et al.* T cell-dependence of Lassa fever pathogenesis. *PLoS Pathog.* **6,** e1000836 (2010).
5. Jahrling, P. B. & Peters, C. J. Passive antibody therapy of lassa fever in cynomolgus monkeys: Importance of neutralizing antibody and lassa virus strain. *Infect. Immun.* **44,** 528–533 (1984).
6. Jahrling, P. B., Peters, C. J. & Stephen, E. L. Enhanced treatment of Lassa fever by immune plasma combined with ribavirin in cynomolgus monkeys. *J. Infect. Dis.* **149,** 420–427 (1984).
7. McCormick, J. B. *et at.* Lassa fever. *N. Engl. J. Med.* **314,** 20-26 (1986)
8. McCormick J. B., Mitchell S. W., Kiley M. P. & Ruo S. Inactivated Lassa virus elicits a non protective immune response in rhesus monkeys. *J. Med. Virol.* **37,** 1-7 (1992).
9. Fisher-Hoch, S. P., Hutwagner, L., Brown, B. & McCormick, J. B. Effective vaccine for lassa fever. *J. Virol.* **74,** 6777–6783 (2000).
10. Pushko, P., Geisbert, J., Parker, M., Jahrling, P. & Smith, J. Individual and bivalent vaccines based on alphavirus replicons protect guinea pigs against infection with Lassa and Ebola viruses. *J. Virol.* **75,** 11677–11685 (2001).
11. Geisbert, T. W. *et al.* Development of a new vaccine for the prevention of Lassa fever. *PLoS Med.* **2,** 537–545 (2005).
12. Jiang, X. *et al.* Yellow fever 17D-vectored vaccines expressing Lassa virus GP1 and GP2 glycoproteins provide protection against fatal disease in guinea pigs. *Vaccine* **29,** 1248–1257 (2011).
13. Burton, D. R. Antibodies, viruses and vaccines. *Nat. Rev. Immunol.* **2,** 706–713 (2002).
14. Botten, J. *et al.* A multivalent vaccination strategy for the prevention of Old World arenavirus infection in humans. *J. Virol.* **84,** 9947–9956 (2010).
15. Kasturi, S. P. *et al.* Programming the magnitude and persistence of antibody responses with innate immunity. *Nature* **470,** 543–547 (2011).
16. Ilyinskii, P. O. *et al.* Adjuvant-carrying synthetic vaccine particles augment the immune response to encapsulated antigen and exhibit strong local immune activation without inducing systemic cytokine release. *Vaccine* **32,** 2882–2895 (2014).
17. Manuscript, A. Nano-microparticles as immune adjuvants: correlating particle sizes and the resultant immune responses. *Expert Rev. Vaccines* **9,** 1095–1107 (2011).
18. Querec, T. *et al.* Yellow fever vaccine YF-17D activates multiple dendritic cell subsets via TLR2, 7, 8, and 9 to stimulate polyvalent immunity. *J. Exp. Med.* **203,** 413–424 (2006).
19. Orr, M. T. *et al.* A dual TLR agonist adjuvant enhances the immunogenicity and protective efficacy of the tuberculosis vaccine antigen ID93. *PLoS One* **9,** e83884 (2014).
20. Kasturi, S. P. *et al.* Programming the magnitude and persistence of antibody responses with innate immunity. *Nature* **470,** 543–547 (2011).
21. Siegrist, C. Vaccine immunology 2. 14–32

http://dx.doi.org/10.1016/B978-1-4557-0090-5.00004-5.

22. Tomai, M. a & Vasilakos, J. P. TLR7/8 Agonists as Vaccine adjuvants. (2013). doi:10.1007/978-1-4614-5380-2
23. Pulendran, B. & Ahmed, R. Immunological mechanisms of vaccination. *Nat. Immunol.* **131,** 509–517 (2011).
24. Irvine, D. J., Hanson, M. C., Rakhra, K. & Tokatlian, T. Synthetic Nanoparticles for Vaccines and Immunotherapy. *Chem. Rev.* (2015). doi:10.1021/acs.chemrev.5b00109
25. Gregory, A. E., Titball, R. & Williamson, D. Vaccine delivery using nanoparticles. *Front. Cell. Infect. Microbiol.* **3,** 1–13 (2013).
26. Reddy, S. T., Swartz, M. a & Hubbell, J. a. Targeting dendritic cells with biomaterials: developing the next generation of vaccines. *Trends Immunol.* **27,** 573–579 (2006).
27. Zhao, L. *et al.* Nanoparticle vaccines. *Vaccine* **32,** 327–337 (2014).
28. Draper, S. J. & Heeney, J. L. Viruses as vaccine vectors for infectious diseases and cancer. *Nat. Rev. Microbiol.* **8,** 62–73 (2010).
29. Crotty, S. Follicular helper CD4 T cells (TFH). *Annu. Rev. Immunol.* **29,** 621–663 (2011).
30. Wiley, S. R. *et al.* Targeting TLRs expands the antibody repertoire in response to a malaria vaccine. *Sci. Transl. Med.* **3,** 93ra69 (2011).
31. Sommerstein, R. *et al.* Evolution of Recombinant Lymphocytic Choriomeningitis Virus/Lassa Virus In Vivo Highlights the Importance of the GPC Cytosolic Tail in Viral Fitness. *J. Virol.* **88,** 8340–8348 (2014).

Chapter 5

Lymphatic endothelial cells scavenge and process exogenous antigen *in vivo* under steady and inflammatory conditions

Marcela RINCON RESTREPO, Efhtymia VOKALI, Sachiko HIROSUE and Melody SWARTZ

5.1 ABSTRACT

Recently there have been described “atypical” modes of antigen presentation by non-hematopoietic cells. In this study, we demonstrated that lymph node lymphatic endothelial cells (LN-LECs), one of main subsets of stromal cells in LNs, selectively internalized and processed foreign exogenous antigen *in vivo*, both during non-inflammatory and inflammatory conditions. Interestingly, in lymphangiogenic LNs LECs displayed a higher uptake of antigen, indicating that, similar to classical antigen presenting cells, LECs can actively sense and integrate dangerous extracellular signals, and thus augment antigen internalization. We assessed whether by interfering with the development of LN lymphangiogenesis by blocking the signalling through VEGFR3 we could gain some insights into the effects of proliferative LECs on adaptive immune responses. However, in our studies we could not demonstrate an effect of blocking VEGFR-3 in reducing LN lymphangiogenesis, perhaps due to the usage of other signaling receptors to promote LEC proliferation. Thus, we suggest that future studies to evaluate the functional roles of stromal cell presentation in adaptive immune responses should be evaluated with more specialized animal models, involving lymphatic-specific conditional ablation of components of the antigen presentation machinery, that will allow a better understanding of the consequences of antigen scavenging by LECs on vaccine-elicited immunity.

5.2 INTRODUCTION

Lymphatic endothelial vessels represent the port of entry of migratory cells, solutes and peripheral antigens that drain from distal sites to lymph nodes (LNs)[1]. LNs are highly structured organs that enhance adaptive immune responses by facilitating the interactions between peripheral solutes and antigen presenting cells (APCs), as well as the encounter of APCs with circulating lymphocytes [2,3]. This is achieved thanks to the LN stroma architecture, composed of a heterogeneous population of non-hematopoietic cells that play important roles in cell trafficking, LN compartmentalization and antigen distribution [4]. The main LN stromal cell subsets are distinguished based on their expression of podoplanin (gp38) and CD31 on fibroblastic reticular cells (FRCs, gp38+CD31-), lymphatic endothelial cells (LECs, gp38+ CD31+), blood endothelial cells (BECs, gp38-CD31+) and a group of double negative cells (DN, CD31-gp38-) [5,6].

Recently, cumulative evidence indicates that stromal cells in LNs not only represent a passive scaffold, but also can play active roles in the regulation of adaptive immunity. For instance, FRCs and LECs can express and present peripheral tissue restricted antigens (PTAs) to CD8 T cells, leading to CD8 T cell tolerance [6,7]. Moreover, Lund *et al.* recently showed that antigen presentation is not only restricted to PTAs, since LECs in tumor draining LNs scavenge and cross-present antigens derived from the tumor. In this scenario, the atypical antigen presentation by LECs led to the induction of CD8 T cells that were dysfunctional and apoptotic [8], suggesting that the interactions between LECs and CD8 T cells have mainly tolerogenic outcomes.

It has been widely observed that during various inflammatory events such as viral infections, subunit immunizations and during cancer, there is a noticeable increase in LEC proliferation in draining LNs, which is termed LN-lymphangiogenesis[8–12]. The main modulators of LN-lymphangiogenesis are members of the VEGF family of growth factors. Among the most important factors are VEGF-C and VEGF-D, which signal through VEGFR-3, a tyrosine kinase receptor whose expression is restricted to the lymphatic endothelium in adults.

LN-lymphangiogenesis was proposed as a mechanism to restore LN homeostasis after an inflammatory challenge by supporting lymphocyte egress[13]. However, there is limited information about the active role of proliferative LECs during an immune response. It was recently reported by Tamburini *et al.* that LECs can capture antigen during viral infections[14]. Notably, this antigen was stored for long periods of time in LECs, which positively correlated with antiviral CD8 T cell responses. What was most interesting was the fact that antigen storage appeared only during inflammatory conditions, and happened only in proliferative LECs. However, in these experiments, the author did not find antigen processing by LECs, and thus these cells played mainly a passive role, serving as a “depot” of antigen, perhaps for maintaining a pool of memory CD8 T cells.

Herein, we wanted to evaluate whether LN-LECs can scavenge and process foreign exogenous antigens in inflammatory and non-inflammatory conditions. For this purpose, we delivered intradermally (i.d.) different macromolecules to naïve mice, or mice pretreated with the TLR-9 ligand, CpG-B, that drives a potent inflammatory response. We showed that LN-LECs internalized and processed soluble Ovalbumin (OVA) 90 minutes after i.d.

administration, while 70KDa and 2000KDa Dextran remained excluded from the LEC population, being mainly taken up by macrophages.

Furthermore, we sought to evaluate which were the implications of antigen uptake by proliferative LECs during a subunit immunization in the outcome of adaptive CD8 T cell responses. For this purpose, we administered the antibody mF4-31C1, which blocks the signaling through VEGRF-3 and affects uniquely proliferative LECs [15], after the immunization with Nanoparticles OVA, together with CpG-B. We demonstrated a modest, although not significant reduction in the number of LN-LECs upon α–VEGFR3 treatment. However, there were not significant differences in the cellular composition of LNs, or any changes in the overall distribution of stromal cells. Consequently, analysis of adaptive immune responses also revealed no significant changes in the numbers and phenotype of expanding CD8 T cells. Although we do not discard the possibility that lymphatic proliferation might have an effect on adaptive responses, we conclude that the effect of solely blocking the VEGFR-3 pathway is either too small to be observed in our system, or there is a compensation of other signalling pathways that promote LEC expansion. We therefore conclude that evaluation of the immunomodulatory effect of LN lymphangiogenesis in vivo should involve selective *in vivo* models, or dual blocking therapy with anti VEGFR-3 and anti VEGFR2, since inflammatory lymphatic expansion is dependent on signalling through both receptors.

5.3 MATERIALS AND METHODS

Animals

C57BL/6 female mice, between 8-12 weeks of age, were purchased from Harlan (France). OTI mice were obtained from an in house colony. All animal experiments were performed under the approval from the Veterinary Authority of the Canton of Vaud (Switzerland) according to Swiss Law.

Nanoparticle preparation

For NP-ss-Ovalbumin preparation, 500μL of NPs previously activated with pyridyl disulfide (as described in Chapter3) were mixed with 286.6 mg of guanidine hydrochloride (GndHCl) to achieve a final concentration of 6M of GndHCl. The solution was filtered through a 0.22μm membrane (Millipore Corporation) and mix with 50μL of OVA at 40mg/mL. The mixture was left overnight at room temperature, and then purified by size exclusion chromatography through a Sepharose CL-6B column equilibrated in PBS. The concentration of OVA in the fractions obtained after purification was determined by a BCA assay following the manufacture's instructions (ThermoScientific). Before and after the coupling, the size of NPs was determined by dynamic light scattering with a Nano Zs Zetasizer (Malvern Instruments). The diameter of NPs varied between 35nm-40 nm.

Immunizations and adoptive transfers

All vaccines were administered i.d. into the 4 limbs. 10 μg of OVA conjugated to NPs were injected per mouse, together with 10 μg of CpG. Before the immunizations, OVA was filtered through a 0.22μm membrane (Millipore Corporation) to remove aggregates. All PSs and proteins batches were tested for endotoxin levels using a TLR activation assay based on HEK-Blue reporter cell lines (Invivogen) before immunization. For the blockage of LEC proliferation, either 500 μg (i.p.) or 100μg (i.d.) of α-VEGFR-3 neutralizing antibody (mF4-31C1, ImClone/Eli Lilly) or IgG control were administered one day before immunization, followed by two extra doses, three days apart between each administration.

For the adoptive transfer of naive antigen specific T cells, single cell suspensions were prepared from spleens of OTI mice. CD8 T cells were isolated using the EasySep™ Mouse T Cell Isolation Kit (Stemcell Technologies). Immediately after isolation, $1x10^6$ cells were adoptively transferred i.v. into naïve host mice.

In vivo antigen drainage and immunostaining

To determine whether LN LECs can actively capture antigens in vivo, fluorescently labeled OVA protein was administered into the limbs of mice and its distribution within various cells in the LN was analyzed after 90 min. C57BL/6 mice were injected intradermally (i.d.) with 15 μg OVA-AF647 in the limbs. After 90 min, mice were transcardially perfused with a heparinized saline solution containing 1 g/l glucose and 20 mM HEPES (pH 7.2). For immunostaining, brachial LNs were removed and fixed overnight in 1% paraformaldehyde in PBS (pH7.4). After three washes in PBS, LNs were embedded in a block of 2% agarose and sectioned (150 μm) using a vibratome (Leica). Sections were blocked in 0.5% of casein and further labeled using Abs against CD3ε (BD Pharmingen) and Lyve-1 (Reliatech). Images were

acquired on a Leica SP5 confocal microscope using an immersion 20x or 63x objective and processed using Imaris software (Bitplane).

Preparation of lymph node and spleen suspensions

Lymph nodes were opened with needles and first digested in DMEM (1.2mM $CaCl_2$, 2% FBS, Pen/Strep) containing collagenase IV (1mg/mL) and DNAse I (40μg/ml) to isolate lymphocytes. In a second digestion step in DMEM with collagenase D (1mg/mL) and DNAse I (40μg/ml), stromal lymph node cells were isolated for further analysis. After digestion, lymph node cell suspensions were filtered through a 70μm nylon cell strainer. For spleen, single cell suspensions were prepared by mechanical disruption through a 70μm nylon cell strainer. Splenocytes were further treated with hypotonic ammonium chloride–potassium bicarbonate buffer to lyse red blood cells.

***Ex vivo* reestimulation**

Up to $3x10^6$ cells were plated in 96-well plates and cultured in 10%FBS -DMEM medium for 2 hours at 37°C in the presence 200μg/mL of OVA. Afterwards, 5 μg/mL of Brefeldin A were added to the culture and left for 3 extra hours.

Flow cytometry.

Up to $3x10^6$ cells were plated in 96 well-plates and washed once with HBSS before staining with live/dead fixable cell viability reagent (Life technologies). For surface staining, cells were washed once with HBSS supplemented with 0.5% bovine serum albumin (BSA, Sigma) (staining buffer) and resuspended in an antibody cocktail using monoclonal antibodies. For intracellular staining, cells were fixed and permeabilized with the Foxp3 / Transcription Factor Fixation/Permeabilization kit (eBiosciences) according to the manufacturer's instructions. Cells were stained in permeabilization buffer with monoclonal antibodies. After staining, cells were resuspended in staining buffer for analysis by flow cytometry.

Data collection

Flow cytometry was performed using a CyAn™ ADP (Beckman Coulter) and data were analyzed with FlowJo (Tree Star). We used the non-parametric Mann-Whitney U test for statistical comparisons. A *P* value of less than 0.05 was used as an indicator of statistical significance. All data was analyzed using the GraphPad Prism 5 Software (GraphPad Software Inc., La Jolla, CA). All data presented as bar graphs represent the mean ± standard deviation.

5.4 RESULTS

Lymphatic endothelial cells capture antigen according to its physicochemical properties under steady state conditions

There is increasing evidence of the potential of stromal cells as antigen presenting cells. For instance, our group has recently shown that in tumor bearing mice, lymph node (LN) LECs presented tumor associated antigen to CD8 T cells, promoting proliferation and cytokine secretion by the activated cells [8]. Motivated by these studies, we wanted to determine whether antigen scavenging by LECs *in vivo* occurred also under steady state conditions, out of the tumor context, and how this uptake varied for antigens with different properties.

To evaluate the *in vivo* antigen uptake by LECs, fluorescently labelled Dextran and Chicken egg Ovalbumin (OVA) protein were used as model antigens. We injected 15μg of lysine fixable dextran (70KDa and 2000KDa), alone or together with 15μg of fluorescently labelled OVA intradermally (i.d.) into the upper limbs of naïve mice. After 90 min, we collected the brachial draining LNs, and analysed them by confocal microscopy for colocalization with Lyve-1, a marker almost exclusively found in LECs.

Already 90 min after administration, all the antigens were observed in the draining LNs (Fig5-1). We took a closer look of the lymphatic sinuses region, which is enriched with LECs, and found that in these areas most of the OVA protein was surrounded by Lyve1+ structures. The elongated shape of the Lyve1+ structures indicated that they undoubtedly correspond to LECs, and not macrophages that also express Lyve1 (Fig1A, top left).

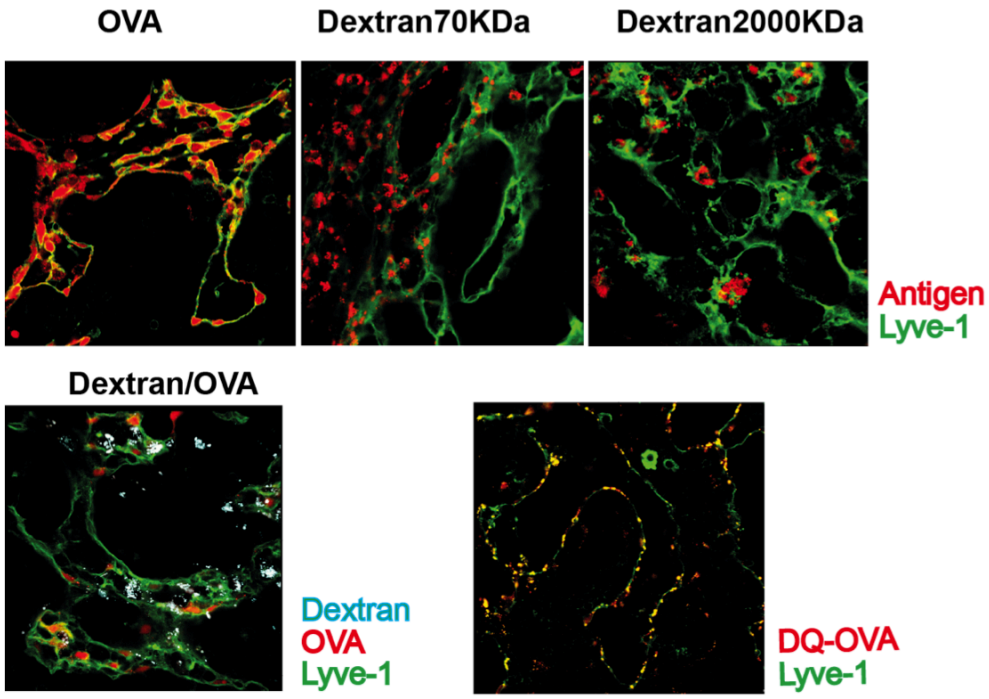

Figure 5–1 Antigen uptake by lymphatic endothelial cells in steady state conditions. Confocal images of brachial lymph nodes 90 minutes after intradermal (i.d.) administration of fluorescently labelled antigen (15μg).

Instead, the signal from both types of dextran was excluded from the LEC cytoplasm, and was most likely associated with macrophages lining the subcapsular sinuses, as reported in previous studies [16,17] (Fig5-1, top middle and right). The same results were obtained independently of whether Dextran (70KDa) was co-administered with OVA (Fig5-1, bottom left) or given alone (Fig1, middle and right). In order to evaluate if the antigen observed inside LECs was also being processed, we injected i.d. DQ-OVA, and analysed LNs 90 min after administration. DQ OVA is heavily labelled with a fluorophore that is autoquenched when the protein structure is intact, but that fluoresces upon proteolytic digestion. Indeed, we observed processing of OVA inside various LECs, as well as other populations in the subcapsular sinus, which could be macrophages (Fig5-1, bottom right)

Uptake of foreign protein antigen occurs in steady state and inflammatory conditions.

There is little information about LEC antigen uptake *in vivo* under inflammatory conditions, outside of the tumor context. We therefore wondered whether antigen uptake happens also in LNs that have been previously inflamed by the administration of a large dose of the TLR-9, CpG-B. We had previously observed that administration of this adjuvant promotes a marked cellular expansion in draining LNs, characterized by the proliferation and remodelling of the lymphatic architecture (LN-lymphangiogenesis).

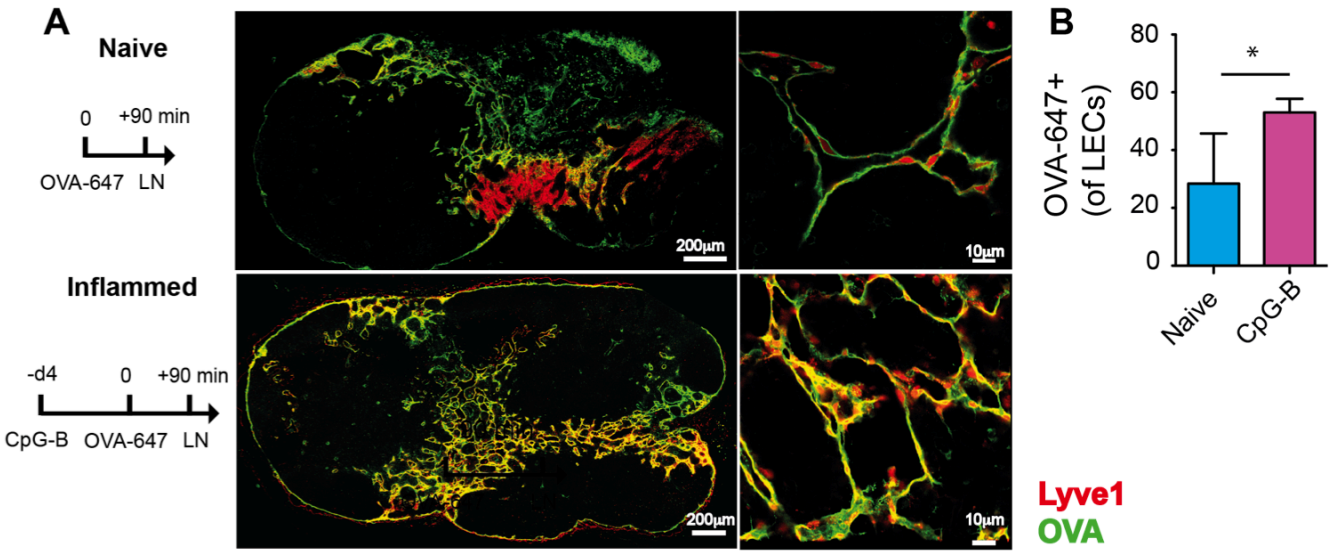

Figure 5–2 OVA uptake by lymphatic endothelial cells in draining lymph nodes in steady state conditions and inflammatory conditions. **A)** *Left*, experimental set up; *right,* confocal images of brachial lymph nodes 90 minutes after intradermal (i.d.) administration of fluorescently labelled OVA in naïve or CpG-B treated mice. **B)** Flow cytometry analysis of the OVA uptake by LECs (CD31+ gp38+) in naïve and CpG-B treated mice.

Mice received 30µg of CpG-B in the left and right side of the upper back, since this location also drains to the brachial LNs. Four days after, we injected fluorescently labelled OVA (15µg) i.d. in the upper limbs, and 90 min later collected brachial LNs for analysis by confocal

imaging and flow cytometry. As a comparison, we used mice that received saline instead of CpG-B (Fig 5-2).

The images clearly revealed that also under inflammatory conditions antigen was indeed taken up by LECs, similarly to the steady state condition. OVA was found in the cytoplasm of LECs, and this was true for all the regions of the LN analysed (Fig5-2, A). Analysis by flow cytometry also revealed that there was an increase in the frequency of OVA+ LECs in inflamed LNs (Fig5-2, B), suggesting that LECs, similarly to classical APCs, may also sense and integrate exogenous dangerous signals, and thus augment antigen internalization.

Administration of α-VEGFR3 during the course of an immunization does not have a significant impact on lymph node composition or lymphocyte activation

Most of the current studies about antigen presentation by LECs indicate that this subset is strongly tolerogenic. In tumors, our group has previously observed that reducing inflammatory lymphangiogenesis upon administration of an α-VEGFR3 antibody (αR3 hereafter) enhances the CD8 T cell antitumoral response [8]. In our studies, we wanted to determine whether this happens also in the context of a subunit immunization.

We decided to use the nanoparticle vaccine platform established in our laboratory, since with this system we can induce larger numbers of antigen specific CD8 T cells when compared to the free OVA, thus making it easier to detect potential changes happening upon the administration of the blocking antibody. Furthermore, these carriers can be also taken up by LECs, and the internalized antigen can be crosspresented to CD8 T cells [18].

We administered 3 doses (3 days apart) of 500μg or αR3 or IgG control, starting at day -1. At day 0, we vaccinated mice with NP-ss-OVA (10μg) together with 10μg of CpG-B, and at day 6 we evaluated draining LNs. As an extra control, we had a group that was not immunized, and did not receive an antibody treatment (Fig5-3, A).

Analysis by confocal imaging revealed no major differences in the lymphatic architecture in LNs between the IgG and the αR3 treated groups (Fig5-3, B). We only observed a reduction of Lyve1+ structures within medullary sinuses in the αR3 treated mice, although this is only a qualitative observation, and its verification would require further analysis. Next, we studied by flow cytometry the numbers of LN-LECs after the diverse treatments, based on the expression of CD31 and gp38 (Fig5-3, C).

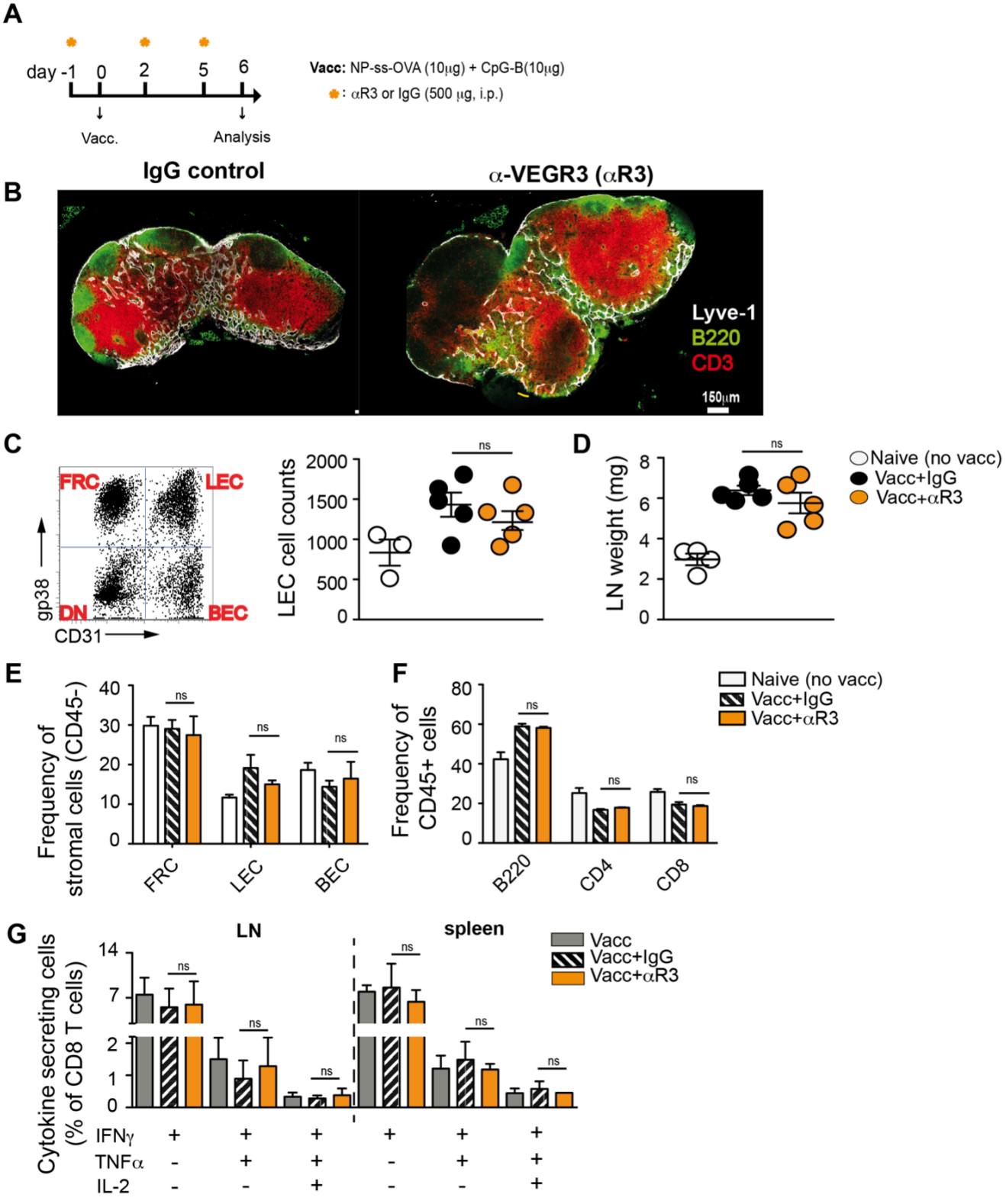

Figure 5–3 Intravenous α-VEGFR3 treatment has no effect on the cellular composition of draining lymph nodes after a subunit immunization. **A)** Immunization and antibody treatment timeline. **B)** Confocal images of brachial LNs at day 6 after the immunization with NP-ss-OVA and CpG, under IgG or α-VEGFR3 treatment. **C)** *Left,* Identification of stromal cells (CD45-) based on the expression of gp38 and CD31; *right,* LECs counts at day 6. D) Weight of individual lymph nodes after immunization and antibody treatment. **E-F)** Frequency of CD45- and CD45+ cells (% of viable cells) in draining lymph nodes at day 6. **G)** Frequency of cytokine secreting CD8 T cells; lymphocytes were restimulated *ex vivo* with SIINFEKL peptide in the presence of Brefeldin A; cytokine expression was assessed by intracellular staining.

The data show that the immunization promoted lymphangiogenesis and LN expansion, as described by the increment in LECs numbers and LN weight (Fig5-3, C-D). However, there were no differences between the antibody treated groups, suggesting that the αR3 blockade did not inhibited LN-lymphangiogenesis. There were also no differences in the cellular composition of draining LNs between the two treated groups. We analyzed the stroma population, (which lack the CD45 antigen, Fig5-3, C) and found no major differences in the CD45- cell compartments, i.e., FRCs, BECs and LECs (Fig 5-3, E). Regarding the number of lymphocytes, both IgG and αR3 groups induced the same changes on the B cell and T cell populations upon vaccination when compared to the untreated control (Fig5-3, F).

Next, we investigated if there were differences in CD8 T cell responses in draining LNs, as well as in the spleen. Herein we also included a control group that was immunized but did not received any antibody treatment, in order to evaluate if there were unspecific effects induced by the type of antibody administrated. We observed that the functionality of CD8 T cells was not affected, and all mice displayed the same capacity to secrete inflammatory cytokines upon an *ex-vivo* restimulation assay with SIINFEKL (Fig 5-3, G).

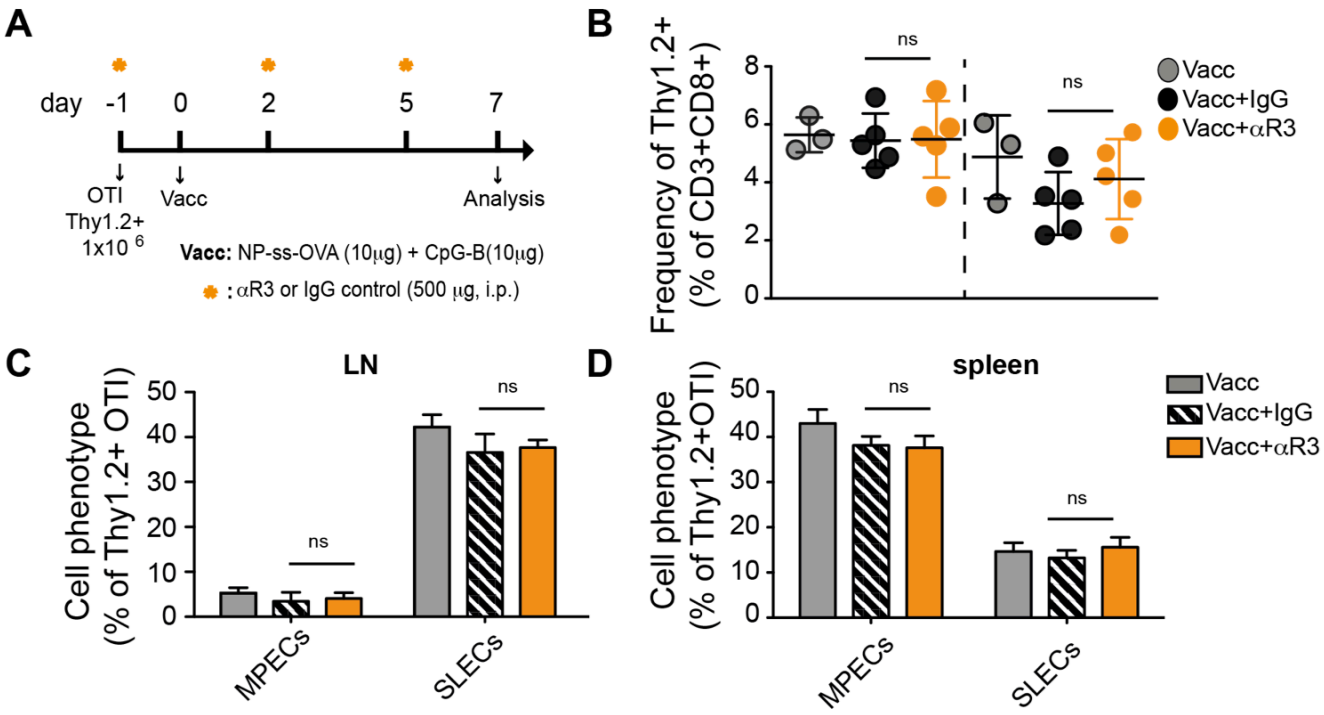

Figure 5–4 α-VEGFR3 treatment has not effect on the expansion and phenotype of adoptively transferred OTI CD8 T cells after a subunit immunization. **A)** Immunization and antibody treatment timeline. **B)** Frequency of Thy1.2+ OTI cells at day 7 after intradermal (i.d.) immunization with NP-ss-OVA and CpG-B, under IgG or αVEGFR3 treated conditions. **C-D)** Phenotype of Thy1.2+ OTI cells in draining lymph nodes and spleen, based ton the expression of killer cell lectin-like receptor G1 (KLRG1) and the interleukin-7 (IL-7) receptor alpha chain (CD127) [19]. Memory precursors cells (MPECs) are defined as CD127+ KLRG1-, while short lived effector cells (SLECs) are defined as CD127-KLRG1+ .

We had comparable results using an OTI adoptive transfer system (Fig5-4, A). We observed a similar expansion of OTI cells on day 7 after the immunization, regardless of the antibody

treatment that the mice received (Fig5-4, B). We also analyzed the phenotype of the Thy1.2+ OTI cells, based on the expression of killer cell lectin-like receptor G1 (KLRG1) and the interleukin-7 (IL-7) receptor alpha chain (CD127) [19], which defines CD127+ KLRG1- as memory precursors effector cells (MPECs), and CD127-KLRG1+ as short lived effector cells (SLECs). OTI cells displayed no differences in none of the markers studied, suggesting that in the short term, the treatment with αR3 has no effect on the induction of adaptive CD8 T cell responses (Fig5-4, C-D). These results were not surprising, considering that there was a no significant reduction in the numbers of LECs upon αR3 treatment.

Intradermal delivery of αVEGR3 does not significantly affect the stromal composition of LNs and the number of antigen-specific CD8 T cells induced after nanoparticle immunization

Finally, we sought to study whether delivering the αR3 antibody intradermally could have a more significant effect on the reduction of LN-lymphangiogenesis, since this delivery route targets effectively the LNs. For this purpose, we injected 25μg of αR3 or IgG control on the back on the mice, since this location also drains to brachial LNs, and thus it does not interferes with the drainage of the NP-ss-OVA immunization, which is administered in the foot pad. Similarly to our previous studies, we gave three doses of antibody three days apart. Mice were immunized one day after the first αR3 or IgG dose, and draining LNs were evaluated on day 6 (Fig5-5, A). We observed no significant differences in the weight of LNs, as well as no changes in the overall frequency of FRCs and LECs (Fig 5-5, B-C). Although we observed a reduction in the LEC counts in the αR3 treated mice, this was not significant compared to the IgG control group (Fig5-5, D). Staining with a pentamer recognizing SIINFEKL-MHCI revealed also no differences in the frequencies of antigen specific CD8 T cells (Fig5-5, E) in the LN. In conclusion, the administration of the αR3 antibody intradermally does not change the functional outcomes of CD8 T cell adaptive immunity after a NP-based immunization.

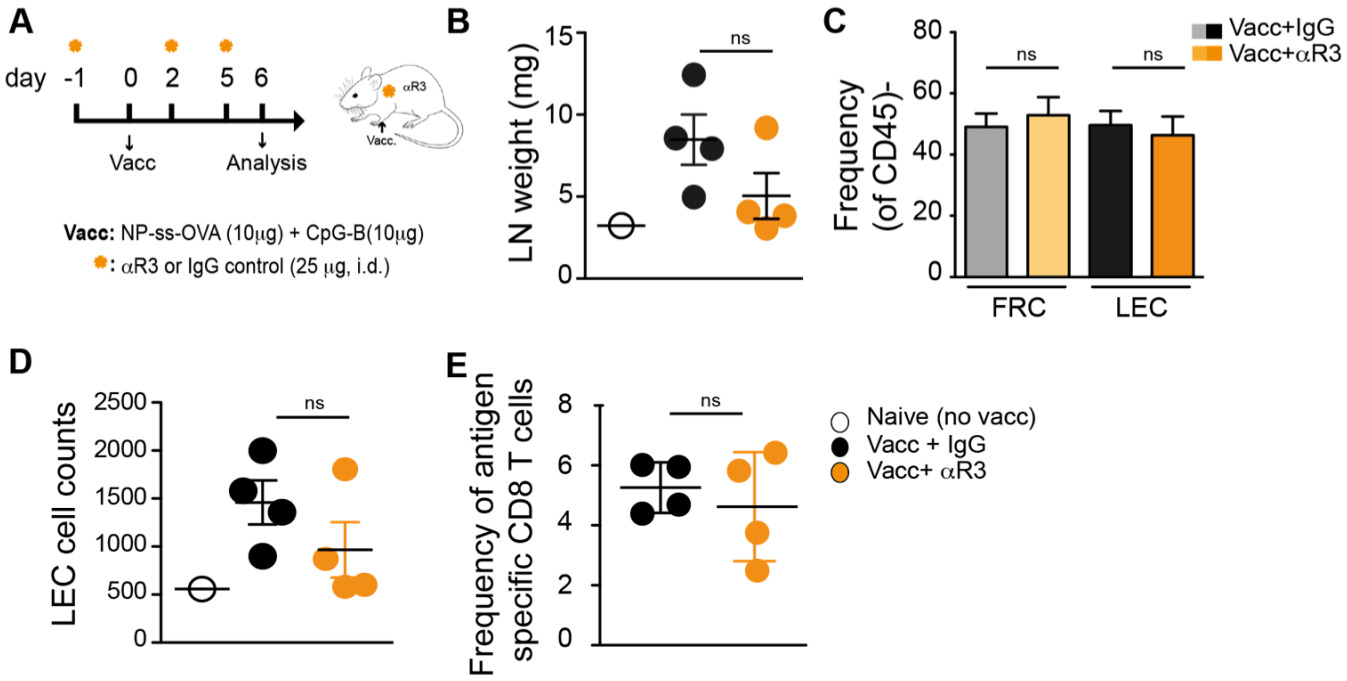

Figure 5–5 Intradermal administration of α-VEGFR3 does not inhibit lymph node lymphangiogenesis. **A)** Immunization and antibody treatment timeline. **B)** Weight of individual LNs after immunization and antibody treatment. **C)** Frequency of Follicular reticular cells (FRCs) and Lymphatic endothelial cells (LECs) , from the total stromal population (CD45-). **D)** LEC counts on day 6 after the NP-ss-OVA immunization. **E)** Frequency of SIINFEKL antigen specific CD8 T cells in draining LNs.

5.5 DISCUSSION

Lymph node stromal cells were once thought to provide only a support for antigen and cellular trafficking. However, we now know that these subsets play active and important roles in shaping immune responses and maintaining immune tolerance.

Herein, we have reported that under steady state LECs take up the exogenous antigen Ovalbumin (OVA) *in vivo*. The consequences of scavenging in steady state conditions were addressed recently in our group by Hirosue *et al.* [18], who demonstrated that antigen presentation by LECs led to CD8 T cells that were dysfunctional and apoptotic *in vitro*. We used fluorescently labelled OVA to show that under inflammatory conditions LECs also scavenged antigen, even at higher rates than those observed under steady-state conditions. In fact, recent studies have shown that LECs express pattern recognition receptors (PPRs), such as Toll like receptors (TLRs) [20,21], which in classical APCs enhance antigen uptake and cross-presentation. Thus, active sensing of dangerous signals in the extracellular environment could have enhanced the antigen scavenging by LECs under inflammatory conditions. It is still not determined which receptors LECs use to internalize antigen, although Hirosue *et al.* [18] reported that both macropinocytosis and clathrin mediated endocytosis were necessary for OVA uptake by LECs *in vitro*.

The fate of the antigen after internalization remains still unknown for us. A transcriptional analysis of stromal cells after stimulation with *Escherichia coli,* LPS and OVA showed that this treatment led to the overexpression of MHCI and MHCII by LECs [21]. Thus, a fraction of the antigen may have been processed for its presentation to T cells in order to contribute to the maintenance of peripheral tolerance. While some antigen may be stored within the LECs, as described by Tamburini *et al.,* it would be interesting to study whether the internalized protein can be also transferred to other APCs, such as DCs, similarly to what has been described between B cells and follicular dendritic cells [22].

We also show that once internalized, OVA was processed inside LECs. This is in agreement with early observations by Sixt *et al.*, that observed by confocal microscopy signal from DQ-OVA, similarly to what we have seen in our experiments [16]. However, recently Tamburini *et al.* reported no DQ-OVA signal, and thus, no processing of the antigen that was archived by LECs after a viral infection or a subunit immunization [14]. The discrepancies between this study and ours are likely arising from the two different timelines between the experiments, since Tamburini studied antigen signalling/processing one week post immunization.

To date there is no information on the active role of LECs in modulating immune responses during inflammatory conditions. Therefore, we assessed whether by interfering with the development of LN lymphangiogenesis we could gain some insights into the effects of proliferative LECs on adaptive immune responses. For this purpose, we administered the mF4-31C1 antibody that blockades signaling through VEGFR3, affecting the growth of new LECs, without disturbing the functionality of pre-existing vessels [15].

However, we did not observe significant differences in the numbers of LECs upon α-VEGFR3 administration. Similarly, there were no significant changes in the weight of the LNs between the αVEGFR3 and IgG control groups, and lymphocyte and stroma composition in LNs were very similar in both groups. We discard the possibility that the absence of any

obvious phenotype was because of the lack of activity of the antibody, since the same compound has been widely used in our group to block the development of lymphangiogenesis in VEGF-C overexpressing tumors[8].

A potential cause of the unnoticeable effects is that a) under CpG-B administration the inflammatory lymphangiogenesis depends mainly on other growth factors or b) LECs are compensating the lack of VEGFR3 signalling with additional growth factors. It has been noted that during inflammation macrophages, neutrophils and B cells can secrete VEGFA and VEGFD, which signal through VEGFR2, and that are recognised to be potent inducers of lymphangiogenesis [23–26]. Moreover, it has been suggested that the fully processed form of VEGF-C can also signal through VEGFR-2 [24]. Considering both scenarios, it is then not surprising that there were no noticeable effects of the blockade of VEGFR3 signalling.

Examination of adaptive immune responses also failed to show an effect of the blockade of the VEGFR3 signalling on the induction of CD8 T cell responses, as well as in their functionality, when compared to the isotype control. This was observed in endogenous CD8 T cell, and also when the response was magnified upon adoptive transfer of OVA specific T cells. The results are not surprising, considering that no remarkable changes in the LEC population were observed after administration of the α-VEGFR3 antibody.

Considering that only 1% of the LN population corresponds to the stromal cell subset, we speculate that assessing the specific role of LECs *in vivo* will require more specialized animal models, such as the ones where Cre-recombinase is expressed in LECs under the control of Lyve1 and Prox1 promoters. In this way, lymphatic-specific conditional mutations can be developed, and the role of antigen presentation by LECs in adaptive immunity could be more easily addressed. Moreover, future studies could also involve dual blockade of α-VEGR3 and α-VEGFR2 signalling, as reported by Tan *et al.* and Angeli *et al.* [12,13], since in this setup the two main signalling receptors of LECs can be blocked, and the probabilities of observing a more significant reduction of LEC numbers are higher.

Overall, this work demonstrated that LECs do sense and integrate signals from their microenvironment in steady state and inflammatory conditions. Future work is necessary to understand the consequences of LEC scavenging of foreign exogenous antigens on vaccine-elicited immunity.

5.6 REFERENCES

1. Girard, J.-P., Moussion, C. & Förster, R. HEVs, lymphatics and homeostatic immune cell trafficking in lymph nodes. *Nat. Rev. Immunol.* **12,** 762–773 (2012).
2. Mueller, S. N. & Germain, R. N. Stromal cell contributions to the homeostasis and functionality of the immune system. *Nat. Rev. Immunol.* **9,** 618–629 (2009).
3. Bajénoff, M. *et al.* Stromal Cell Networks Regulate Lymphocyte Entry, Migration, and Territoriality in Lymph Nodes. **25,** 989–1001 (2009).
4. Malhotra, D., Fletcher, A. L. & Turley, S. J. Stromal and hematopoietic cells in secondary lymphoid organs: Partners in immunity. *Immunol. Rev.* **251,** 160–176 (2013).
5. Turley, S. J., Fletcher, A. L. & Elpek, K. G. The stromal and haematopoietic antigen-presenting cells that reside in secondary lymphoid organs. *Nat. Rev. Immunol.* **10,** 813–825 (2010).
6. Fletcher, A. L. *et al.* Lymph node fibroblastic reticular cells directly present peripheral tissue antigen under steady-state and inflammatory conditions. *J. Exp. Med.* **207,** 689–697 (2010).
7. Nichols, L. a *et al.* Deletional self-tolerance to a melanocyte/melanoma antigen derived from tyrosinase is mediated by a radio-resistant cell in peripheral and mesenteric lymph nodes. *J. Immunol.* **179,** 993–1003 (2007).
8. Lund, A. W. *et al.* VEGF-C promotes immune tolerance in B16 melanomas and cross-presentation of tumor antigen by lymph node lymphatics. *Cell Rep.* **1,** 191–199 (2012).
9. Kumar, V. *et al.* Global lymphoid tissue remodeling during a viral infection is orchestrated by a B cell-lymphotoxin-dependent pathway. *Blood* **115,** 4725–33 (2010).
10. Hirakawa, S. *et al.* VEGF-C induced lymphangiogenesis in sentinel lymph nodes promotes tumor metastasis to distant sites. *Hematology* **109,** 1010–1017 (2007).
11. Tobler, N. Tumor and lymph node lymphangiogenesis — impact on cancer metastasis. *J. Leukoc. Biol.* **80,** 691–696 (2006).
12. Angeli, V. *et al.* B cell-driven lymphangiogenesis in inflamed lymph nodes enhances dendritic cell mobilization. *Immunity* **24,** 203–215 (2006).
13. Tan, K. W. *et al.* Expansion of cortical and medullary sinuses restrains lymph node hypertrophy during prolonged inflammation. *J. Immunol.* **188,** 4065–4080 (2012).
14. Tamburini, B. a, Burchill, M. a & Kedl, R. M. Antigen capture and archiving by lymphatic endothelial cells following vaccination or viral infection. *Nat. Commun.* **5,** 3989 (2014).
15. Pytowski, B. *et al.* Complete and specific inhibition of adult lymphatic regeneration by a novel VEGFR-3 neutralizing antibody. *J. Natl. Cancer Inst.* **97,** 14–21 (2005).
16. Sixt, M. *et al.* The conduit system transports soluble antigens from the afferent lymph to resident dendritic cells in the T cell area of the lymph node. *Immunity* **22,** 19–29 (2005).
17. Gretz, J. E., Norbury, C. C., Anderson, a O., Proudfoot, a E. & Shaw, S. Lymph-borne chemokines and other low molecular weight molecules reach high endothelial venules via specialized conduits while a functional barrier limits access to the lymphocyte microenvironments in lymph node cortex. *J. Exp. Med.* **192,** 1425–1440 (2000).
18. Hirosue, S. *et al.* Steady-State Antigen Scavenging, Cross-Presentation, and CD8+ T Cell Priming: A New Role for Lymphatic Endothelial Cells. *J. Immunol.* **192,** 5002–5011 (2014).
19. Joshi, N. S. *et al.* Inflammation Directs Memory Precursor and Short-Lived Effector CD8+ T Cell Fates via the Graded Expression of T-bet Transcription Factor. *Immunity* **27,** 281–295 (2007).

20. Fletcher, A. L. *et al.* Lymph node fibroblastic reticular cells directly present peripheral tissue antigen under steady-state and inflammatory conditions. *J. Exp. Med.* **207,** 689–697 (2010).
21. Malhotra, D. *et al.* Transcriptional profiling of stroma from inflamed and resting lymph nodes defines immunological hallmarks. *Nat. Immunol.* **13,** 499–510 (2012).
22. Batista, F. D. & Harwood, N. E. The who, how and where of antigen presentation to B cells. *Nat. Rev. Immunol.* **9,** 15–27 (2009).
23. Jussila, L. & Alitalo, K. Vascular growth factors and lymphangiogenesis. *Physiol. Rev.* **82,** 673–700 (2002).
24. Angeli, V. *et al.* B cell-driven lymphangiogenesis in inflamed lymph nodes enhances dendritic cell mobilization. *Immunity* **24,** 203–215 (2006).
25. Tan, K. W. *et al.* Neutrophils contribute to inflammatory lymphangiogenesis by increasing VEGF-A bioavailability and secreting VEGF-D. *Blood* **122,** 3666–3677 (2013).
26. Kang, S. *et al.* Toll-like receptor 4 in lymphatic endothelial cells contributes to LPS-induced lymphangiogenesis by chemotactic recruitment of macrophages. *Blood* **113,** 2605–2613 (2009).

Chapter 6

Conclusions, implications and future directions

6.1 CONCLUSIONS

In this thesis we explored the use of nanocarriers as antigen vectors for the development of subunit vaccines. We assessed their efficacy when delivered together with TLR ligands on modulating the magnitude and quality of cellular and humoral responses against the model protein OVA, as well as peptides and proteins derived from real pathogenic viruses, such as the LCMV and LASV.

Initially, we have confirmed the efficacy of PEG-PPS NPs to generate high frequencies of cytotoxic T cell responses when delivered together with the TLR9 ligand CpG-B. Moreover, we achieved a deep characterization of the phenotype of the elicited CD8 T cells, and demonstrated that the NPs generated a durable immunity, promoting long-lasting memory T cells that persist in lymphoid and non-lymphoid organs, suggesting that intradermal immunization with NPs has the potential to generate a broad protection to pathogens with diverse tissue tropism.

In the following study, we studied two nanocarrier platforms, PSs and NPs, in order to understand the mechanisms by which these two vectors preferentially activate CD4 or CD8 T cell responses. We demonstrated that the size of the nanocarrier, together with the mode of antigen loading, impacts the intracellular trafficking of the antigen, as well as its localization in lymphoid organs upon *in vivo* administration. We further assessed the consequences of having antigen in PSs or NPs on humoral immunity. We showed that PSs enhance significantly the number of T follicular helper CD4 cells, a subset that is a crucial component in B cell-based vaccines. Thus, these studies highlight the potential of PSs as a vector for the development of vaccines aimed to elicit antibodies.

Indeed, in our following chapter, we demonstrated that the quality of the cellular and humoral response against an antigen derived from LASV is dramatically enhanced by the PSs platform. The PSs increase the number of epitopes recognized by serum antibodies, thus enhancing the recognition of the viral protein when displayed in its native conformation. We thus confirm the potential of PSs for the development of B cell vaccines, and moreover, proved the feasibility of developing nanoparticle-based vaccine against an important, although neglected diseases, Lassa fever.

Finally, we demonstrated that not only professional APCs capture antigen delivered intradermally. We showed that lymphatic endothelial cells do capture antigen *in vivo* during steady state and non inflammatory conditions. We envision that the understanding of the implication of antigen scavenging by stromal cells will bring novel methods of immunomodulation that can be directly applied for tuning the outcome of adaptive immune responses.

To conclude, we have proved that NPs and PSs are effective vectors for the development of subunit vaccines, and moreover, we accomplished our aims to establish new insights and immediately applicable guidelines for the development of rationally designed vaccines.

6.2 IMPLICATIONS AND FUTURE DIRECTIONS

Establishing correlates of protection for T cell-based vaccines

The development of T cell memory is a key component for the success of T cell-based vaccines. Memory T cells are comprised of subsets that vary in important properties such as cytotoxic activity, trafficking patterns, tissue residence and proliferative capacity. Establishing which of these subsets is promoting protective capacity has been an intense subject of research. Our group has developed and applied the PEG-PPS nanoparticle technology in therapeutic and prophylactic T cell based vaccines. This antigen carrier has proven to be effective in promoting protection against influenza, as well as reducing tumor burden, thus providing enhanced host survival in a melanoma murine model [1,2]. However, the question that remains open after these studies are: how did the NP vaccines mediate protection or enhanced survival?

T cell phenotype is commonly used as a surrogate of protection. Herein, we made use of an adoptive transfer system to characterize in deep the phenotype of T cells after the nanoparticle vaccination. We demonstrated that a prime boost immunization with a peptide derived from the LCMV promotes a large memory pool of T cells that hold an effector phenotype characterized by a large population of CD43- CD27- cells, which also lack the expression of CD62L and CD127, and display high levels of KLRG-1. This subset was found in large frequencies in the spleen, as well as in peripheral organs such as lung and liver. Thus, it might be possible that previous studies involving NPs could have mediated protection or enhanced tumor killing because of the capacity of this vector to elicit effector memory T cells. Indeed, there is cumulative evidence that the effector memory subset, previously believed to be "senescent", has important roles in protective immunity [3–6]. What it is interesting in these studies are the mechanisms by which the effector subset contributed to protection. For instance, Olson *et al.* [3] demonstrated that the T effector memory cells were better in protecting against *Listeria monocytogenes* thanks to an enhanced cytotoxic activity of the effector subset, combined with their strategic position in the red pulp of the spleen, which is likely the main point of encounter between cytotoxic lymphocytes and *Listeria* infected cells. Hansen *et al.* [5] also demonstrated that protection against a simian immunodeficiency virus (SIV) by a viral vector that promoted effector memory CD8 T cells was acknowledged to the location of T cells in the surface of mucosal tissues, which helped to impaired virus replication early during infection, thus avoiding disease dissemination.

Overall, what these studies suggest is that is the combination of various factors, such as T cell functionality, tissue residence and T cell magnitude, that will determinate the protective capacity of T cell memory. However, considering the broad tissue tropism of pathogens, it is likely that for each disease a correlate of protection has to be determined. Therefore, our future work will be focus towards understanding how the effector memory cells obtained after an NP immunization vary in their protective capacity when compared to the central-memory like cells obtained upon the DC vaccination, in an acute and a chronic model of LCMV, as well as in a bacterial challenge model with *Listeria monocytogenes.* Moreover, we aim to evaluate the impact of other TLR adjuvants on the T cell memory phenotype. The overall

goal is to be able to tailor the immune response elicited by the NPs to the desired immune outcome that is beneficial for each pathogen.

Polymersomes as a promising system for B cell vaccines: applications for a vaccine against Lassa fever

For most of vaccines approved to date, the success of the immunization depends on the ability of the vector to elicit neutralizing antibodies against the microbial agent. However, eliciting neutralizing antibodies is not always an easy task, as is the case for HIV and influenza, which have proven to be major challenges for the vaccinology field.

In our third chapter, we evaluated potential mechanism by which the PS platform enhances CD4 T cell responses over the NP platform. We observed that PSs protected the antigen from endosomal escape and deliver it to lysosomes, which are specialized compartments for MHCII loading. This had direct implications on the numbers of antigen specific CD4 T cells. Moreover, a large proportion of the CD4 T cells elicited displayed an enhanced T follicular helper phenotype. These results are very promising, since development of immunizations that favor Tfh differentiation is an important goal in B cell-vaccine development. For instance, results from last phase III clinical trial of HIV (RV 144) have demonstrated that HIV-infected individuals that make broadly neutralizing antibodies (bnAbs) have a higher frequency of CD4 T follicular helper cells in blood than those who did not make bnAbs[7]. In fact, we have demonstrated that the implementation of the PSs platform for the development of a vaccine against the surface glycoprotein 1 from Lassa leads to a broadening of the serum antibody targeting regions. In the context of an infection, this indicates that these antibodies will be able to recognize and fight more strains of Lassa. This is crucial for a future vaccine against Lassa fever, since more than 54 strains of LASV have been identified in West Africa. Among these strains there is a high genetic diversity, especially in the glycoprotein precursor (GPC, encoding for GP1 and GP2) [8,9], and thus elicited antibodies with a broad targeting spectrum will be a crucial component of a successful vaccine candidate.

Our current studies are focus on a) evaluating the protective efficacy of the antibodies elicited upon PS-LASV immunization and b) optimization of the adjuvant platform, in order to further modulate the humoral immune response to LASV-GP1. In our first study, we will challenge mice with a chimeric LCMV strain expressing the glycoprotein of LASV [10]. This strain has a similar kinetic persistence than the clone-13 of LCMV. Hence, we aim to evaluate if the antibodies elicited upon a PS-LASV immunization could avoid the establishment of a chronic viral infection. Secondly, we are currently working on the encapsulation of TLR7/8 and TLR9 ligands on PSs for their codelivery with PS-LASV. We could then evaluate if the delivery of immunomodulatory signals in nanoparticle carriers can simultaneously target the same APC as the antigen and thus enhance the quantity as well as the quality of the antibodies elicited.

Capture of antigen by LECs: Implications for adaptive immunity

With the aim to understand the active role of lymphatic endothelial cells (LECs) in adaptive immunity, we evaluated the capacity of these cells to capture antigen in vivo. We used steady state conditions to prove the LEC scavenge antigen in steady state and inflammatory

conditions. In steady state, we have proven that the crosspresentation of exogenous antigens leads to T cell dysfunction and tolerance in a PD-L1 dependent manner [11]. *In vivo,* the role of LEC scavenging in an inflammatory environment still needs to be elucidated. We hypothesize two potential outcomes for this uptake: First, based on the strong evidence of the tolerogenic nature of the stromal cell subsets, we believed that an active antigen presentation in MHCI and MHCII complexes might drive T cell tolerance. This could be a mechanism of protection, as previously described for FRCs, in order to counterbalance the immune response and avoid T cell-mediated immunopathology, and thus, excessive damage of the lymphoid architecture [12].

In a second scenario, antigen uptake by LECs can also promote immunity, although not directly by presenting processed antigen to T cells. As described by Tamburini *et al*., [13] antigen archiving by proliferative LECs was beneficial for the maintenance of T cell memory. Considering the close location of LECs with DCs, it is also possible that the scavenged antigen is transferred to lymph node resident DCs for its further presentation to T cells, in order to initiate an early immune responses

Nanoparticle-based vaccines: promising vectors for programming the quality of the immune response

Herein we have demonstrated the potential of nanocarriers as future components of subunit vaccines. Even though there is strong evidence indicating the efficacy of synthetic nanoparticles for vaccination purposes, it would take several years until a synthetic vaccine can be approved for their use in humans, as most of the current companies based on nanoparticles are currently in Phase I studies [14]. However, we believe that in the future nanoparticles will offer a potent system of antigen delivery with a good safety profile, which is indeed needed in the context of various vaccine candidates, specially those targeting people in zones of high prevalence of endemic diseases.

6.3 REFERENCES

1. Jeanbart, L., Ballester, M., Titta, A. De & Swartz, M. Enhancing Efficacy of Anticancer Vaccines by Targeted Delivery to Tumor-Draining Lymph Nodes. *Cancer Immunol Res* **6,** 436–447 (2014).
2. Nembrini, C. *et al.* Nanoparticle conjugation of antigen enhances cytotoxic T-cell responses in pulmonary vaccination. *Proc. Natl. Acad. Sci. U. S. A.* **108,** E989–E997 (2011).
3. Olson, J., McDonald-Hyman, C., Jameson, S. & Hamilton, S. Effector-like CD8+ T Cells in the Memory Population Mediate Potent Protective Immunity. *Immunity* **38,** 1250–1260 (2013).
4. Wherry, E. J. & Ahmed, R. Memory CD8 T-Cell Differentiation during Viral Infection. *J. Virol.* **78,** 5535–5545 (2004).
5. Hansen, S. G. *et al.* Effector memory T cell responses are associated with protection of rhesus monkeys from mucosal simian immunodeficiency virus challenge. *Nat. Med.* **15,** 293–299 (2009).
6. Van Duikeren, S. *et al.* Vaccine-Induced Effector-Memory CD8+ T Cell Responses Predict Therapeutic Efficacy against Tumors. *J. Immunol.* **189,** 3397–3403 (2012).
7. Locci, M. *et al.* Human circulating PD-1+CXCR3-CXCR5+ memory Tfh cells are highly functional and correlate with broadly neutralizing HIV antibody responses. *Immunity* **39,** 758–769 (2013).
8. Bowen, M. D. *et al.* Genetic diversity among Lassa virus strains. *J. Virol.* **74,** 6992–7004 (2000).
9. Leski, T. A. *et al.* Sequence Variability and Geographic Distribution of Lassa virus, Sierra Leone. *Emerg. Infect. Dis.* **21,** 609–618 (2015).
10. Sommerstein, R. *et al.* Evolution of Recombinant Lymphocytic Choriomeningitis Virus/Lassa Virus In Vivo Highlights the Importance of the GPC Cytosolic Tail in Viral Fitness. *J. Virol.* **88,** 8340–8348 (2014).
11. Hirosue, S. *et al.* Steady-State Antigen Scavenging, Cross-Presentation, and CD8+ T Cell Priming: A New Role for Lymphatic Endothelial Cells. *J. Immunol.* **192,** 5002–5011 (2014).
12. Mueller, S. N. *et al.* Viral targeting of fibroblastic reticular cells contributes to immunosuppression and persistence during chronic infection. *Proc. Natl. Acad. Sci. U. S. A.* **104,** 15430–15435 (2007).
13. Tamburini, B. a, Burchill, M. a & Kedl, R. M. Antigen capture and archiving by lymphatic endothelial cells following vaccination or viral infection. *Nat. Commun.* **5,** 3989 (2014).
14. Irvine, D. J., Swartz, M. a & Szeto, G. L. Engineering synthetic vaccines using cues from natural immunity. *Nat. Mater.* **12,** 978–990 (2013).

Marcela Rincon-Restrepo

1 Avenue du Rond Point, 1006, Lausanne
marcela.rincon-restrepo@epfl.ch
+41(0)766154120

20/08/1984
Nationality: Colombian

EDUCATION

2011 – Ongoing: **Ph.D. in Biotechnology and Bioengineering**

École Polytechnique Fédérale de Lausanne (EPFL), Laboratory of Lymphatics And Cancer Bioengineering (LLCB). **Mentor**: Melody Swartz

- Working on a comprehensive description of the humoral and cellular responses to viral and model antigen upon immunization with nano-sized particles.
- Developed expertise in the characterization of innate and adaptive immune responses
- Gained strong experience in animal models and *in vitro* cell models.
- Multiple collaboration with research groups within Switzerland, including the group of Professor Stefan Kunz at the CHUV, and Professor Sai Reddy at ETH Zurich.

2009-2011 ***Msc.*** **Biomedical Engineering, emphasis in Molecular Bioengineering**

Eidgenössische Technische Hochschule Zürich (ETHZ). Master thesis at the Laboratory of Lymphatics And Cancer Bioengineering (LLCB). **Mentor**: Melody Swartz

- Worked on the formulation of a synthetic vaccine against Machupo virus.
- Developed skills on the formulation of nanoparticles and synthesis of polymers.

2002-2006 **Bsc. Biomedical Engineering**

Escuela de Ingeniería de Antioquia (EIA) **Thesis Title:** Fabrication and characterization of synthetic hydroxyapatite scaffolds for their application in bone tissue engineering

EMPLOYMENT HISTORY

2007 –2008 University of Oxford, Group of Professor Hagan Bayley

- Scientific position. Working towards “Single molecule DNA sequencing with the α-Haemolysin nanopore” project, emphasizing on the understanding of DNA translocation through nanopores.
- Working closely and frequently with Oxford Nanolabs Ltd. on the progress of a collaborative project towards the development of a chip for next generation sequencing.
- Contributed to two publications and one patent.

2006-2007 Colombian Institute of Tropical Medicine

- Project internship implementing the software AM (Administration and Maintenance) in order to increase cost/effective ratio of maintenance procedures.
- Responsible for the administration and maintenance of the medical equipment in the Institute.

SKILLS AND TECHINIQUES

Immunology techniques: Strong experience on cell flow cytometry, immuno-histochemistry and ELISA. Primary cell isolation and *in vitro* cultures.

Molecular biology and biochemical techniques: RNA extraction, cDNA synthesis, RT-PCR , DNA and protein electrophoresis

Software: GraphPad Prism, Adobe Illustrator, FlowJo, Microsoft Office

PUBLICATIONS

Nanoparticle-based vaccine augments cytotoxic CD8 T cells responses and promotes an effector-like memory phenotype. **Rincon-Restrepo M.,** Goncalves-Cabecinhas AR., Utzschneider D., Vokali E., Hirosue S., Kunz S., Swartz MA. *In preparation.*

Implications for the quality of cellular and humoral responses after antigen delivery on Nanoparticles and Polymersomes. **Rincon-Restrepo M.,** Mayer A., Hauert S., Haessler U., Hirosue S., Reddy S., Swartz MA. *In preparation*

Steady-state antigen scavenging, cross-presentation, and CD8+ T cell priming: a new role for lymphatic endothelial cells. Hirosue S, Vokali E, Raghavan VR, **Rincon-Restrepo** M, Lund AW, Corthésy-Henrioud P, Capotosti F, Halin Winter C, Hugues S, Swartz MA. J Immunol. 2014 Jun 1;192(11):5002-11

Controlled translocation of individual DNA molecules through protein nanopores with engineered Molecular Brakes. **Rincon-Restrepo M**.,Mikhailova E., Bayley H., G. Maglia. Nano Lett., 2011, 11, pp 746–750.

Enhanced translocation of single DNA molecules through α-hemolysin nanopores by manipulation of internal charge. Maglia G., **Rincon-Restrepo M**., Mikhailova E., Bayley H. Prot. Natl. Acad. Sci. USA, 2008,105, pp 19720-1972.

Designing nanosensors based on charged derivatives of gramicidin A. Capone R., Blake S., **Rincon-Restrepo M**., Yang J., Mayer M. J. Am. Chem. Soc, 2007, 129, pp 9737-9745.

Fabricación y caracterización de una matriz tridimensional de hidroxiapatita macroporosa para su aplicación en ingeniería de tejidos óseos. **Rincón-Restrepo M**., Rodríguez-Barrera A., Londoño-Puerta M., Echevarria-Velásquez A. Revista EIA, 2007, 7, pp 87-95.

CONFERENCES

Keystone conference, Seattle, 2014. Mechanisms of action of vaccine adjuvants. **Rincon-Restrepo M.,** Mayer A., Hauert S., Haessler U., Hirosue S., Reddy. *Oral presentation.*

5th International Conference on Tumor-Host Interaction and Angiogenesis. Monte Verita, 2013 **Rincon-Restrepo M**., Vokali E., Hirosue S., Swartz MA. *Poster.*

Keystone conference, Ottawa, 2012. Immunological mechanisms of vaccination. **Rincon-Restrepo M**., Goncalvez AR., Hirosue S., Kunz S., Swartz MA. *Poster.*

Biophysical Society Annual Meeting, Long Beach, 2008. Maglia G., **Rincon-Restrepo M**., Bayley H. *Poster.*

III Symposium- Biofabrics. Medellín, 2007. **Rincón-Restrepo M**., Rodríguez-Barrera A., Londoño-Puerta M., Echevarria-Velásquez A. *Oral presentation.*

OTHER SKILLS

English : Fluently spoken and written

Italian : Proficient

French: Basic

Spanish : Mother tongue